Magnetic Reconnection, a Celestial Phenomenon in the Laboratory

Jan Egedal

In collaboration with the WiPPL team,

Including J. Olson, S. Greess, H. Gurram, B. Wetherton, A. Millet-Ayalla, P. Gradney, J. Schroeder, C. Kuchta, A. Le, W. Daughton, M. Clark, J. Wallace, and C. B. Forest

Introduction to Fusion Energy and Plasma Physics Course
SULI, June 16th, 2022

My Journey into Space Plasma Physics

Grew up in a small village "Brylle" in Denmark

Went to the Technical University of Denmark

Attended a colloquium on fusion ➔ Internship at JET (the largest tokamak in the world)

Did PhD at JET/Oxford Uni. UK. ("Experimental Verification of Murphy's law")

Lunch offer: ➔ PostDoc Building a Magnetic Reconnection Experiment "VTF" at MIT, MA, USA.

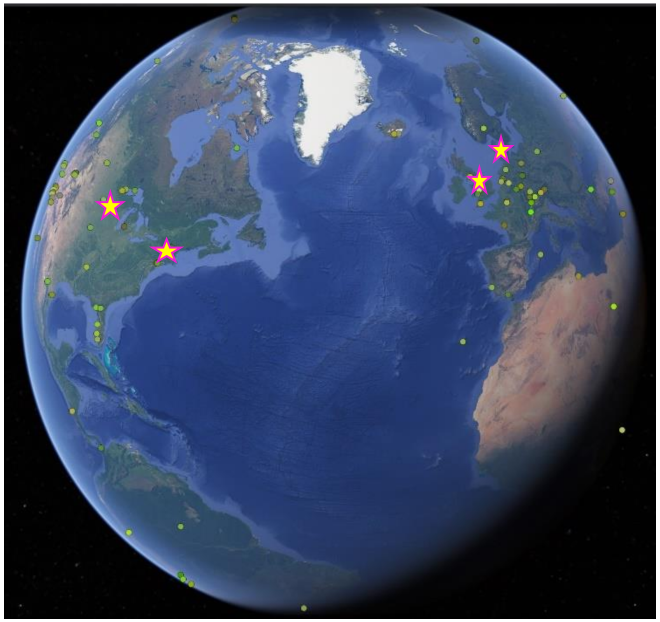

Stayed at MIT for 15 years

Since 2013, working at UW-Madison mainly on magnetic reconnection.

Background in fusion very helpful!

Magnetic Reconnection

- *A change in magnetic topology in the presence of a plasma*

Consider a small perturbation

Plasma carrying a current

Magnetic fields

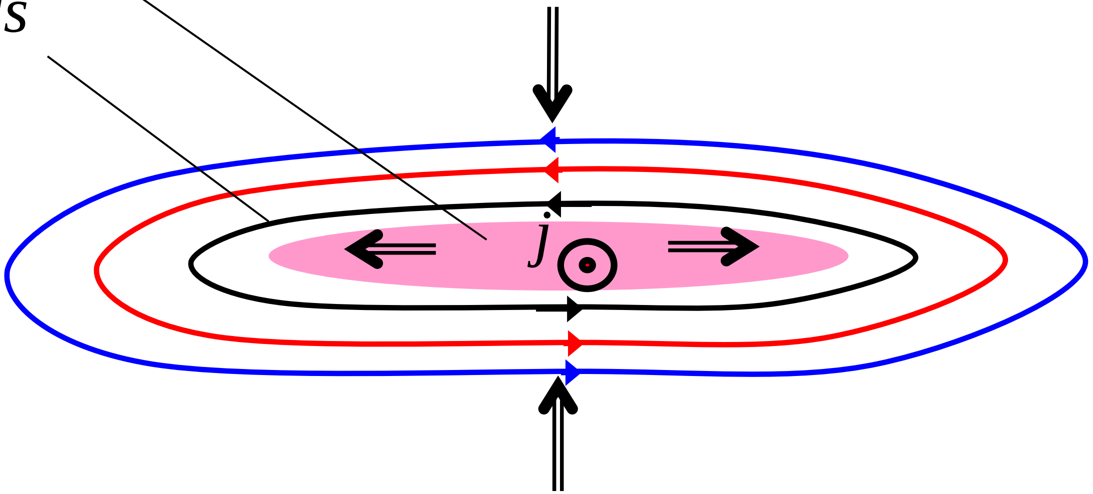

- *A change in magnetic topology in the presence of a plasma*

Consider a small perturbation

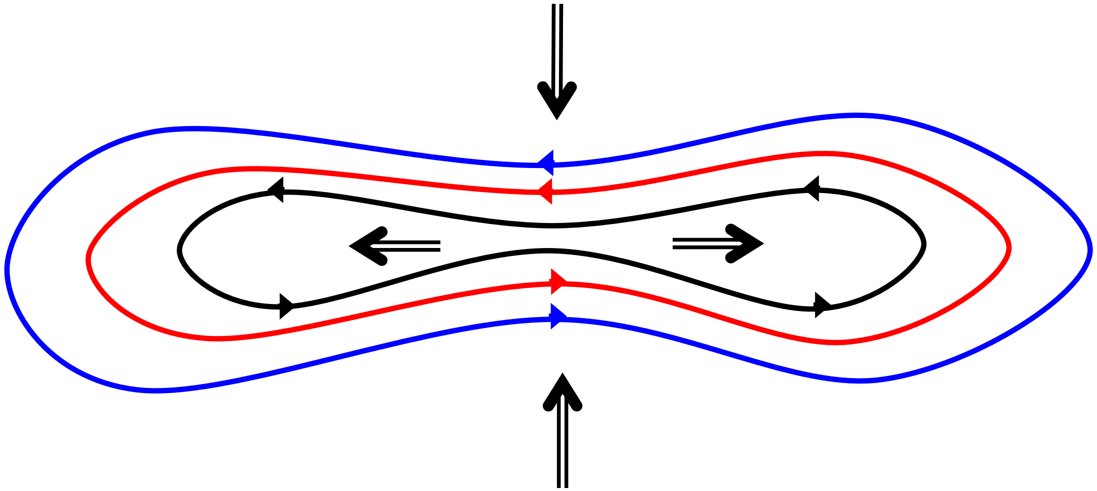

Magnetic Reconnection

- *A change in magnetic topology in the presence of a plasma*

Consider a small perturbation

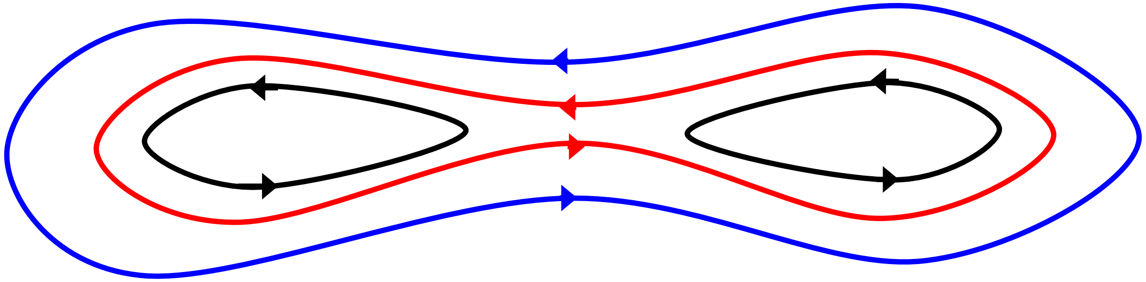

Magnetic Reconnection

- *A change in magnetic topology in the presence of a plasma*

Consider a small perturbation

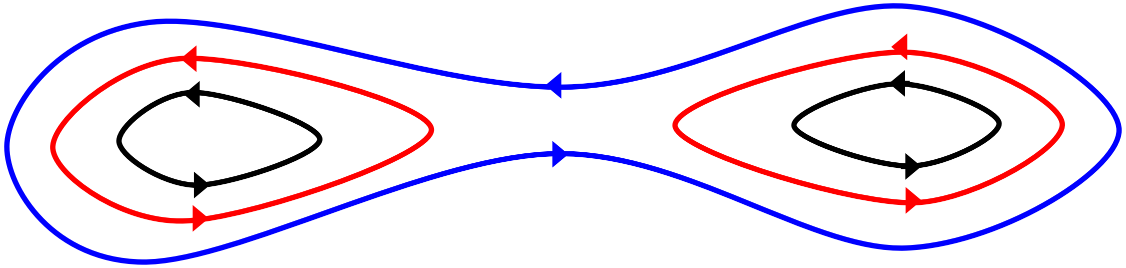

Magnetic Reconnection

- *A change in magnetic topology in the presence of a plasma*

Consider a small perturbation

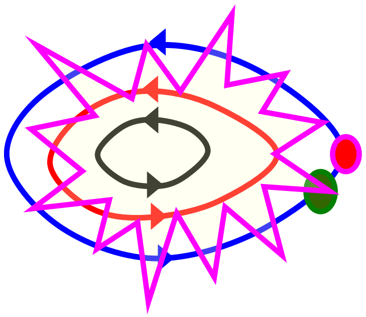

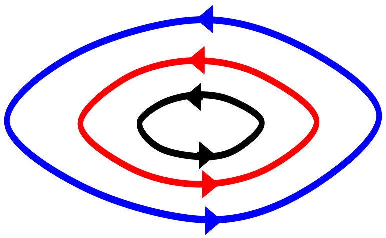

Nearly all the initial magnetic energy is converted into:

1. *thermal energy*
2. *kinetic energy on fast electrons and ions*
3. *kinetic energy of large scale flows*

Coronal Mass Ejections

The most powerful explosions in our solar system

Can power the US consumption of electricity for 10 million years

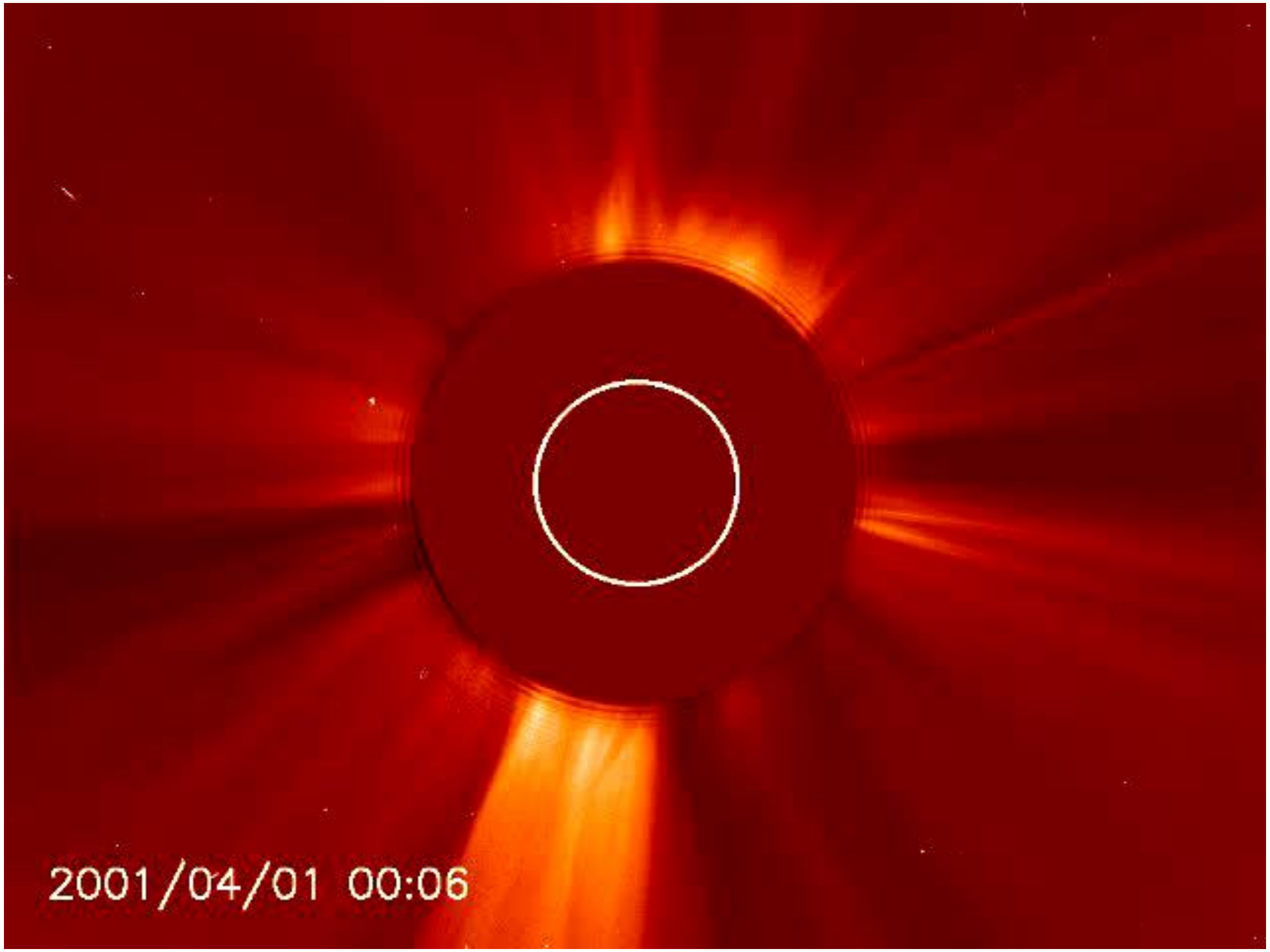

Outline

- Magnetic Reconnection and Space Weather
- Pressure anisotropy and electron trapping, MMS
- TREX, the Terrestrial Reconnection Experiment
  - Supersonically driven reconnection
  - Shock formation yields magnetic pile-up
  - Magnetic pile-up regulates the normalized Rec.-Rate.
    [Olson+, JPP, 2021]
  - Width of the TREX electron diffusion region, ~ $2d_e$
    [Greess+, JGR, 2021]
  - Upgrade to reach fully kinetic reconnection regime
- Conclusions

Space Weather

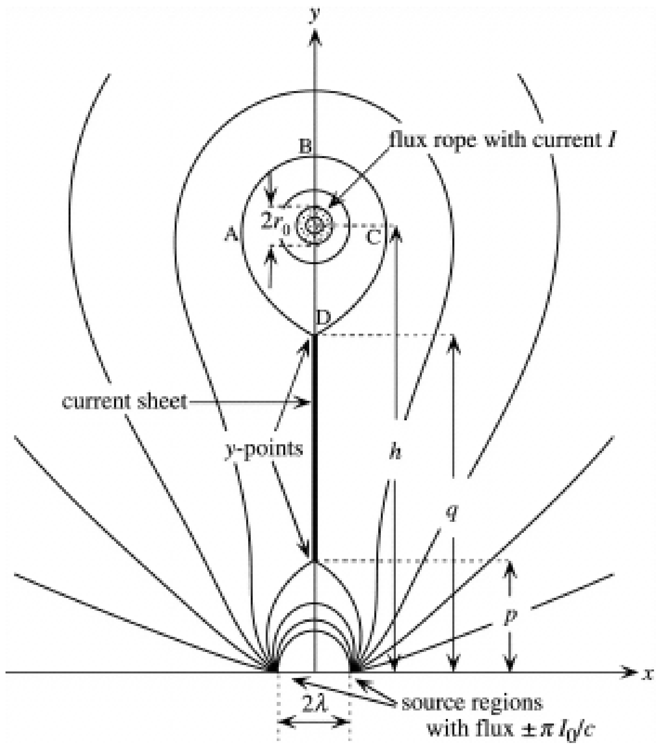

Lin & Forbes (2000)

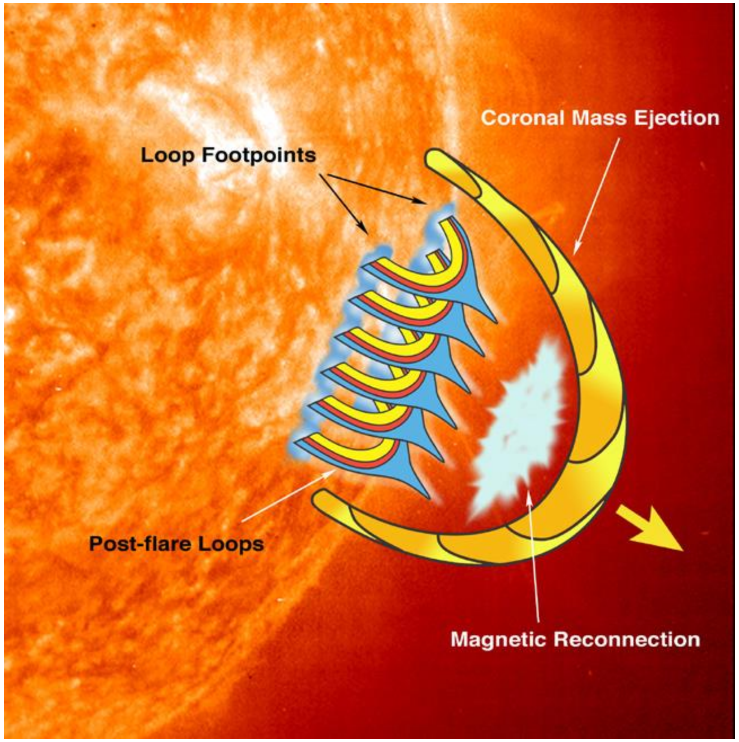

Space Weather

MHD-simulations

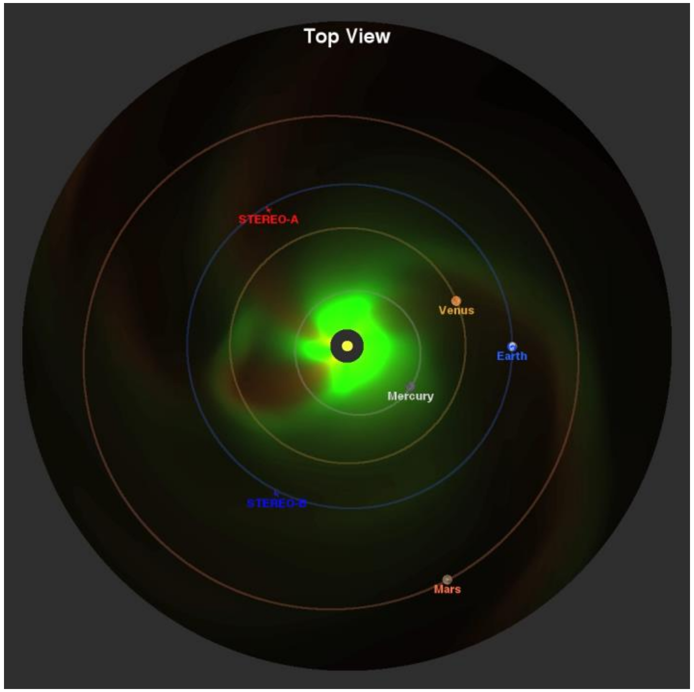

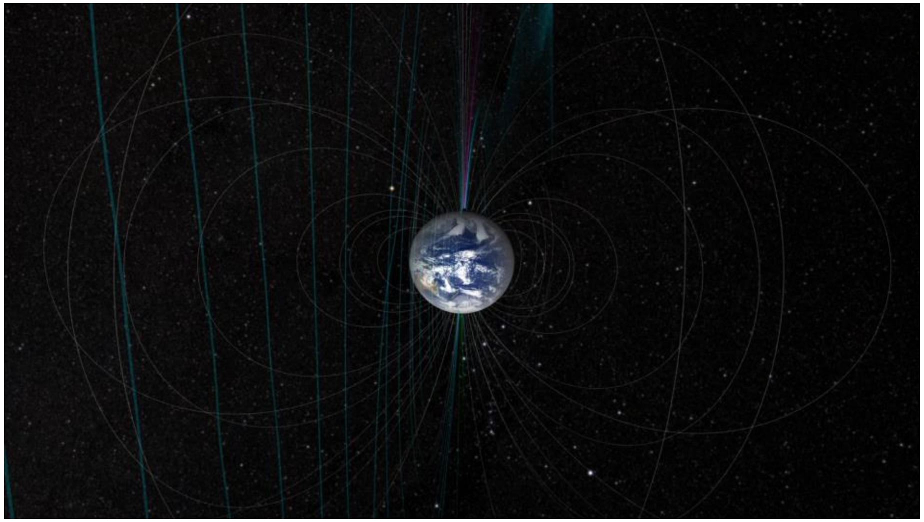

www.nasa.gov/content/goddard/mms-studying-magnetic-reconnection-near-earth
Coronal Mass Ejection July 2012

The Earth’s Magnetic Shield

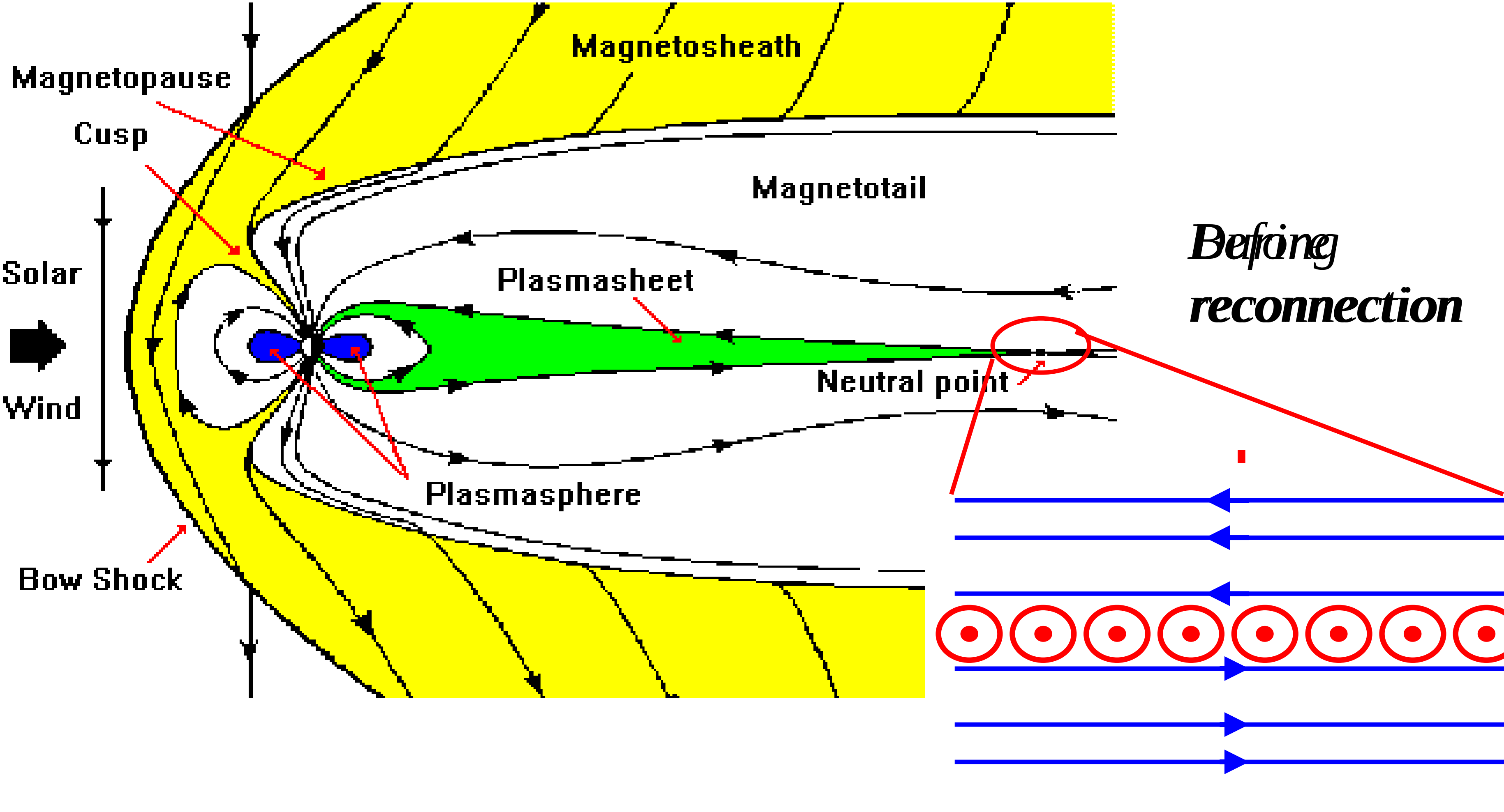

Magnetic sub-storms

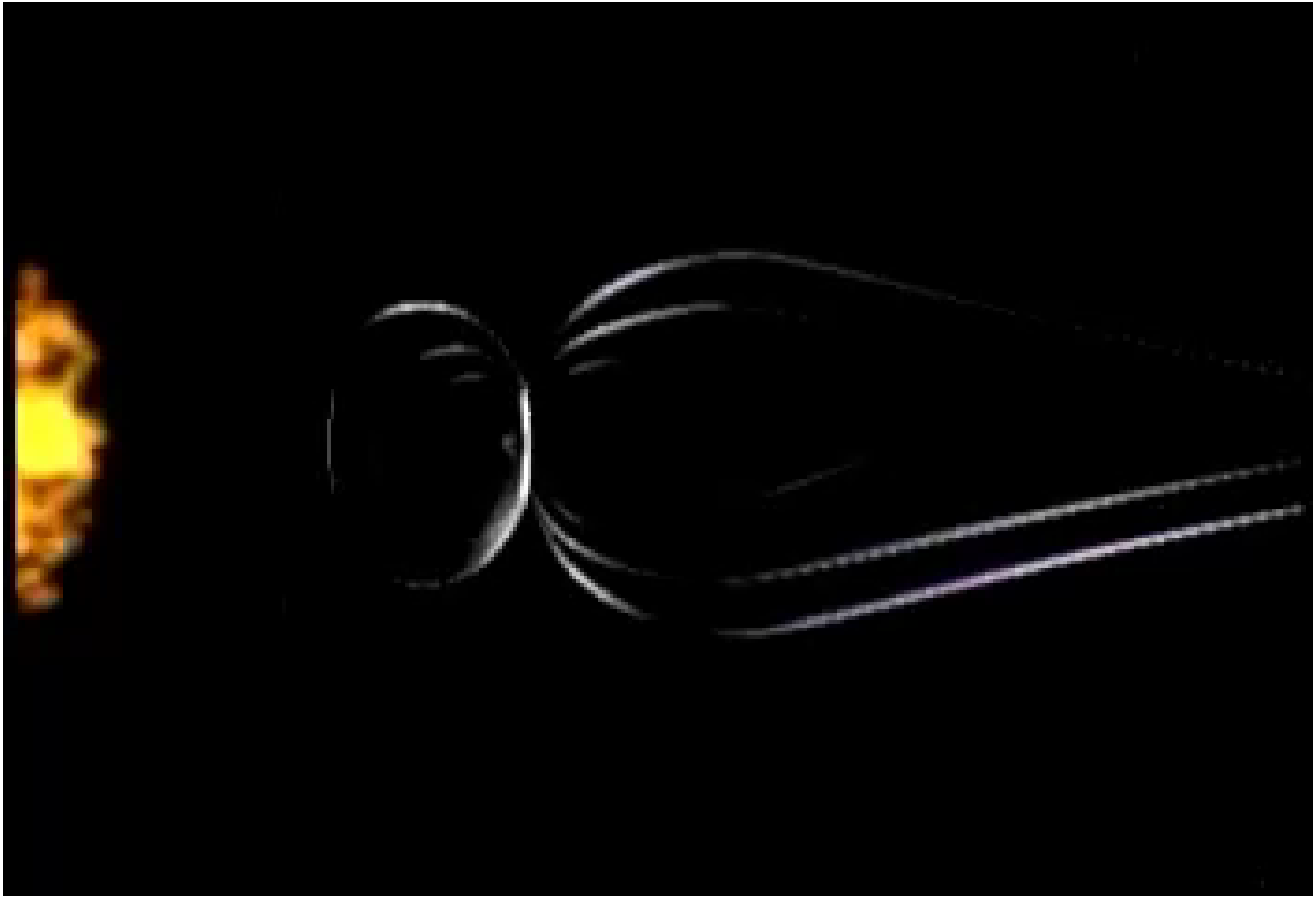

Aurora Borealis

October 26th, 2011, Kola Peninsula, Russia

Carrington Flare (1859, Sep 1, am 11:18)

WiPPL

- Richard Carrington (England) first observed a solar flare in 1859.
- White flare for 5 minutes.
- Very bright aura appeared next day in many places on Earth including Cuba, the Bahamas, Jamaica, El Salvador and Hawaii.
- Largest magnetic storm in recent 200 years (> 1000 nT).

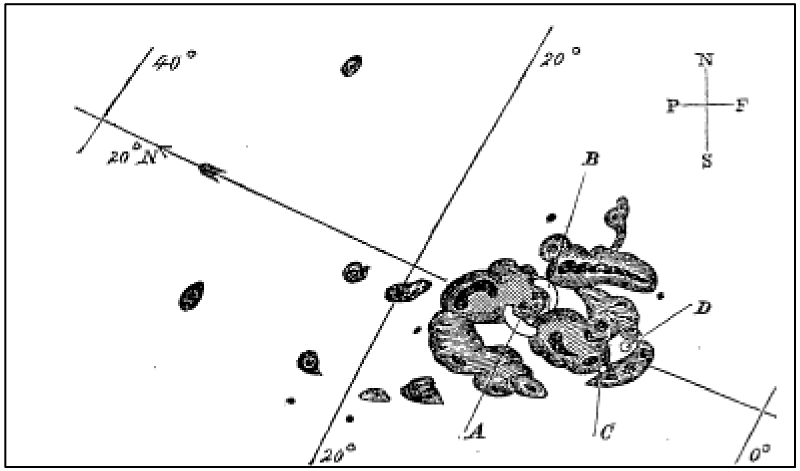

Telegraph systems all over Europe and North America failed, in some cases even shocking telegraph operators. Telegraph pylons threw sparks and telegraph paper spontaneously caught Fire. (Loomis 1861)

http://en.wikipedia.org/wiki/Solar_storm_of_1859

The Solar Wind affects the Earth's environment

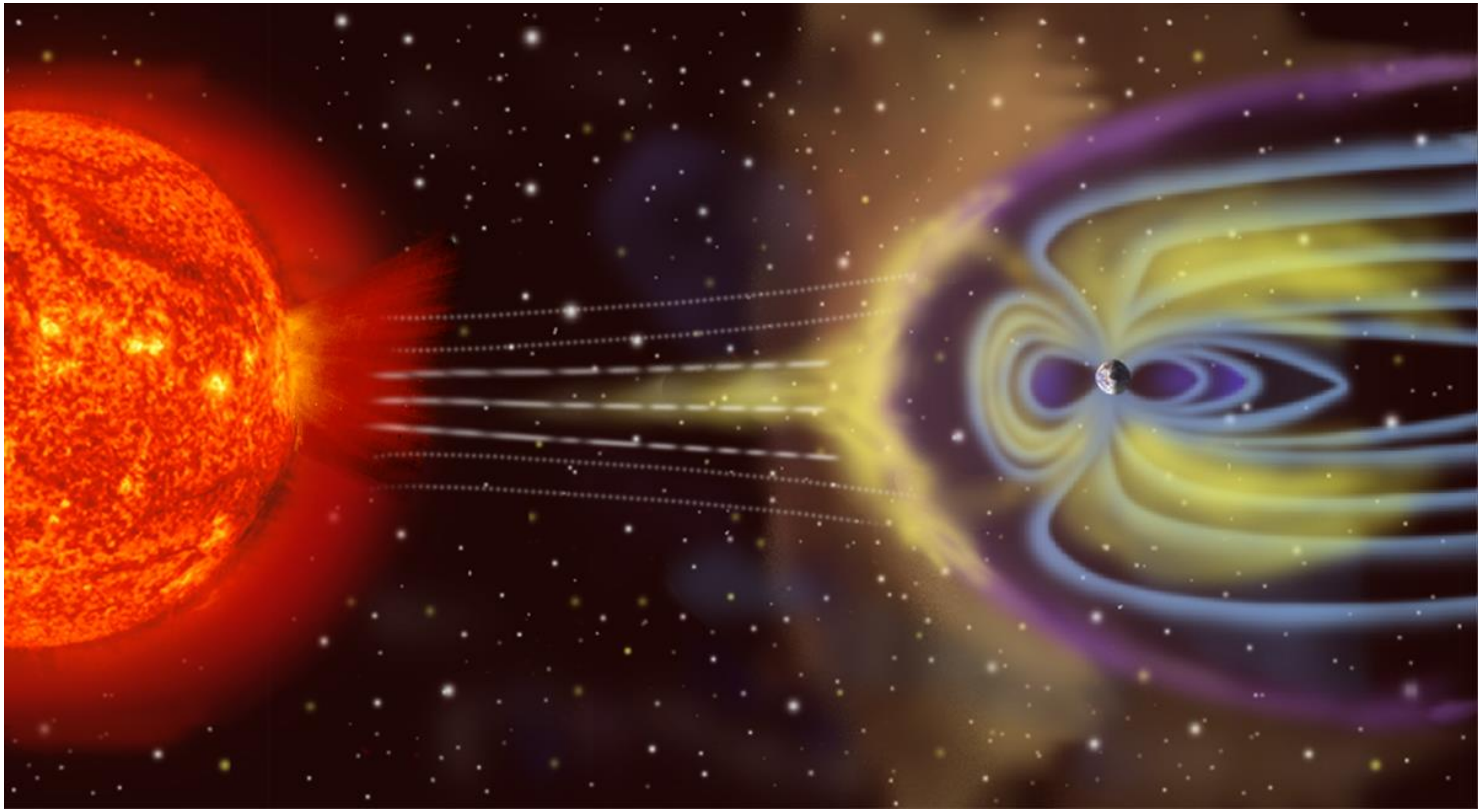

Magnetic storm and aurora on March 13, that lead to Quebeck blackout (for 6 million people)

PJM Public Service
Step Up Transformer
Severe internal damage caused by the space storm of 13 March, 1989

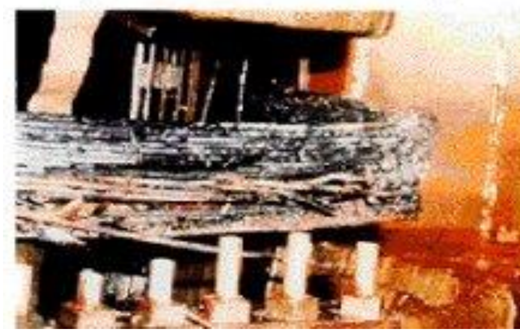

Magnetic storm ~ 540 nT, Solar flare X4.6.

A Carrington Flare today ➔ 30 – 70 billion dollars of damage

Occurrence frequency of flares?

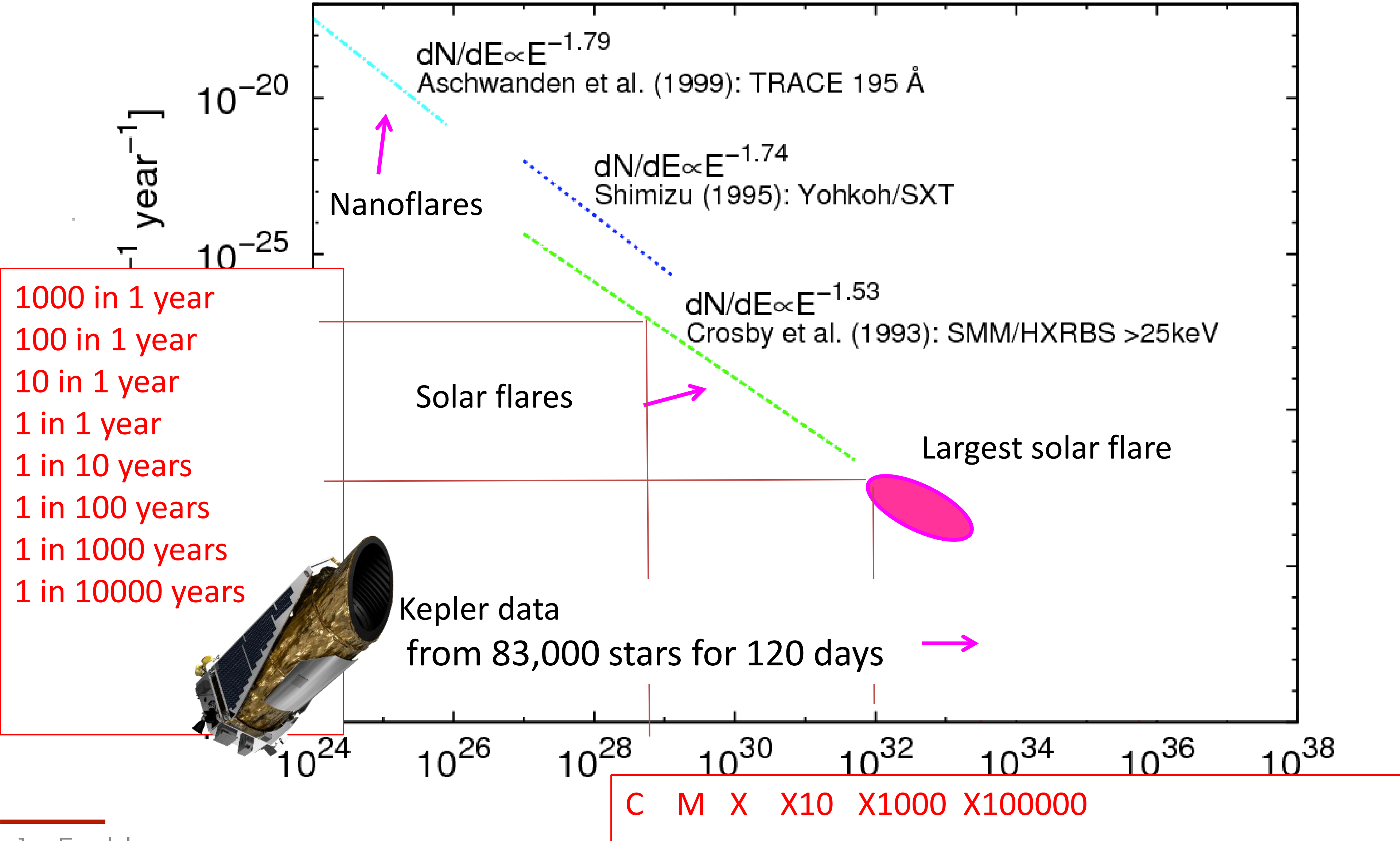

The Tokamak Device

Best plasma confinement device on Earth

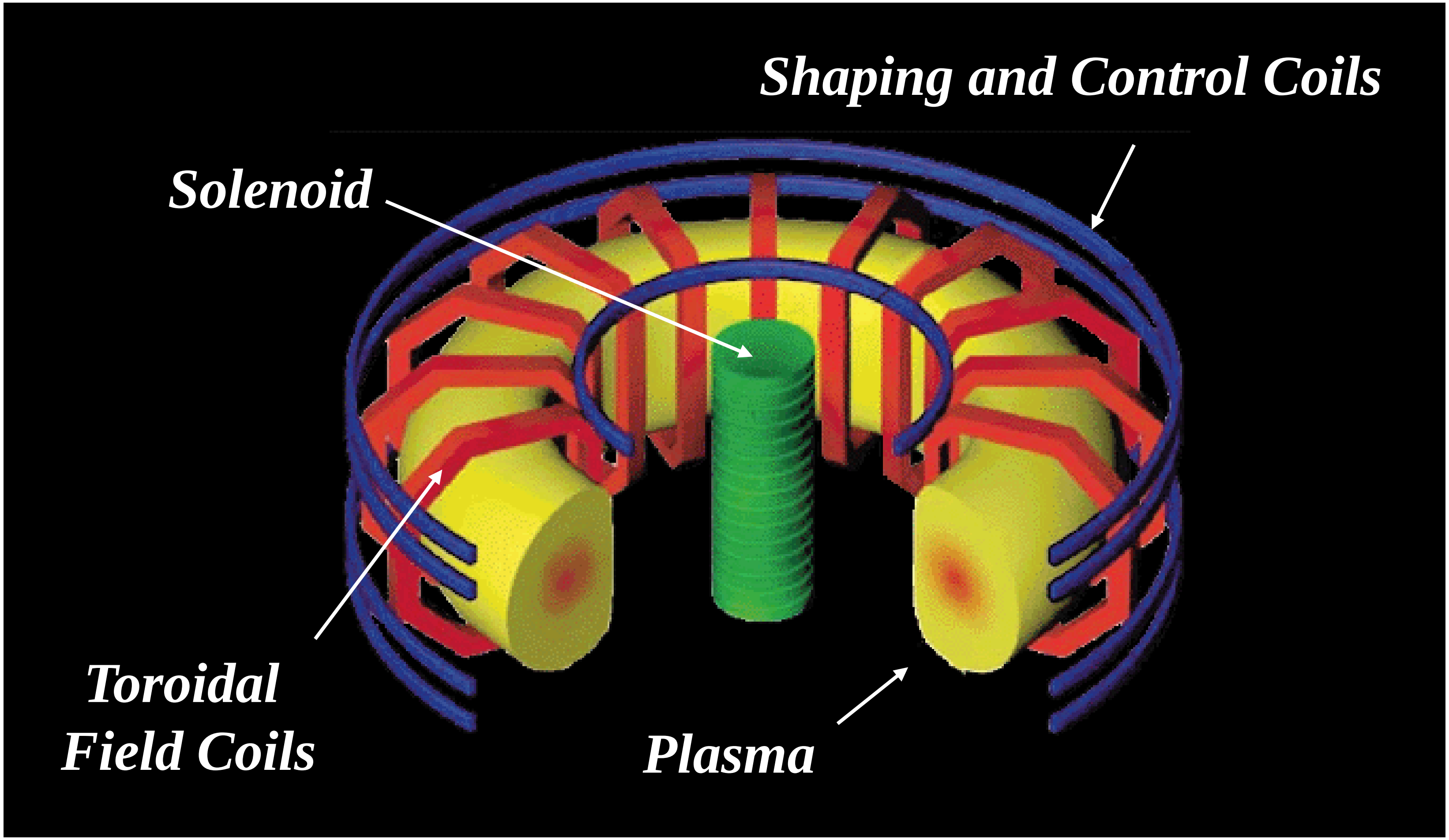

Magnetic Fusion Devices

International Thermonuclear Experimental Reactor

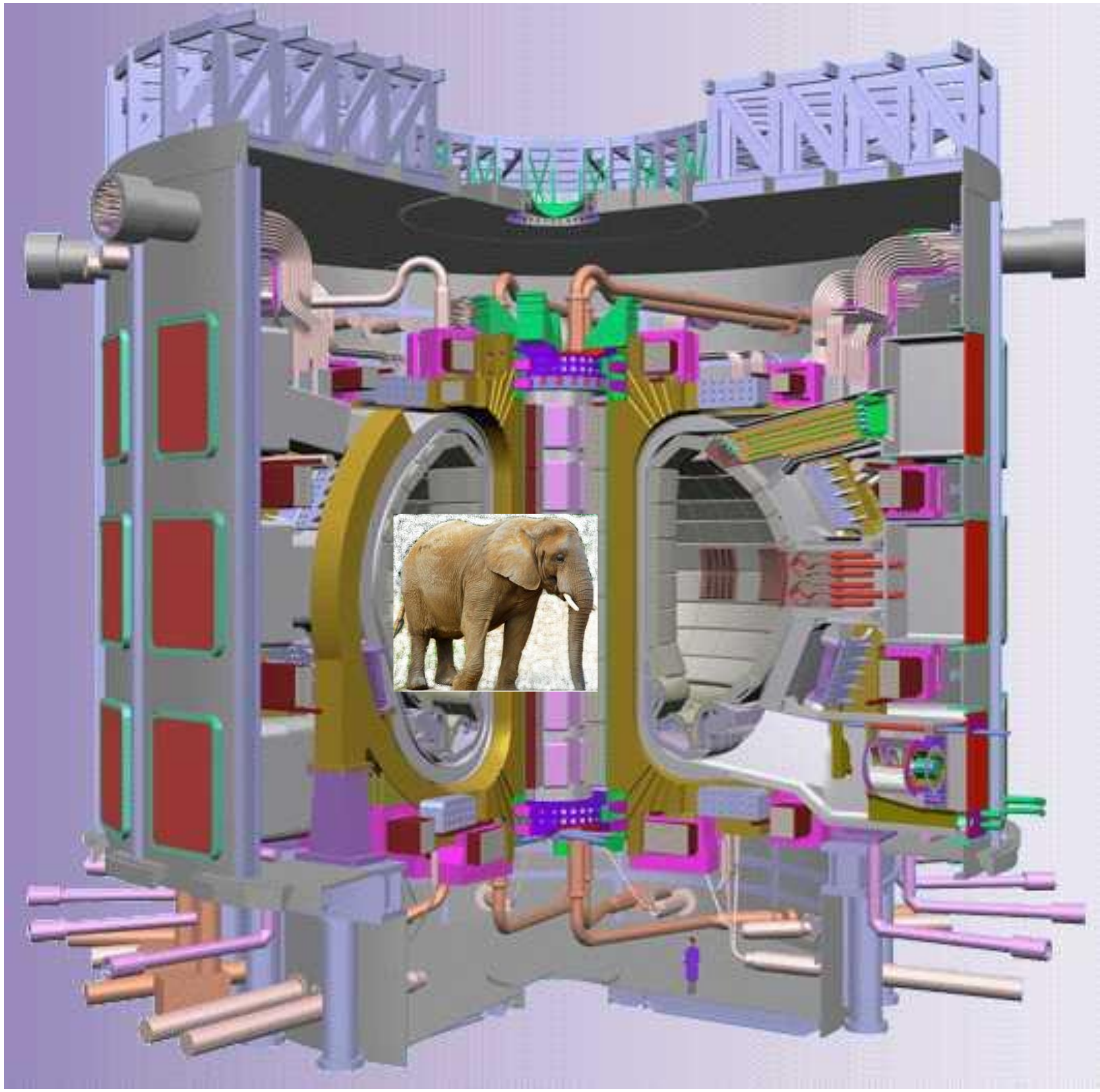

Magnetic Fusion Devices

International Thermonuclear Experimental Reactor

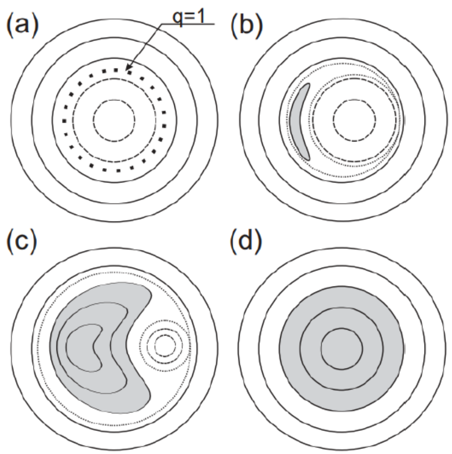

Sawtooth Crashes seen on all tokamaks (T_e perturbations)

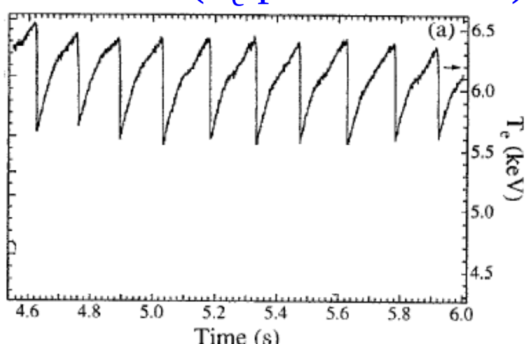

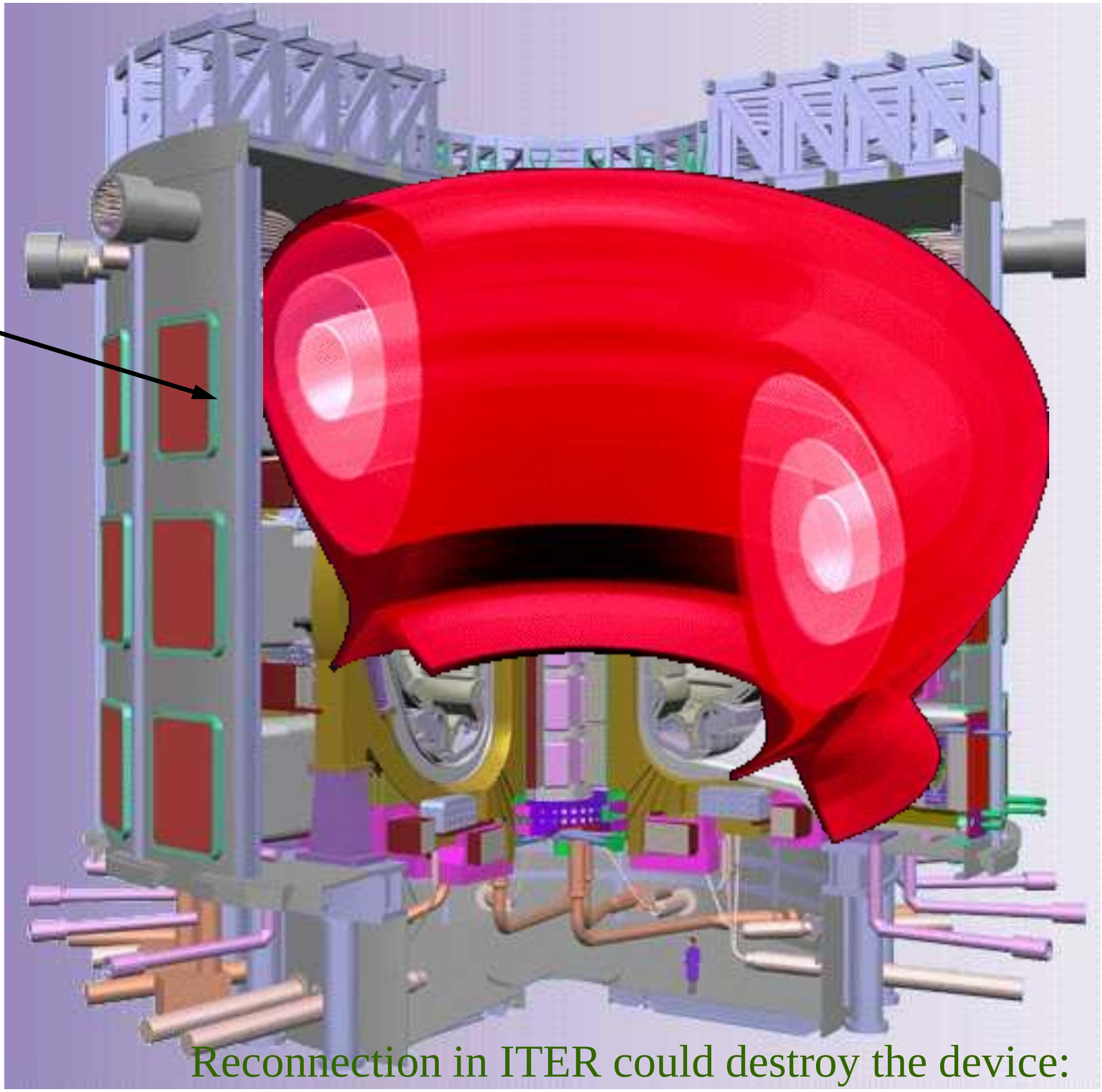

Reconnection in ITER could destroy the device:

Plasma in a Magnetic Field

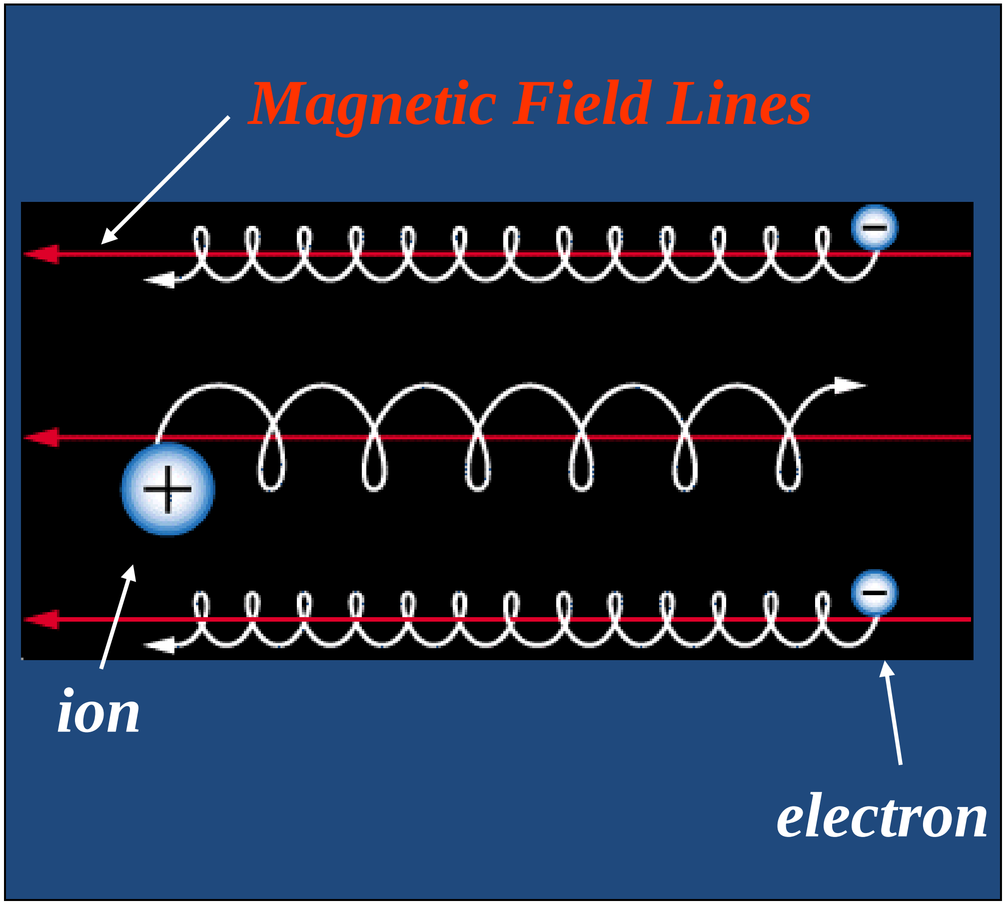

- *The plasma feels a force from the magnetic field*
- *Ions and electrons follow the field lines*
- *Plasmas are highly conductive*
- *Heliosphere like a conductive fluid of liquid copper*

Electromagnetism 101

- *Faraday's law:*

$$EMF = -Area \cdot \frac{dB}{dt}$$

- *Faraday's law for a conducting ring: EMF=0.*

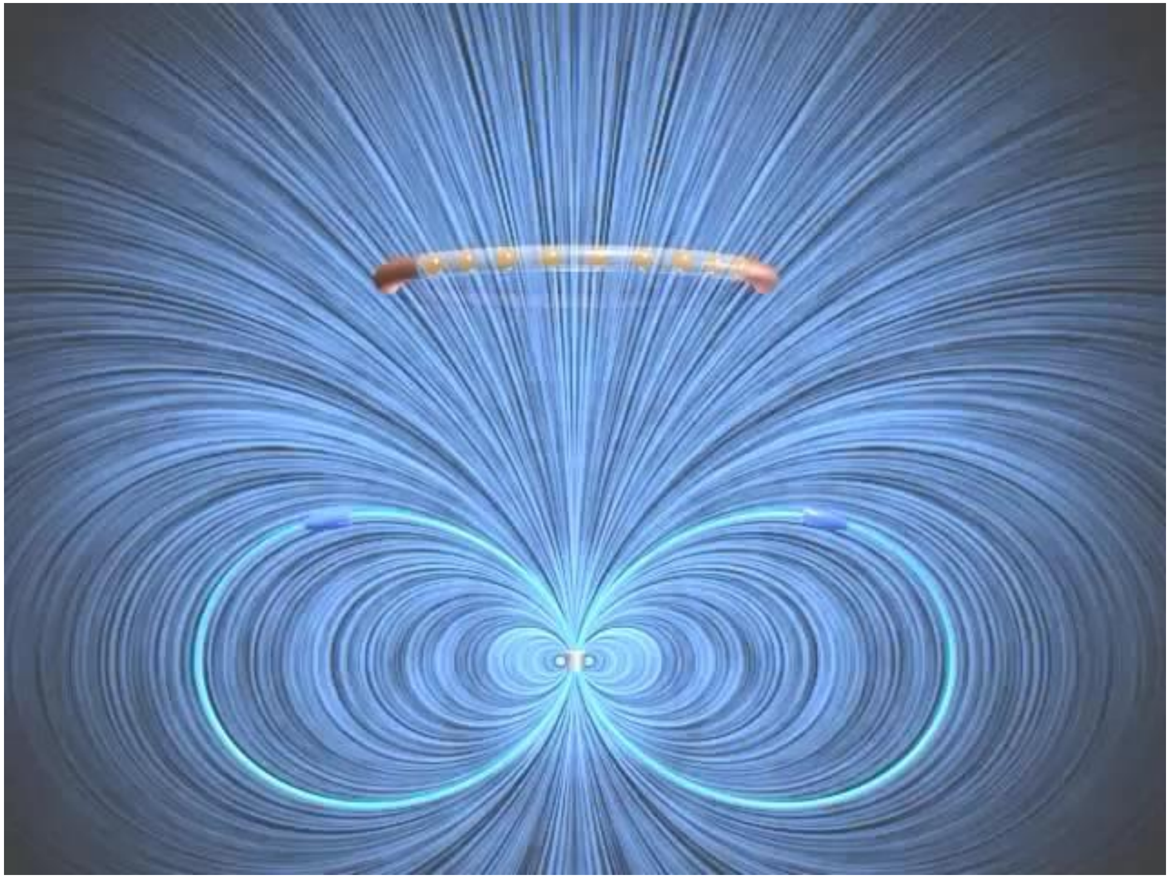

Electromagnetism 101

- *Faraday's law:*

$$EMF = -Area \cdot \frac{dB}{dt}$$

- *Faraday's law for a conducting ring: EMF=0.*
- *The magnetic flux through the ring is trapped*
- *This also holds if the ring is made of plasma*

➔ *plasma frozen in condition*

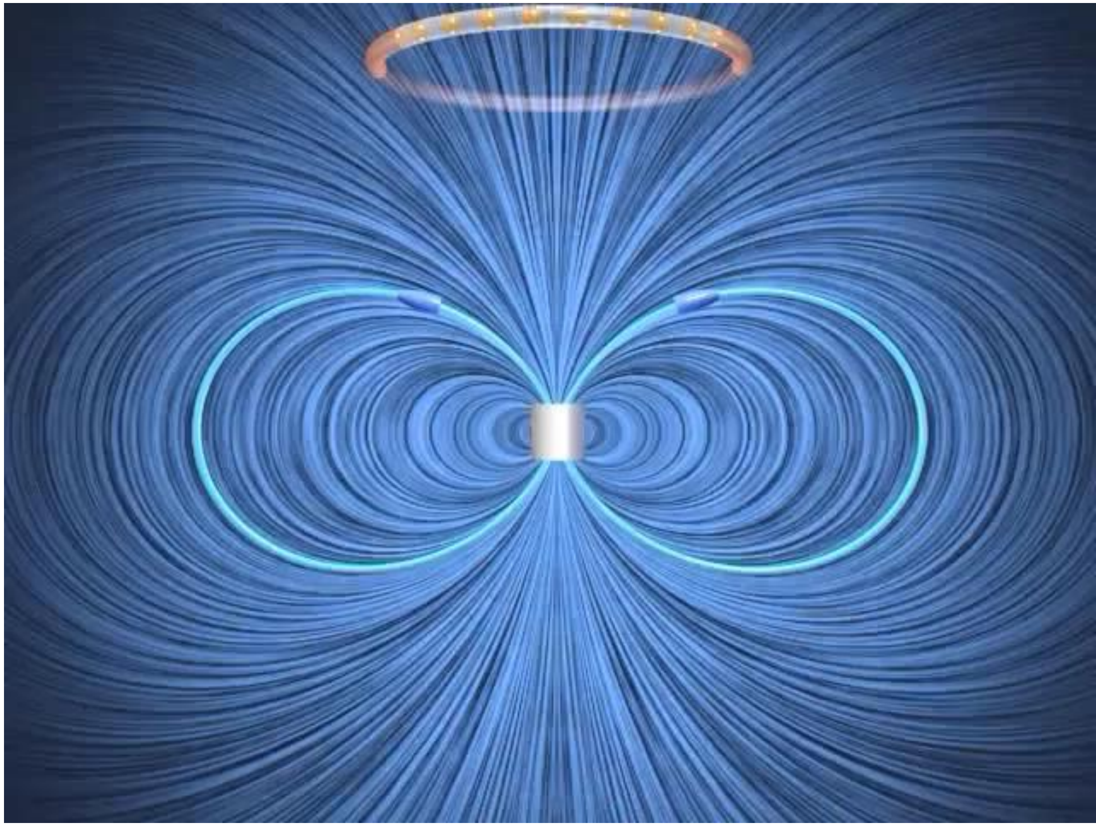

Magnetic topology constant in Ideal plasmas

– Ideal Plasma $\mathbf{E}' = \mathbf{E} + \mathbf{v} \times \mathbf{B} = 0$ ➔ Plasma and B frozen together

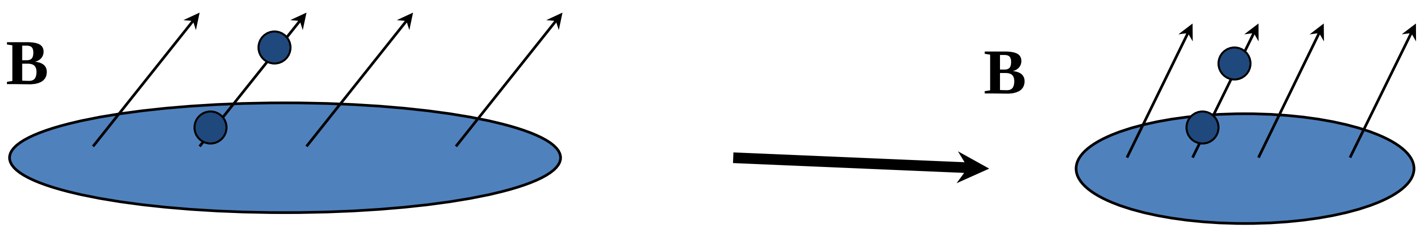

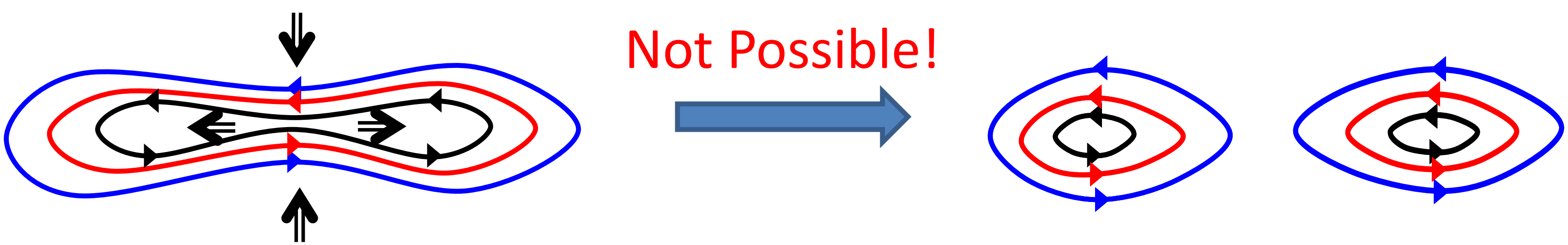

Resistive effects can be important

- *Faraday's law:*

$$EMF = -Area \cdot \frac{dB}{dt}$$

- *Faraday's law for a conducting ring: EMF=0.*
- *The magnetic flux through the ring is trapped*
- *This also holds if the ring is made of plasma*

➔ *plasma frozen in condition*

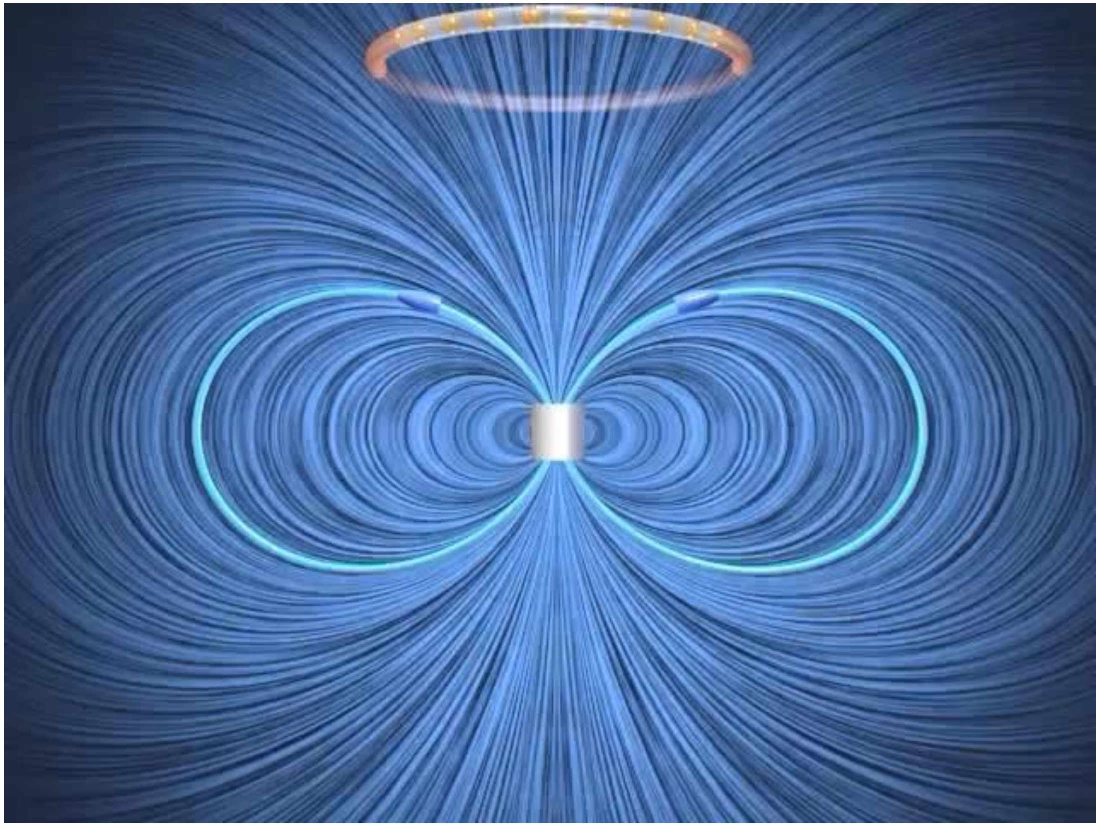

However, the field can go through a resistive ring!

Reconnection: A Long Standing Problem

Simplest model for reconnection:

$\mathbf{E} + \mathbf{v}\times\mathbf{B} = \eta\mathbf{j}$ [*Sweet-Parker* (1957)]

$$-\left.\frac{\partial\Psi}{\partial t}\right|_X = E_X = \eta j_x$$

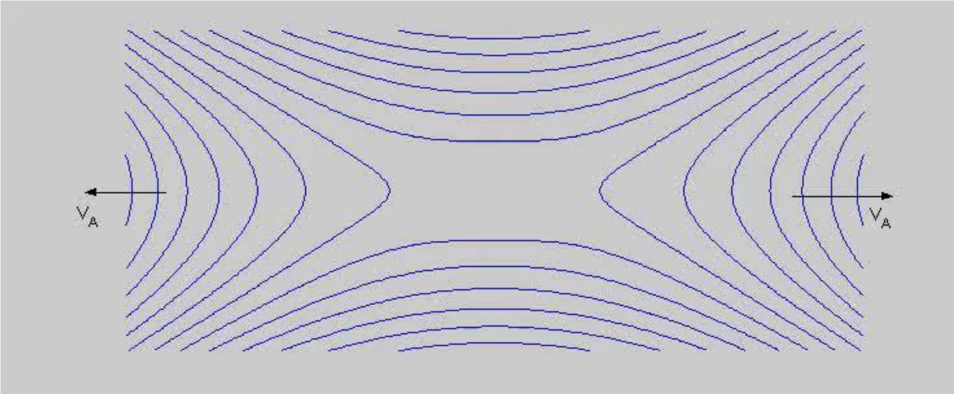

Reconnection: A Long Standing Problem

WiPPL

Simplest model for reconnection:

$\mathbf{E} + \mathbf{v}\times\mathbf{B} = \eta\mathbf{j}$ [*Sweet-Parker* (1957)]

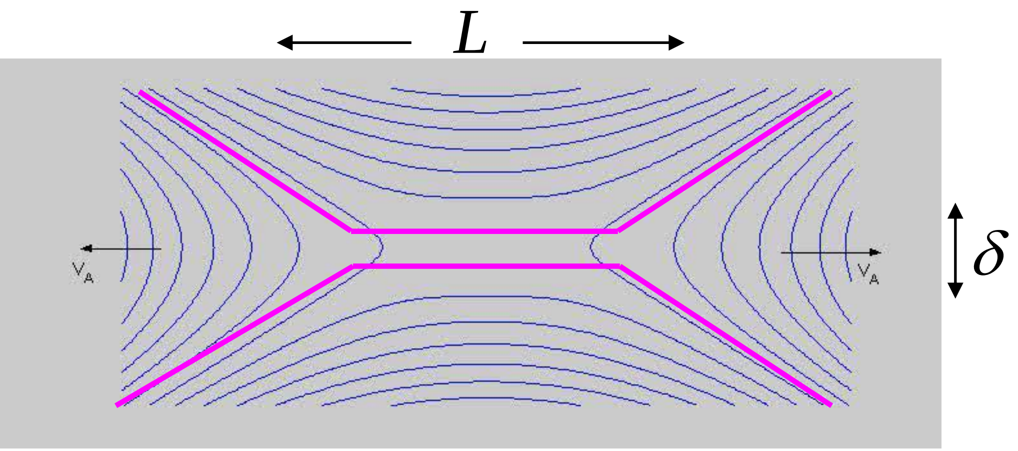

Outflow speed:

$$v_A = \frac{B}{\sqrt{\mu_0 n m_i}}$$

(Alfven speed)

Sweet-Parker: L >>δ:

$$t_{sp} = \sqrt{t_R t_A} = \sqrt{\frac{\mu_0 L^2}{\eta}}\sqrt{\frac{L}{v_A}}$$

Unfavorable for fast reconnection

Two months for a coronal mass ejections

Plasma Kinetic Description

The collisionless Vlasov equation:

$$\left(\frac{\partial}{\partial t} + \mathbf{v}\ \frac{d}{dt} f_j(\mathbf{x}, \mathbf{v}, t) = 0\ )\cdot \nabla_v\right) f_j = 0$$

$$n_j = \int f_j d^3 v \qquad\qquad \mathbf{J}_j = q_j \int \mathbf{v} f_j d^3 v$$

$+$ Maxwell's eqs.

Vlasov-Maxwell system of equations

Can be solved numerically (PIC-codes)

Fluid Formulation (Conservation Laws)

mass:

$$\frac{\partial n}{\partial t} + \frac{\partial (n u_j)}{\partial x_j} = 0,$$

momentum:

$$mn\left(\frac{\partial u_j}{\partial t} + u_k \frac{\partial u_j}{\partial x_k}\right) + \boxed{\frac{\partial \mathsf{P}_{jk}}{\partial x_k}} \overbrace{- en(E_j + \epsilon_{jkl} u_k B_l) - F_j^{\mathrm{coll}}}^{\text{Sweet-Parker}} = 0,$$

energy:

$$\cancel{\frac{\partial \mathsf{P}_{jk}}{\partial t} + \frac{\partial}{\partial x_l}(\mathsf{P}_{jk} u_l + \boxed{\mathsf{Q}_{jkl}}) + \frac{\partial u_{[j}}{\partial x_l}\mathsf{P}_{lk]} - \frac{e}{m}\epsilon_{[jlm} B_m \mathsf{P}_{lk]} - \mathsf{G}_{jk}^{\mathrm{coll}} = 0}$$

$$\vdots$$

Isotropic (scalar) pressure is the standard closure!

$$p = n\,T$$

Add Maxwell's eqs to complete the fluid model

Two-Fluid Simulation

GEM challenge (Hall reconnection)

$\mathbf{E} + \mathbf{v}\times\mathbf{B} = (\mathbf{j} \times \mathbf{B})/ne$ [Birn,… Drake, et al. (2001)]

Out of plane current

Isotropic pressure

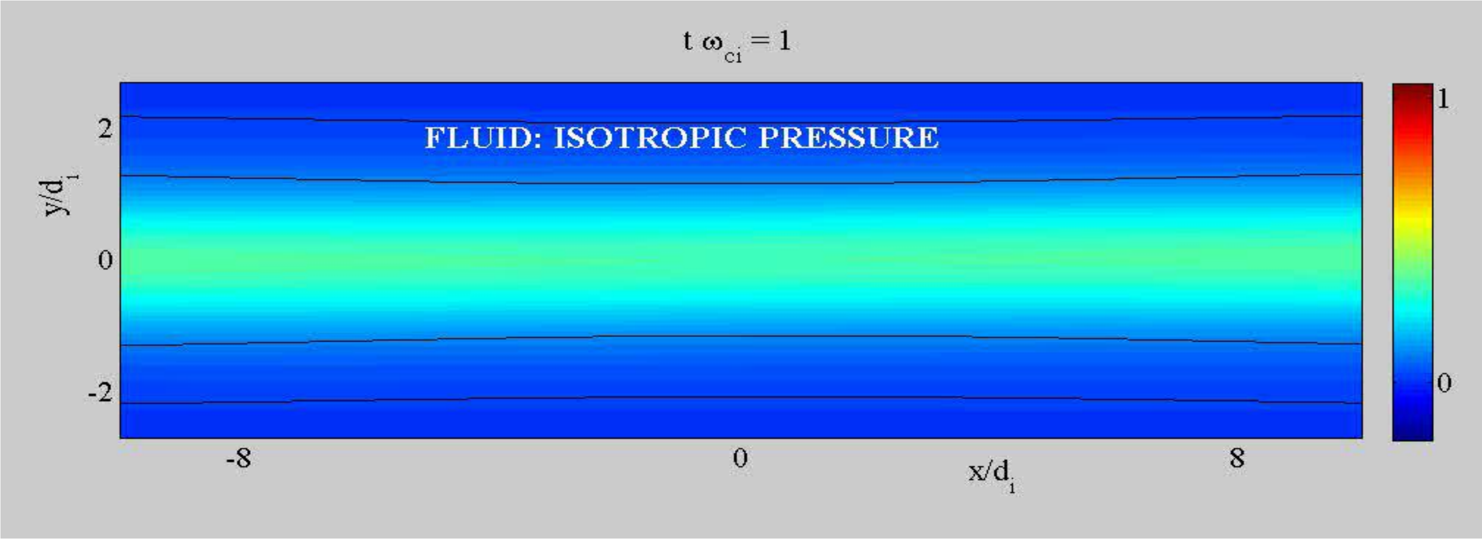

Two-Fluid Simulation

GEM challenge (Hall reconnection)

$\mathbf{E} + \mathbf{v}\times\mathbf{B} = (\mathbf{j}\times\mathbf{B})/ne$ [Birn,… Drake, et al. (2001)]

Out of plane current

Isotropic pressure

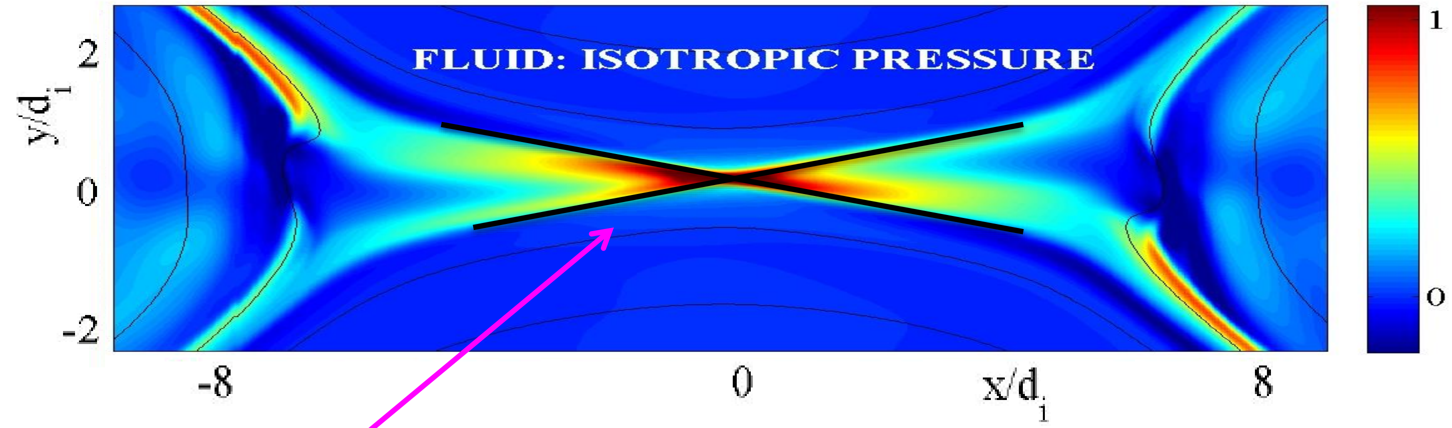

Aspect ratio: 1 / 10

➔ $v_{in} \sim v_A / 10$

Two-Fluid Simulation

GEM challenge (Hall reconnection)

$\mathbf{E} + \mathbf{v}\times\mathbf{B} = (\mathbf{j}\times\mathbf{B})/ne$ [Birn,… Drake, et al. (2001)]

Out of plane current

Isotropic pressure

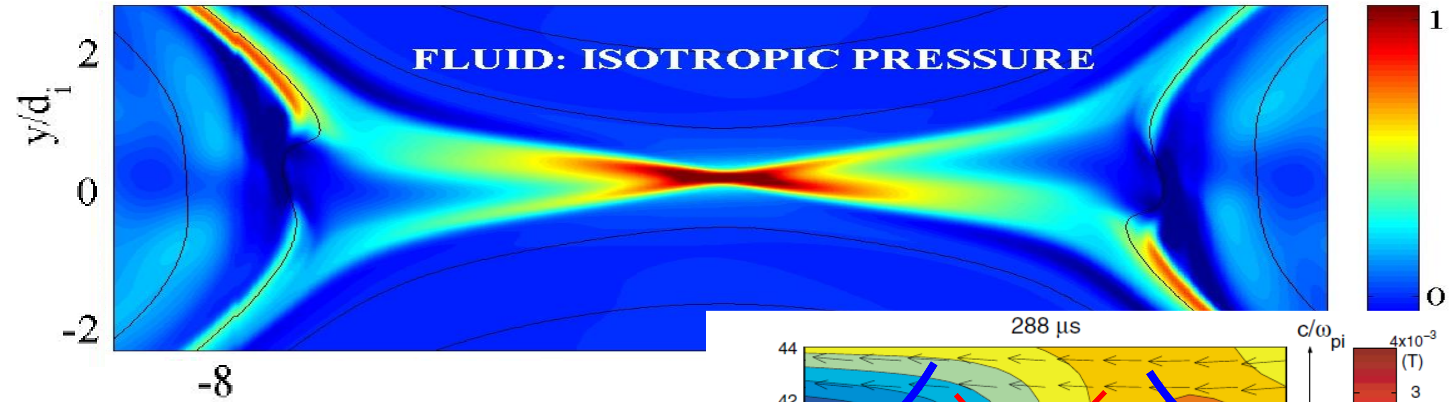

The Hall term is associated with quadrupolar out of plane fields, as observed in the Magnetic Reconnection Experiment (MRX) [Ren, PRL, 2005]

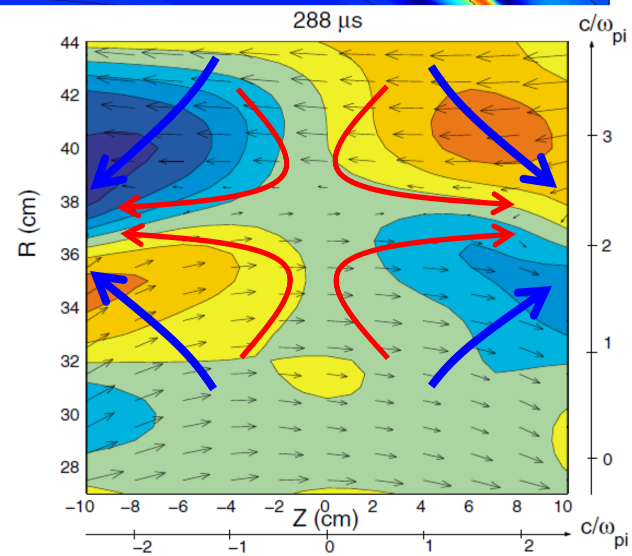

Mechanism for Electron Heating

Fermi heating in contracting magnetic island [Drake et al., 2006]

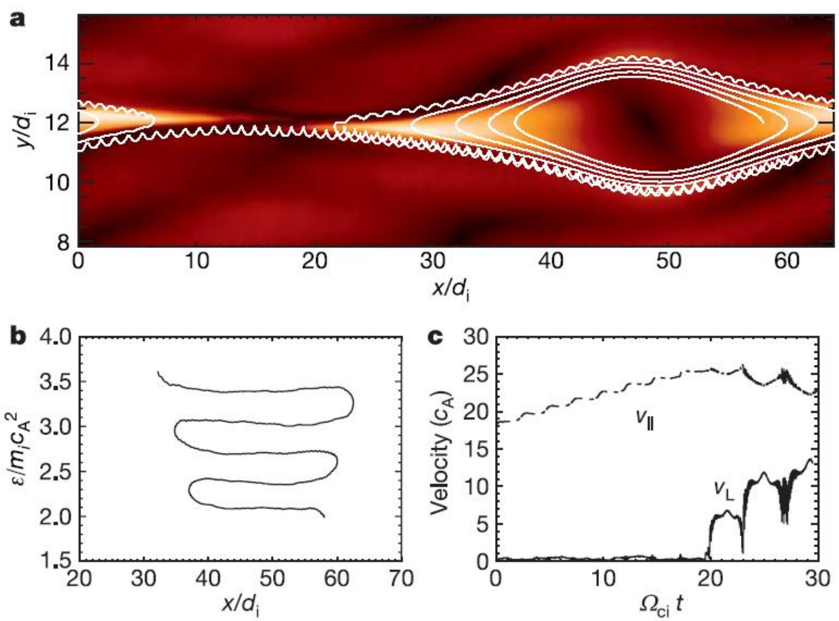

But often reconnection is embedded in an open system:

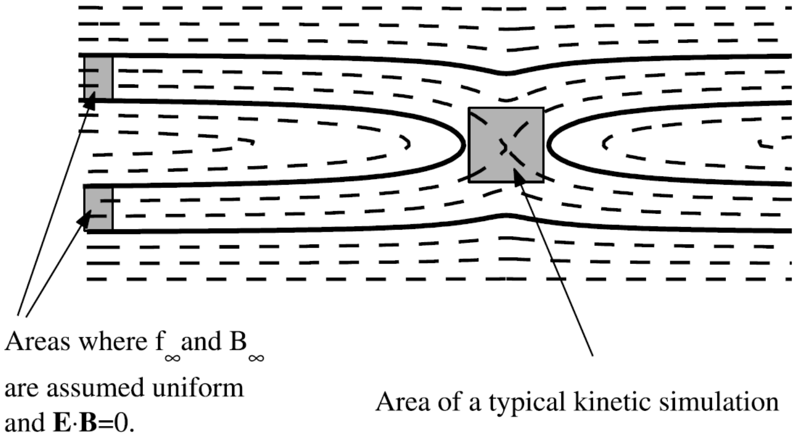

Fresh electrons streaming in from the ambient plasma sets the form of the electron distribution function.

[Egedal et al. 2008]

With $v_{the} >> v_A$ we may expect Boltzman electrons with T_e = constant. [Snyder+ 1997]

Electrons Trapped by $\Phi_{\|}$, $B_g = 0.4$

$$\Phi_{\|}(\mathbf{x}) = \int_{\mathbf{x}}^{\infty} \mathbf{E} \cdot d\mathbf{l}$$

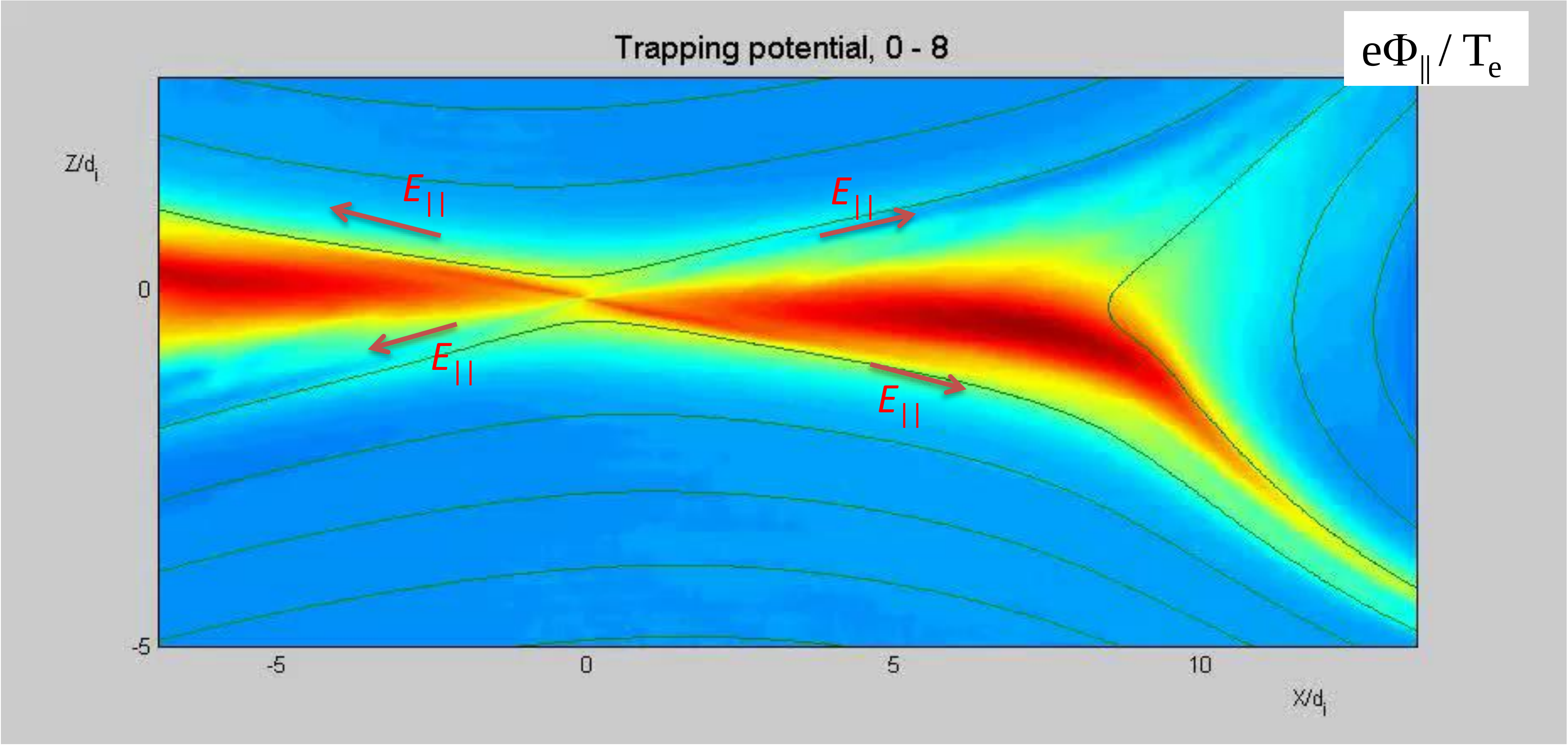

Electrons Trapped by $\Phi_{||}$, $B_g = 0.4$

When / where trapping dominates
➔ Zero Heat Flux:
➔ CGL-scaling laws

$$\boxed{p_{||} \propto \frac{n^3}{B^2}, \quad p_\perp \propto nB}$$

$$\Phi_{||}(\mathbf{x}) = \int_{\mathbf{x}}^{\infty} \mathbf{E} \cdot d\mathbf{l}$$

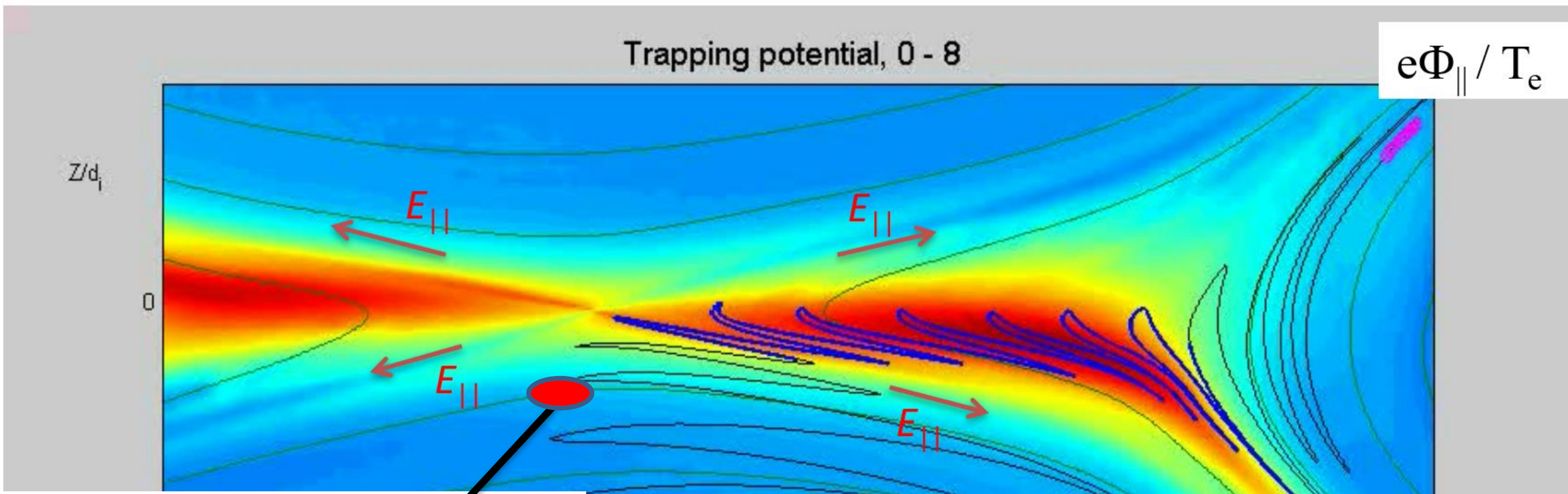

[Øieroset, 2001]

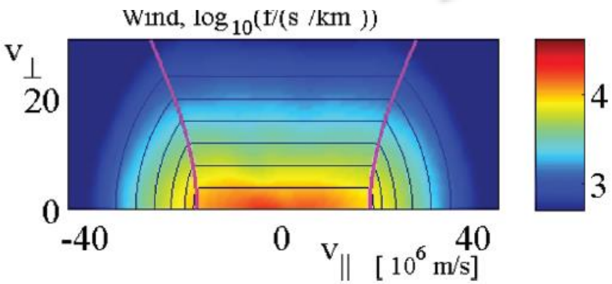

Drift kinetic model with m_i/m_e ➔ ∞

$$\bar{f}_0(\mathcal{E}_{||}, \mathcal{E}_\perp) = \begin{cases} \bar{f}_\infty(\mu B_\infty), & \text{trapped} \\ \bar{f}_\infty(\mathcal{E} - e\Phi_{||}), & \text{passing.} \end{cases}$$

[Egedal, et al., 2005, 2007, 2013]

The Magnetosphere as a Laboratory

MMS, Launched
March 12, 2015.

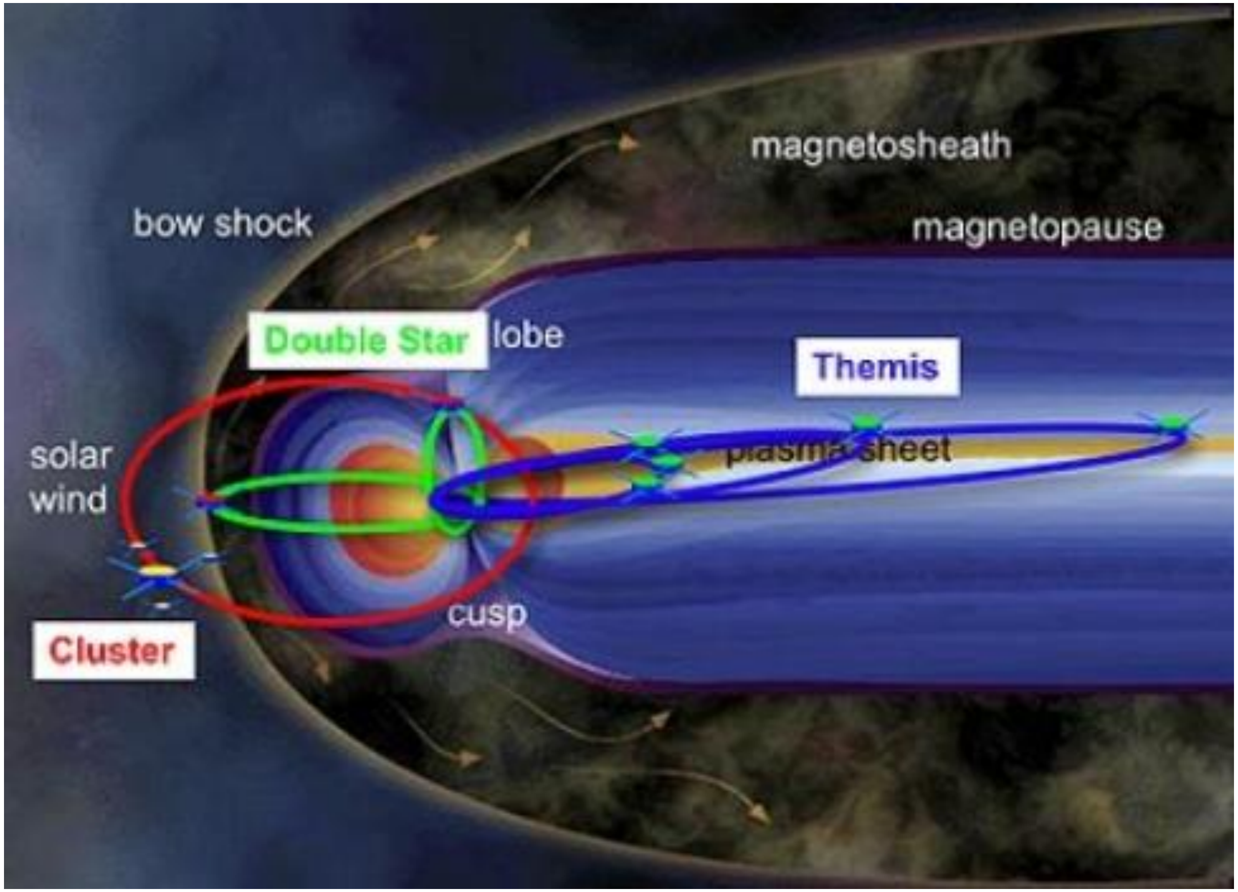

Model Tested Against MMS data

[Øieroset, GRL, 2016], $B_g \sim 2.5\,B_r$

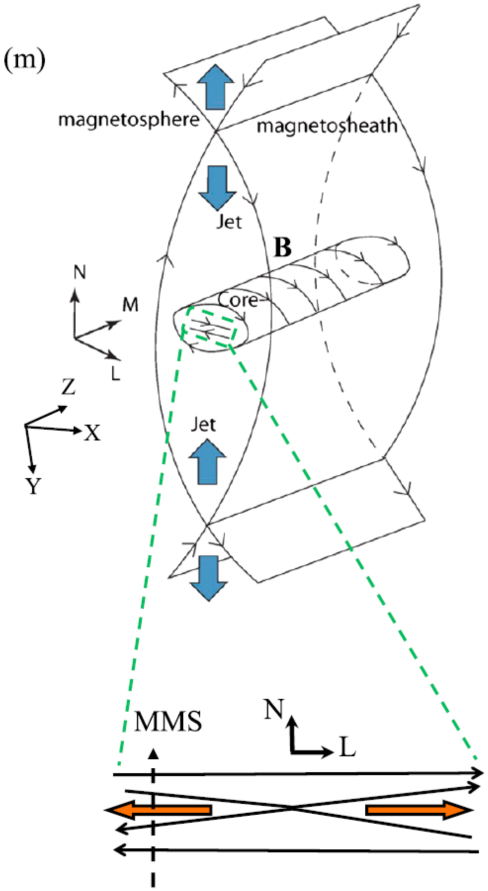

$L \sim 10\,d_i$

Model Tested Against MMS data

[Øieroset, GRL, 2016], $B_g \sim 2.5\, B_r$

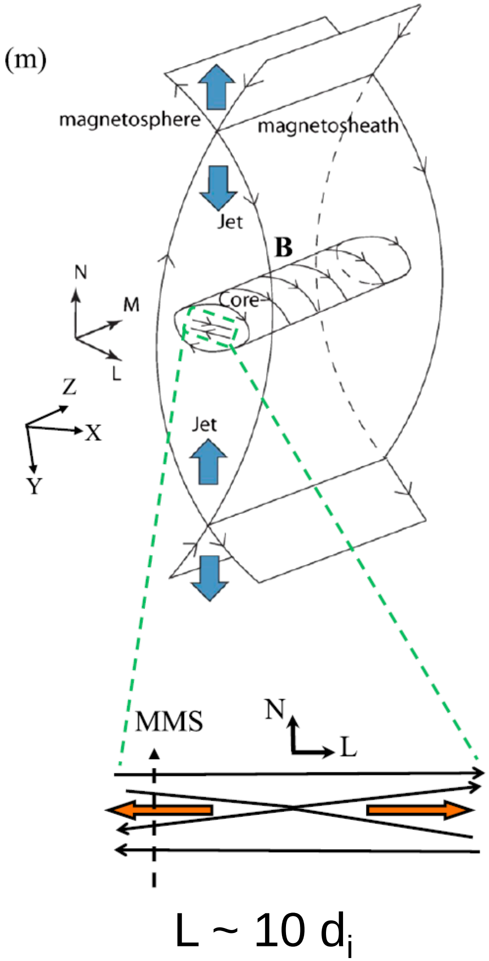

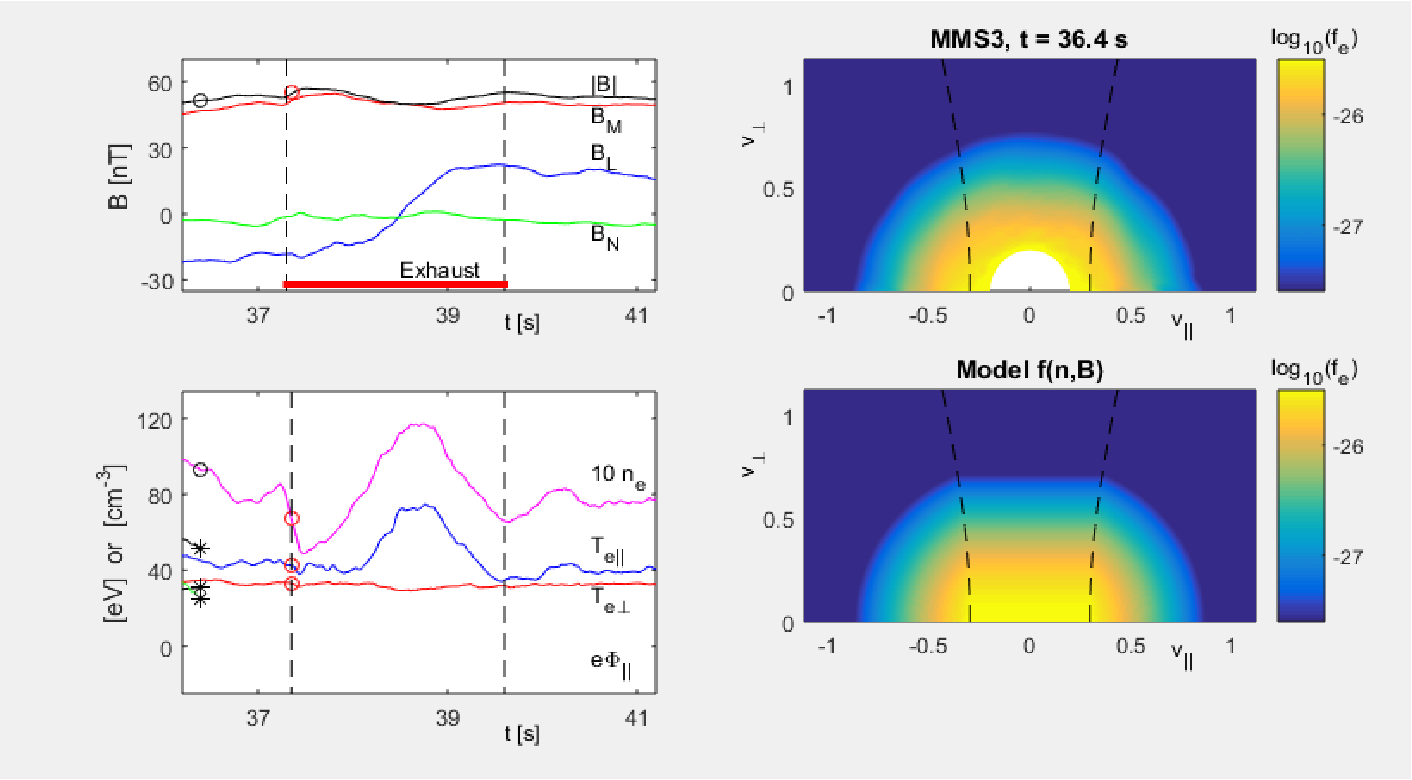

$$f(\mathbf{x}, \mathbf{v}) = \begin{cases} f_\infty(\mathcal{E} - e\Phi_{\|}) & , \text{ passing} \\ f_\infty(\mu B_\infty) & , \text{ trapped} \end{cases}$$

Fit to match $n(t)$

EoS Confirmed by MMS

[Wetherton, GRL, 2019],

Model parameterized in Le et al., PRL 2009

Boltzmann *CGL*

$$\bar{\mathbf{P}} = p_i\bar{\mathbf{I}} + \bar{\mathbf{P}}_e = p_i\bar{\mathbf{I}} + p_\perp\bar{\mathbf{I}} + (p_\parallel - p_\perp)\frac{\mathbf{BB}}{B^2},$$

$$\tilde{p}_\parallel = \tilde{n}\frac{2}{2+\alpha} + \frac{\pi\tilde{n}^3}{6\tilde{B}^2}\frac{2\alpha}{2\alpha+1},$$

$$\tilde{p}_\perp = \tilde{n}\frac{1}{1+\alpha} + \tilde{n}\tilde{B}\frac{\alpha}{\alpha+1}.$$

Here, $\alpha = \tilde{n}^3/\tilde{B}^2$ and $\tilde{Q} = Q/Q_\infty$

Anisotropic pressure model

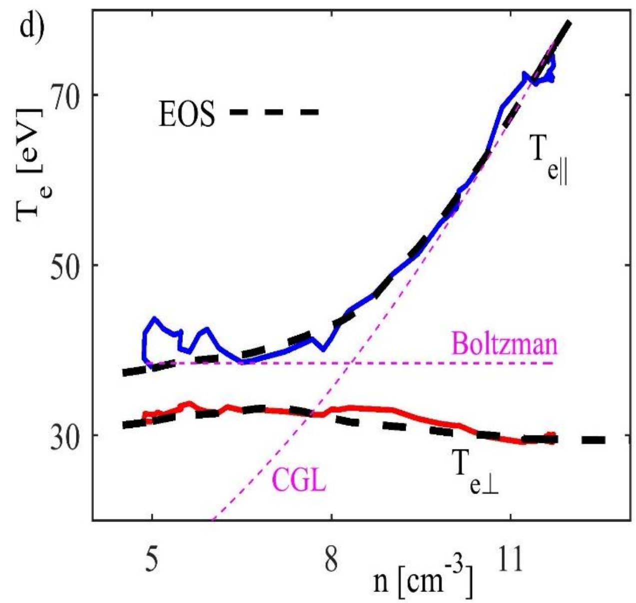

CGL limit
$n \gg n_0$ ➔

$$p_\parallel \propto \frac{n^3}{B^2}$$

$$p_\perp \propto nB$$

EoS Implemented in Two-Fluid Code

WiPPL

- *EoS* implemented by O Ohia using the HiFi framework developed in part by VS Lukin

Model parameterized in Le et al., PRL 2009

Boltzmann CGL

$$\bar{\mathbf{P}} = p_i \bar{\mathbf{I}} + \bar{\mathbf{P}}_e = p_i \bar{\mathbf{I}} + p_\perp \bar{\mathbf{I}} + (p_\parallel - p_\perp) \frac{\mathbf{BB}}{B^2},$$

$$\tilde{p}_\parallel = \tilde{n} \frac{2}{2+\alpha} + \frac{\pi \tilde{n}^3}{6\tilde{B}^2} \frac{2\alpha}{2\alpha+1},$$

$$\tilde{p}_\perp = \tilde{n} \frac{1}{1+\alpha} + \tilde{n}\tilde{B} \frac{\alpha}{\alpha+1}.$$

Here, $\alpha = \tilde{n}^3/\tilde{B}^2$ and $\tilde{Q} = Q/Q_\infty$

Anisotropic pressure model

$$\frac{\partial n}{\partial t} + \nabla \cdot (n\mathbf{V}_i) = 0$$

$$m_i n \left(\frac{\partial \mathbf{V}_i}{\partial t} + \mathbf{V}_i \cdot \nabla \mathbf{V}_i \right) = \mathbf{J} \times \mathbf{B} - \nabla \cdot \bar{\mathbf{P}} + m_i n \nu_i \nabla^2 \mathbf{V}_i$$

$$\frac{\partial}{\partial t} \left(\frac{p_i}{n^\Gamma} \right) = -\mathbf{V}_i \cdot \nabla \frac{p_i}{n^\Gamma}$$

$$\frac{\partial \mathbf{B}'}{\partial t} = -\nabla \times \mathbf{E}'$$

$$\mathbf{E}' + \mathbf{V}_i \times \mathbf{B} = \frac{1}{ne} \left(\mathbf{J} \times \mathbf{B}' - \nabla \cdot \bar{\mathbf{P}}_e \right) + \eta_R \mathbf{J} - \eta_H \nabla^2 \mathbf{J}$$

$$\mathbf{B}' = \left(1 - d_e^2 \nabla^2\right) \mathbf{B}$$

$$\mu_0 \mathbf{J} = \nabla \times \mathbf{B}$$

Standard two-fluid equations

Out of plane current

[Ohia et al., PRL, 2012]

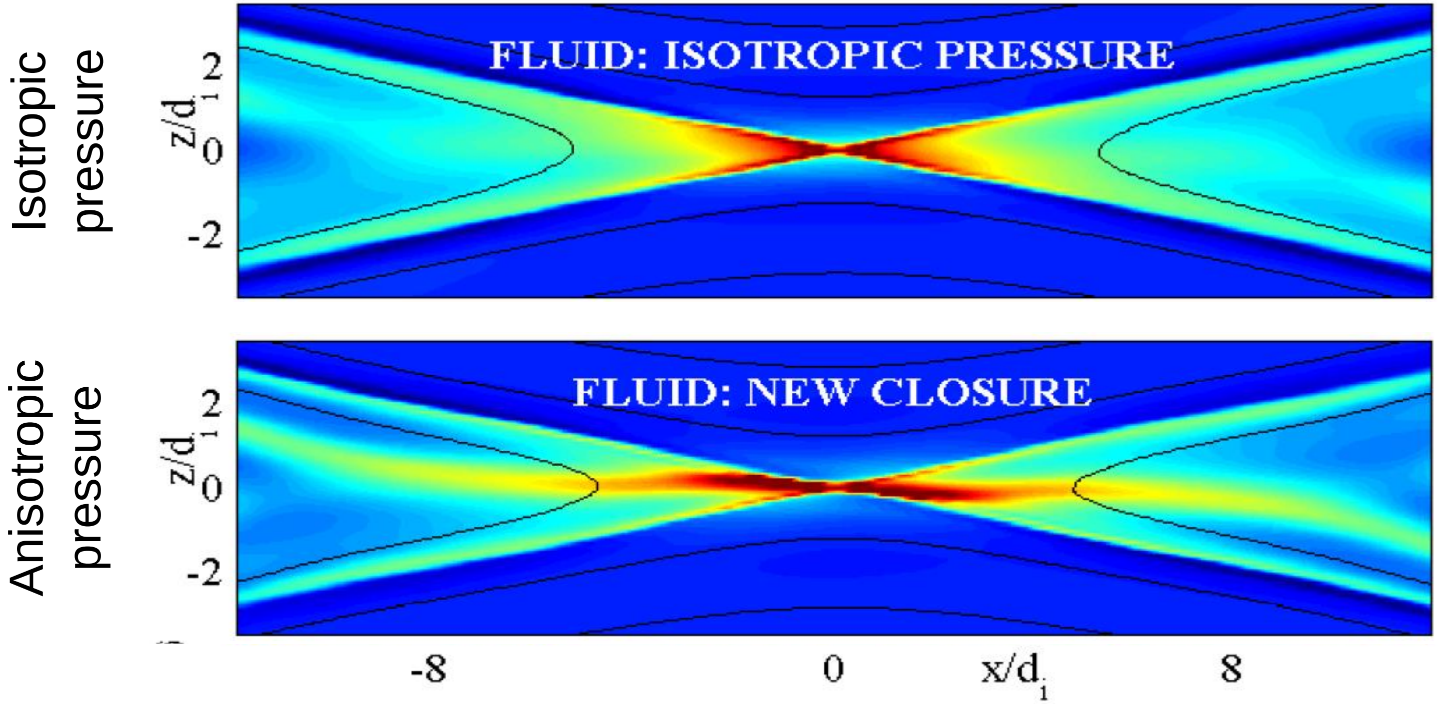

Embedded current layers for anisotropic electrons

Out of plane current

[Ohia et al., PRL, 2012]

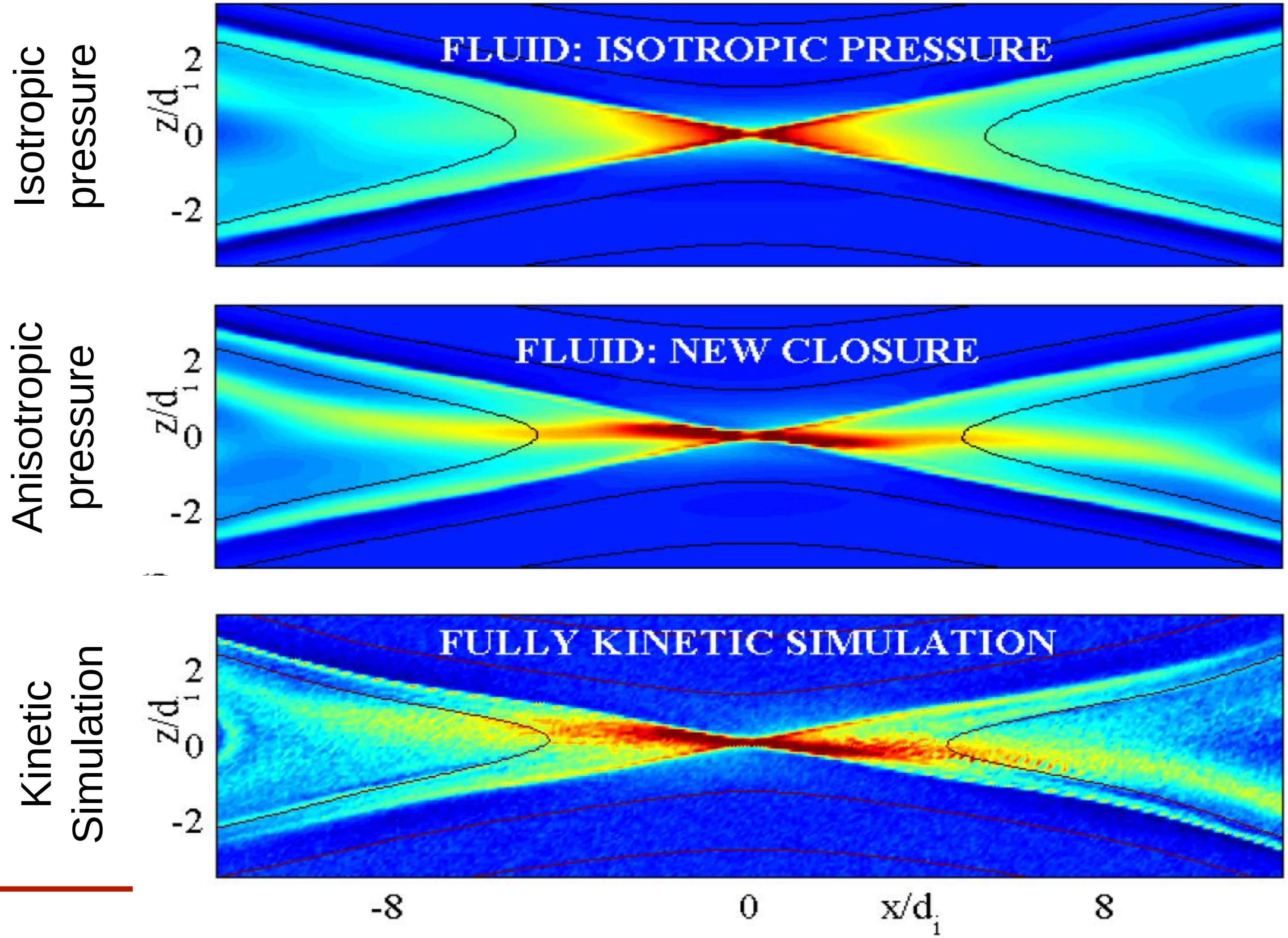

The WiPPL User Facility

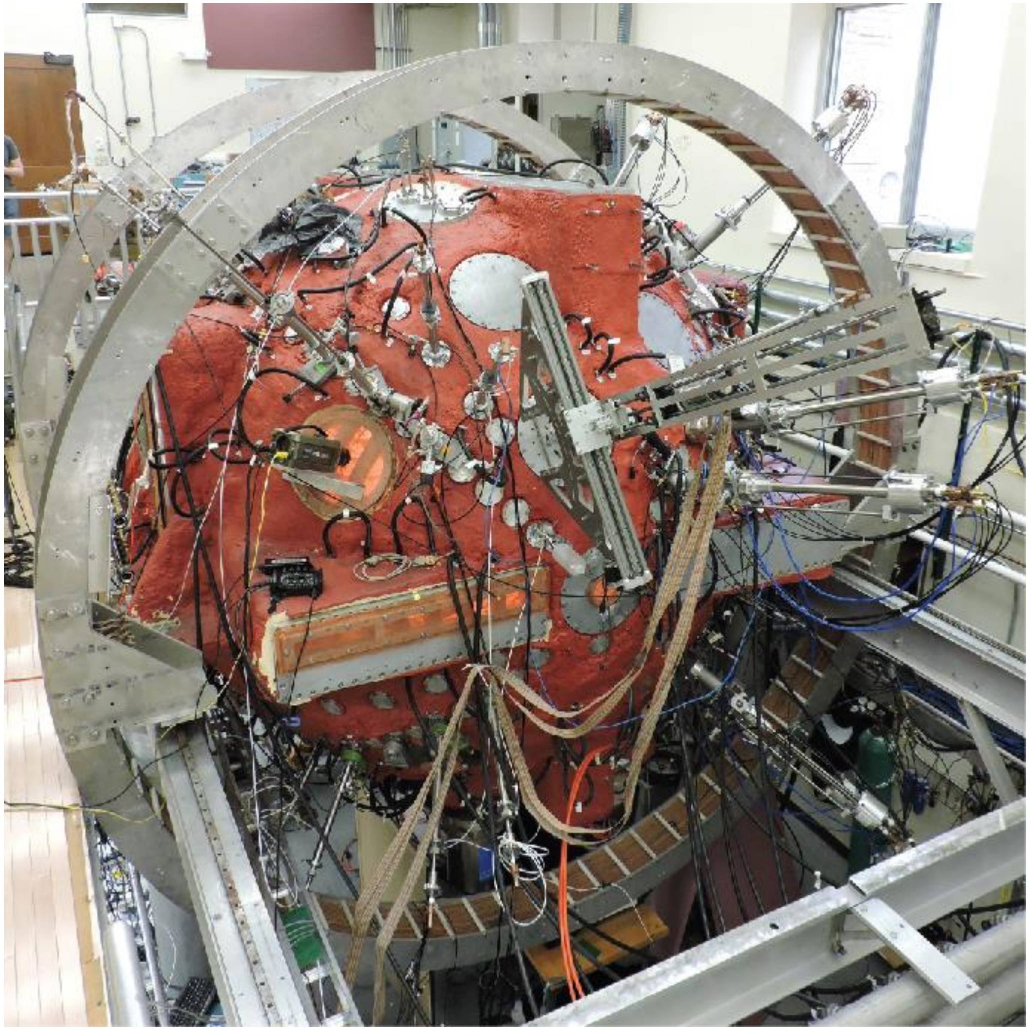

The BRB (Big Red Ball) is comprised of a 3m diameter vacuum vessel.

Highly flexible plasma sources and magnetic configurations are available.

Temperatures:	4 – 30 eV
Densities:	10^{18} – 10^{19} m^{-3}
Magnetic fields:	0 – 80 mT

The Terrestrial Reconnection Experiment (TREX) is one among several user configurations.

New Capabilities Continues to be Developed

New insert provides improved diagnostic access, as well as quick turn-around between experimental configurations

TREX implemented at the WiPPL user facility

Asymmetric reconnection is driven by 4 single turn internal drive coils, energized by capacitor bank at 10kV

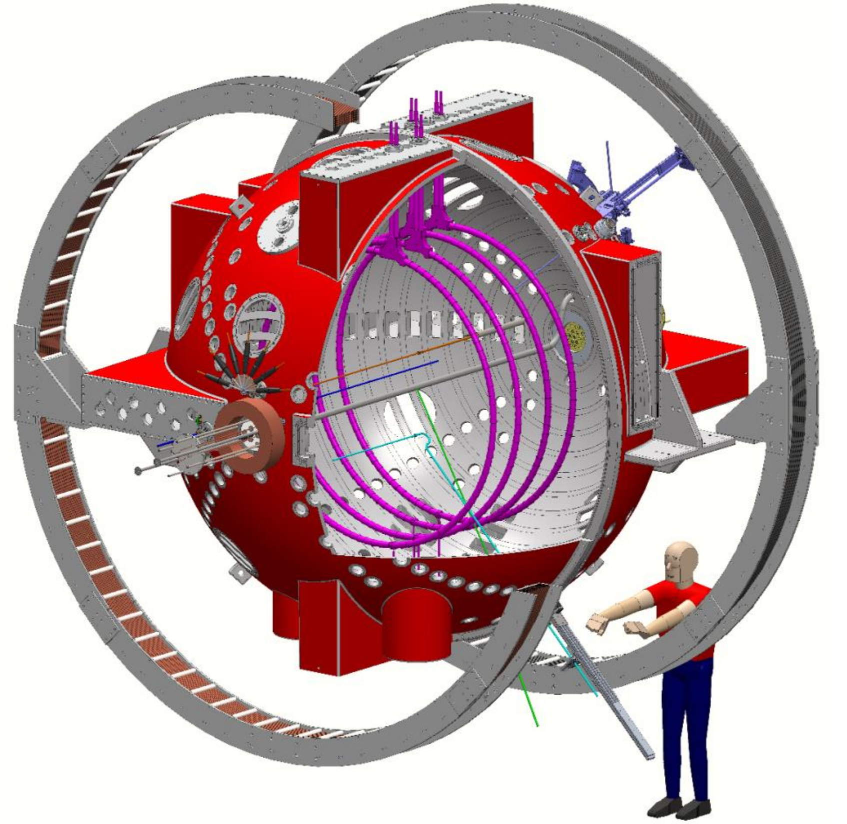

TREX implemented at the WiPPL user facility

Asymmetric reconnection is driven by 4 single turn internal drive coils, energized by capacitor bank at 10kV

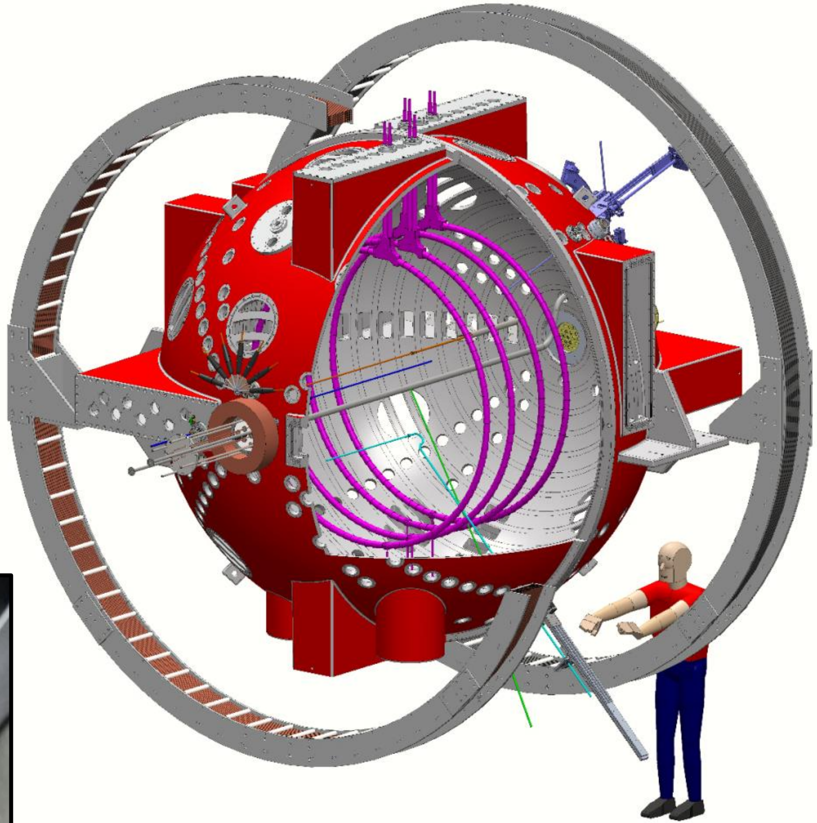

View during the TREX installation:

TREX implemented at the WiPPL user facility

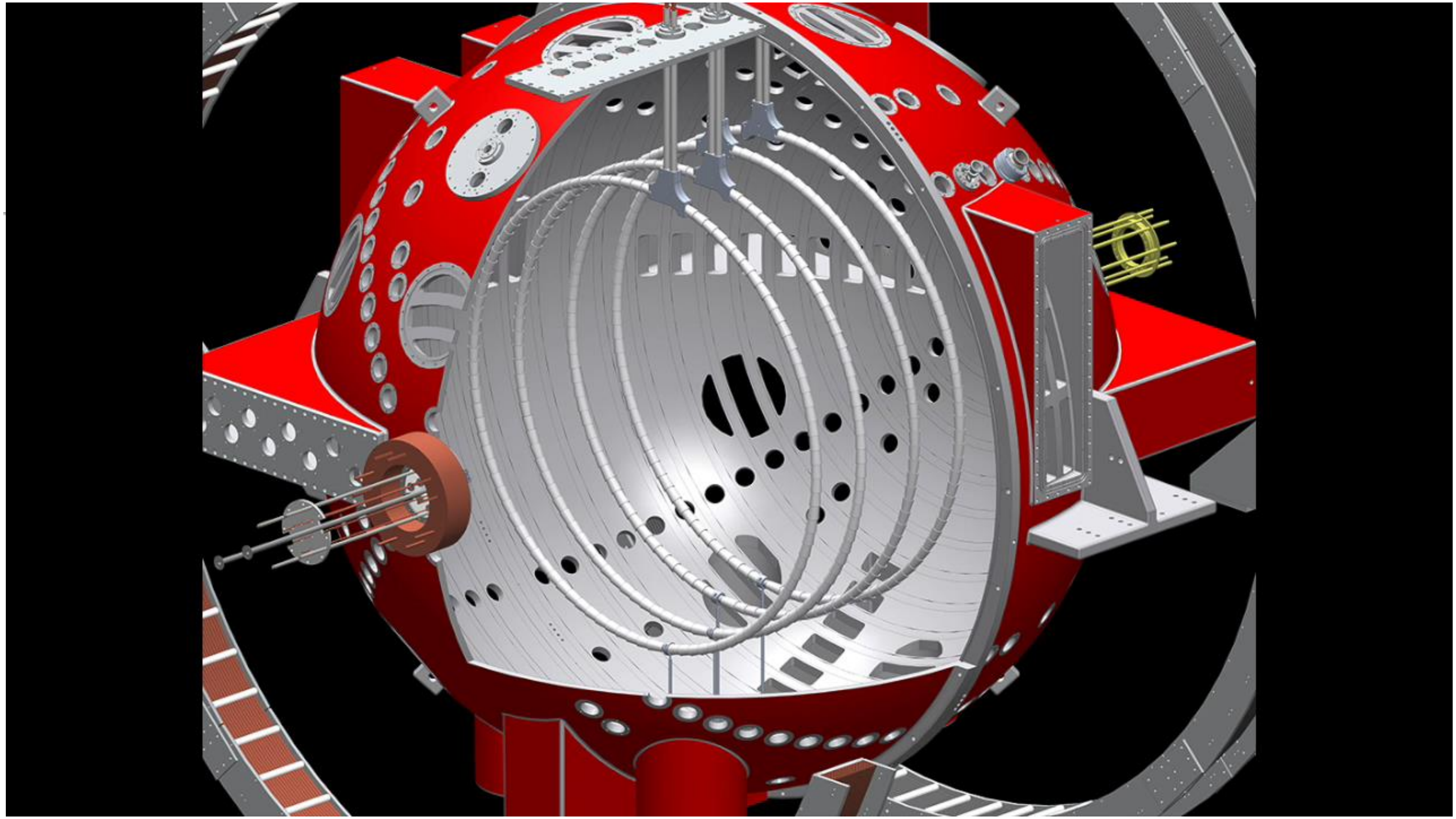

TREX Configuration in Cylindrical VPIC

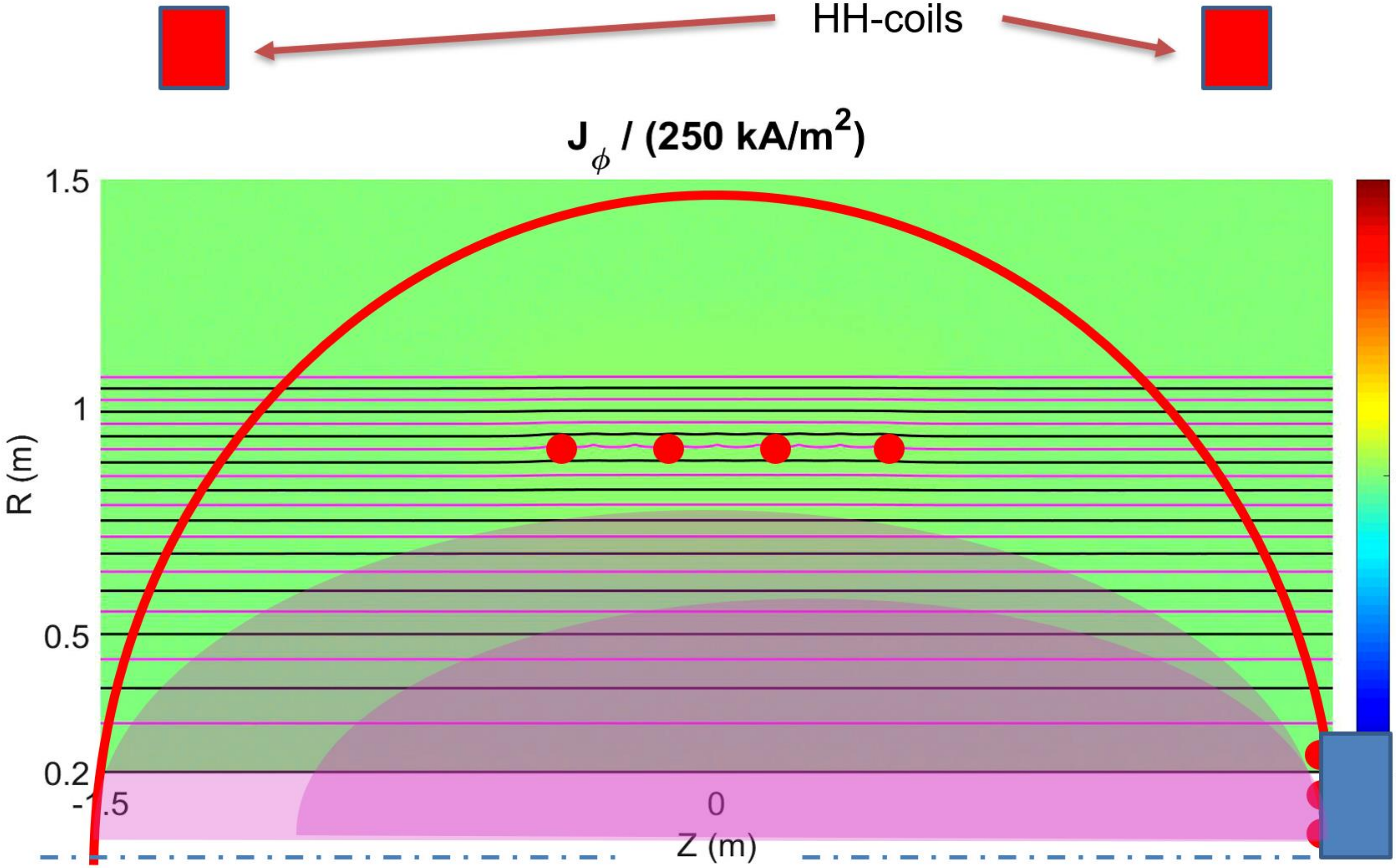

TREX Configuration in Cylindrical VPIC

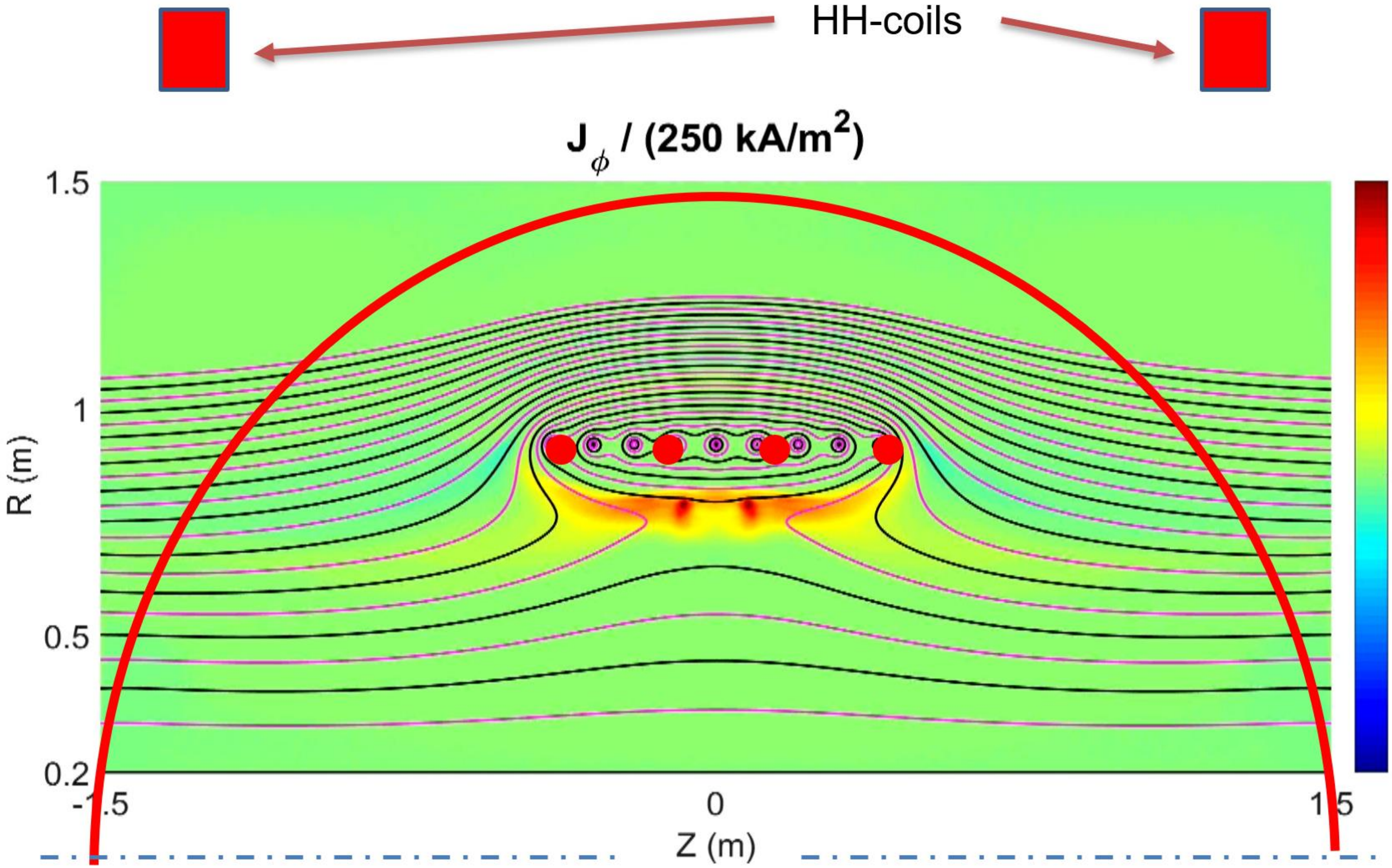

TREX Configuration in Cylindrical VPIC

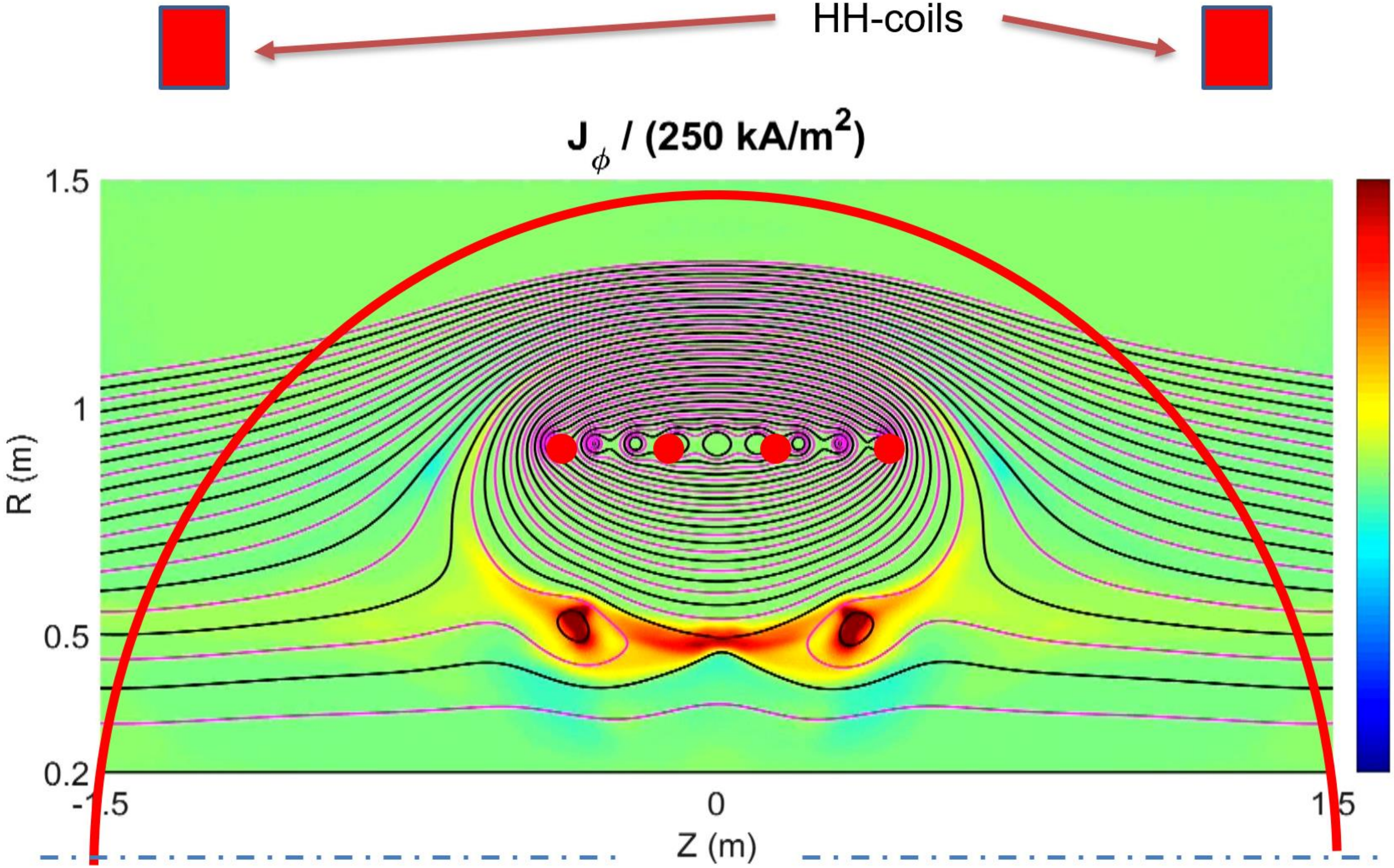

TREX Configuration in Cylindrical VPIC

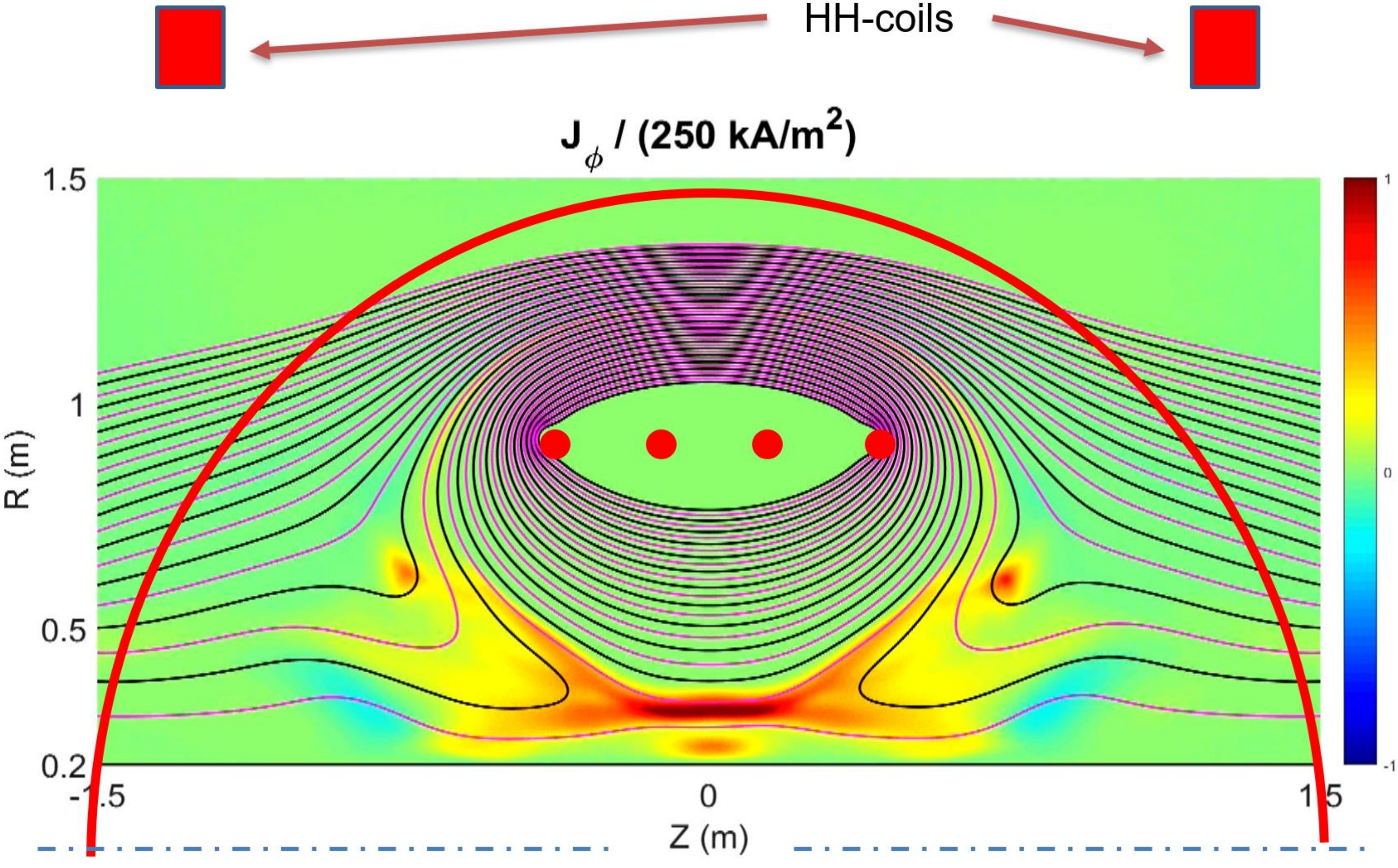

Visible light recorded by Phantom camera

The drive coils
are out of view

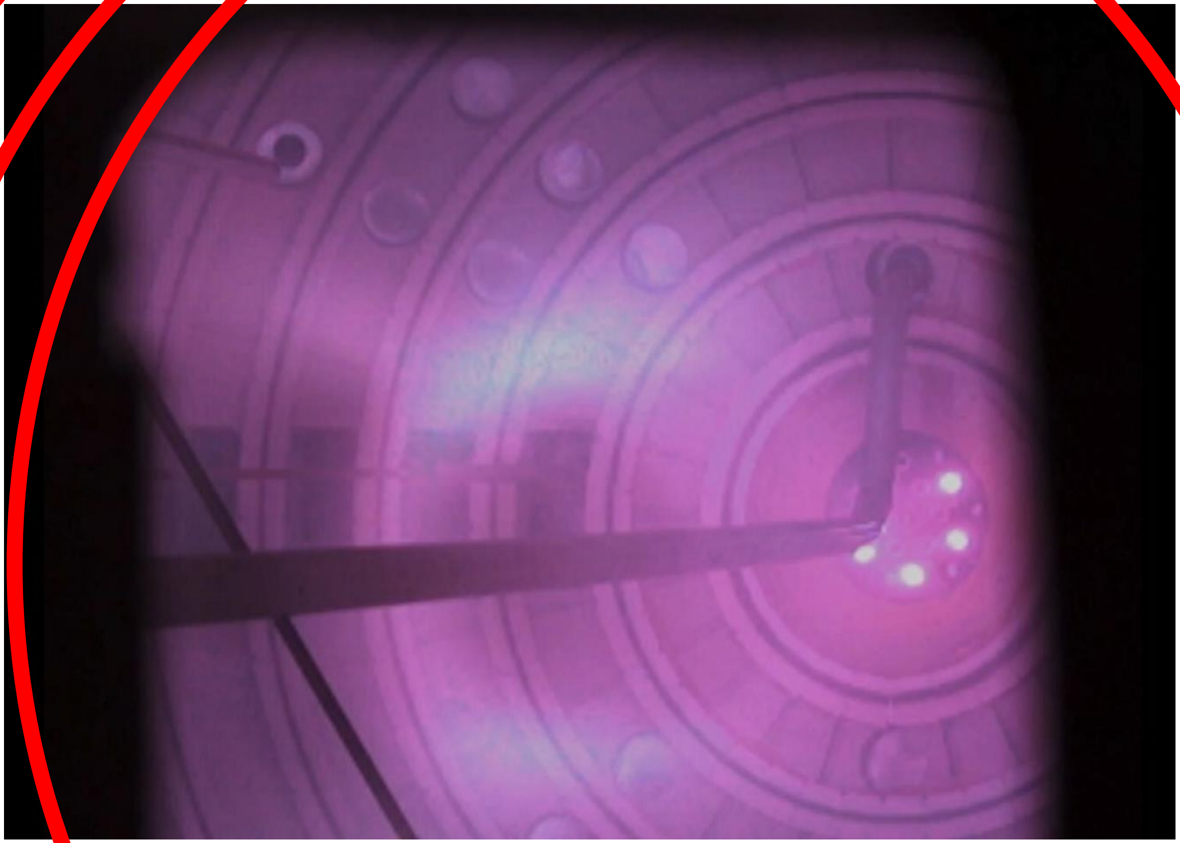

Visible light recorded by Phantom camera

Reconnection pulse last ~ 20μs,
One frame recorded per shot.

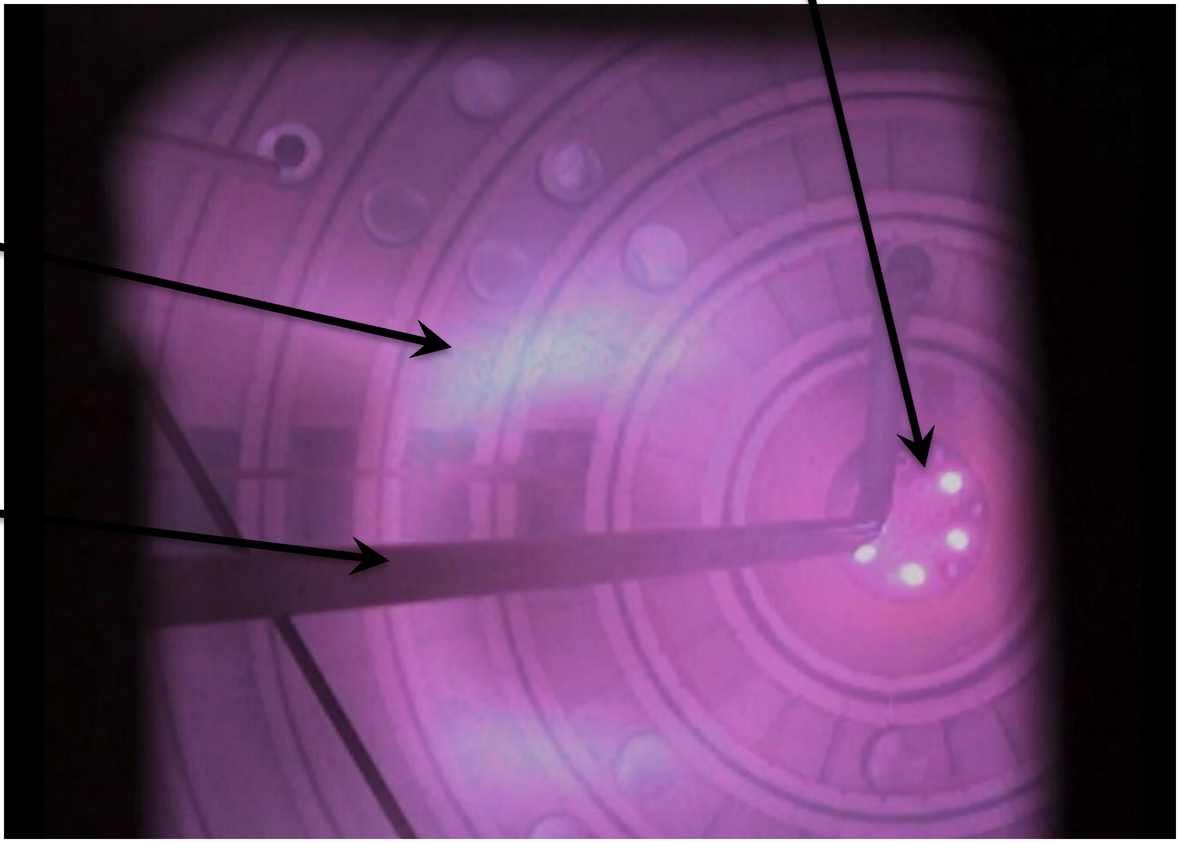

Visible light recorded by Phantom camera

Frames combined from ~ 50 shots.

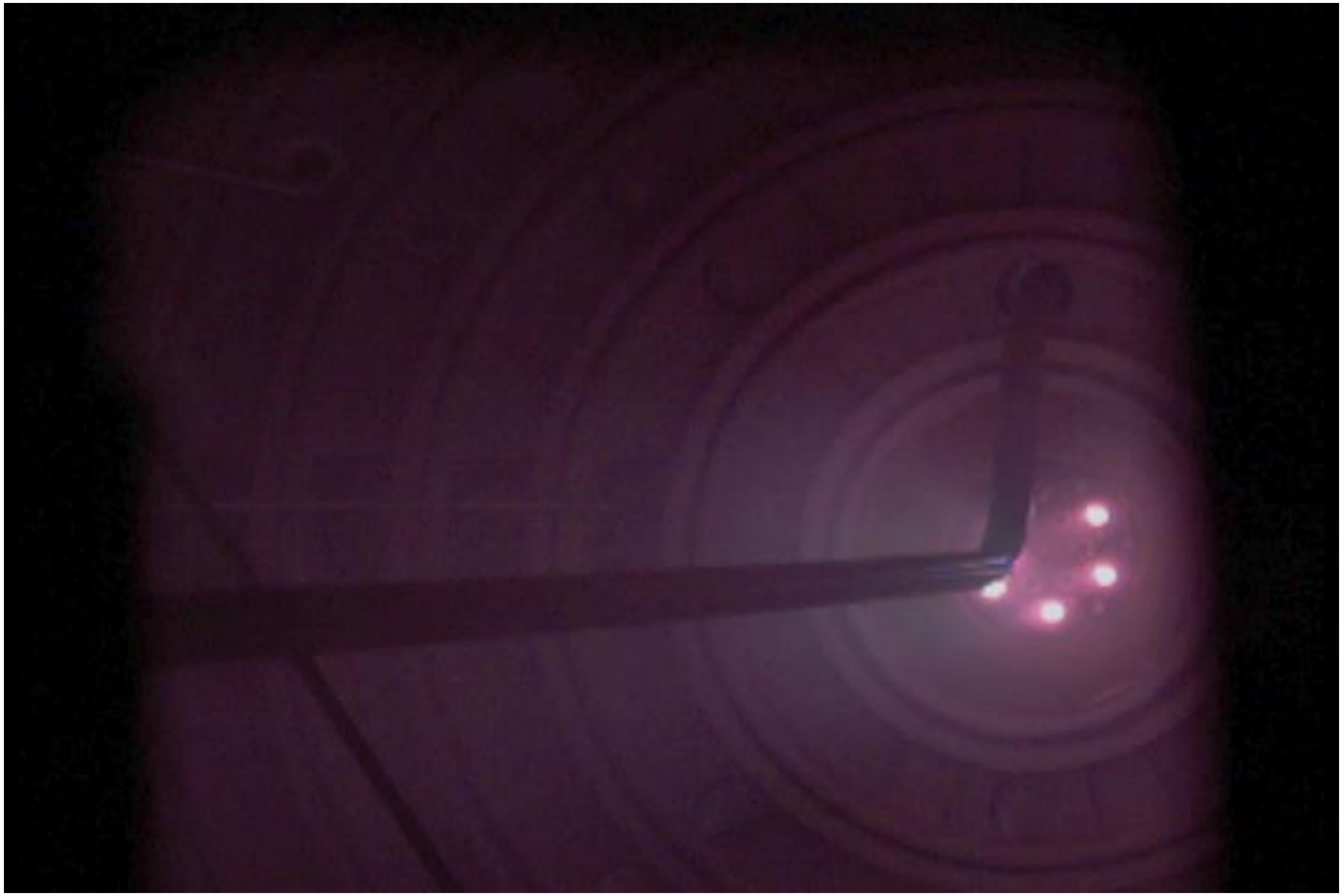

3D Perturbations Observed

TREX geometry implemented in Cylindrical VPIC

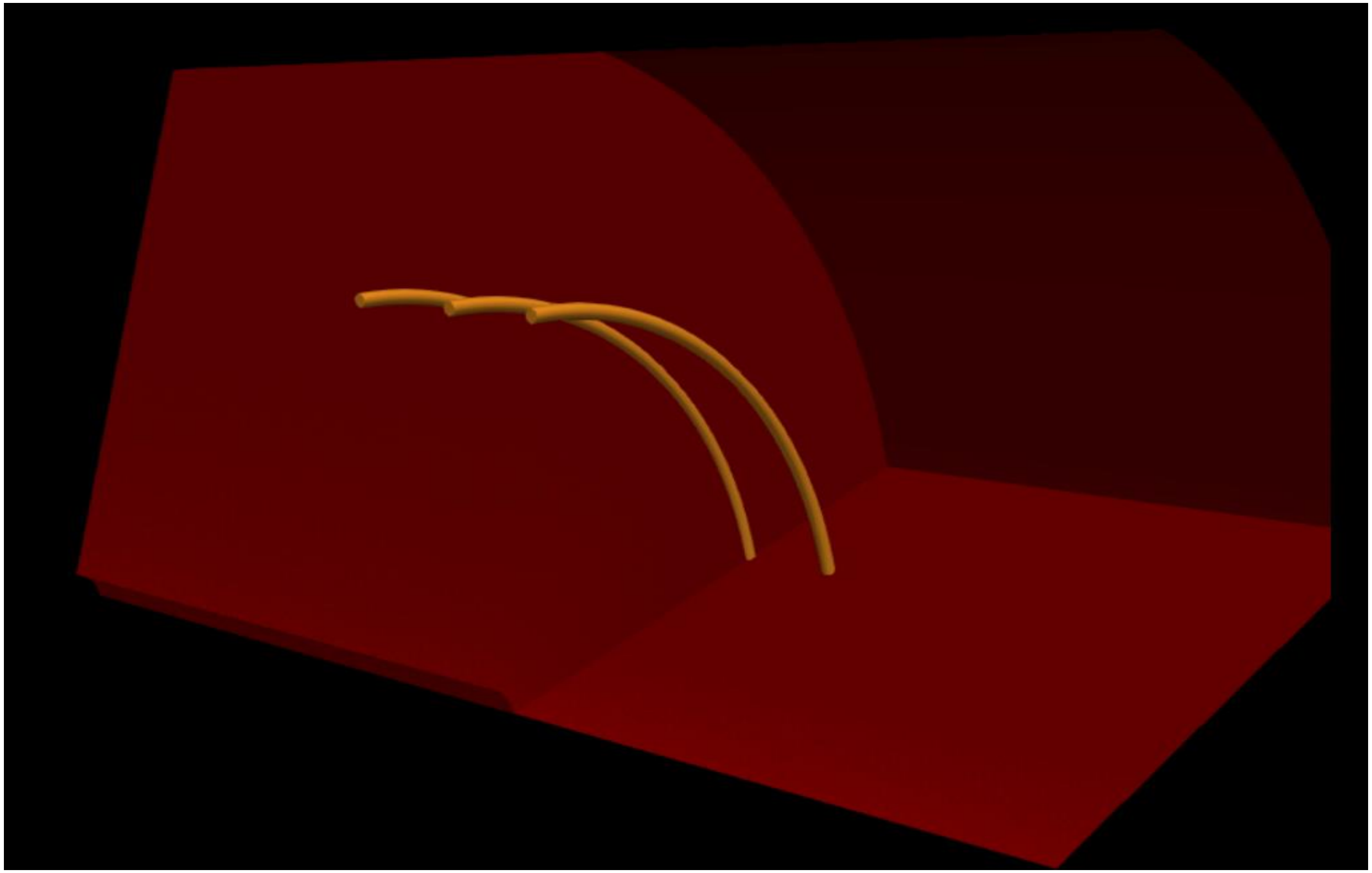

3D Perturbations Observed

TREX geometry implemented in Cylindrical VPIC

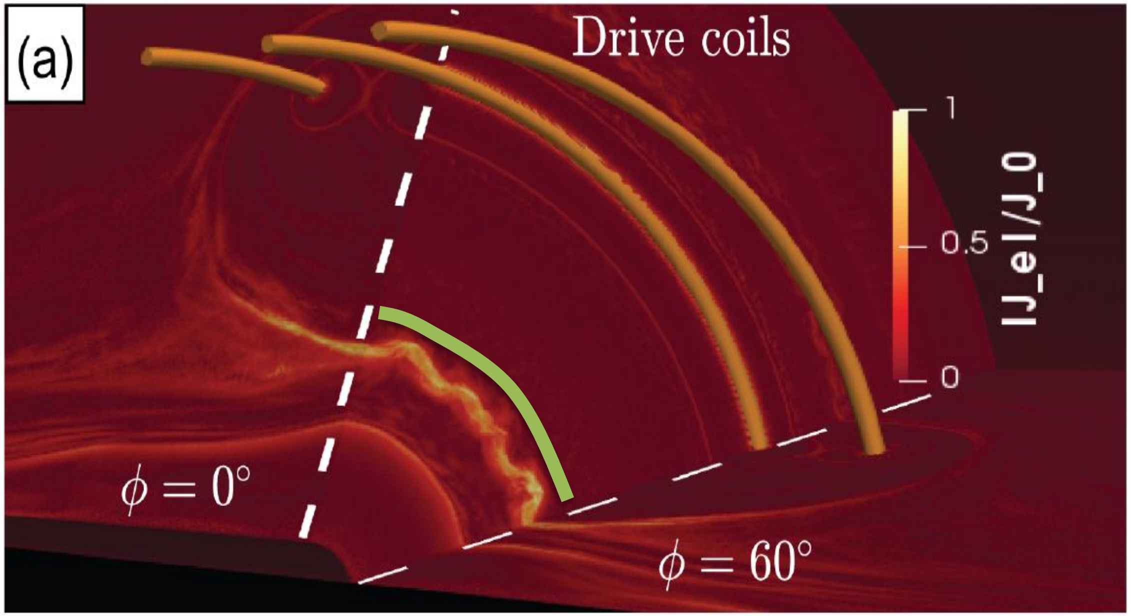

Magnetic field measurements

Magnetic probes

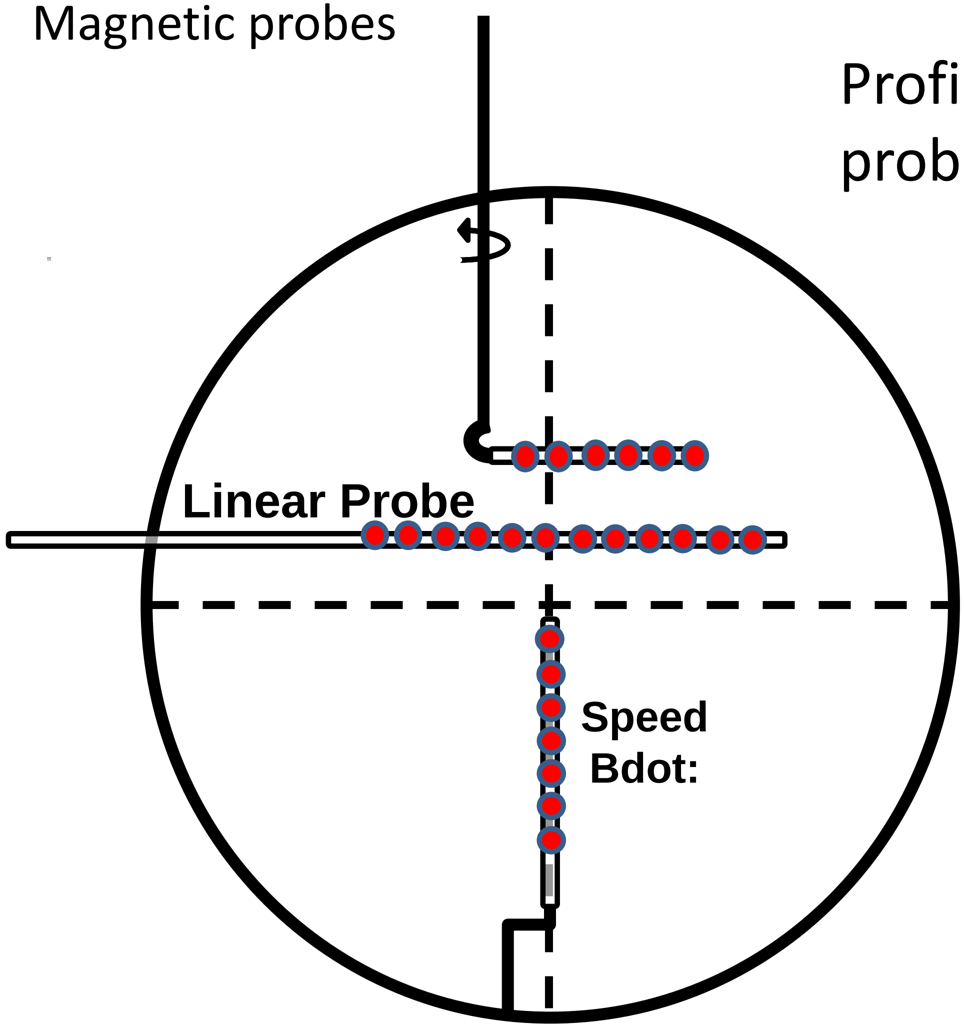

Profiles can be built from movable probe, using multiple shots

Magnetic field measurements

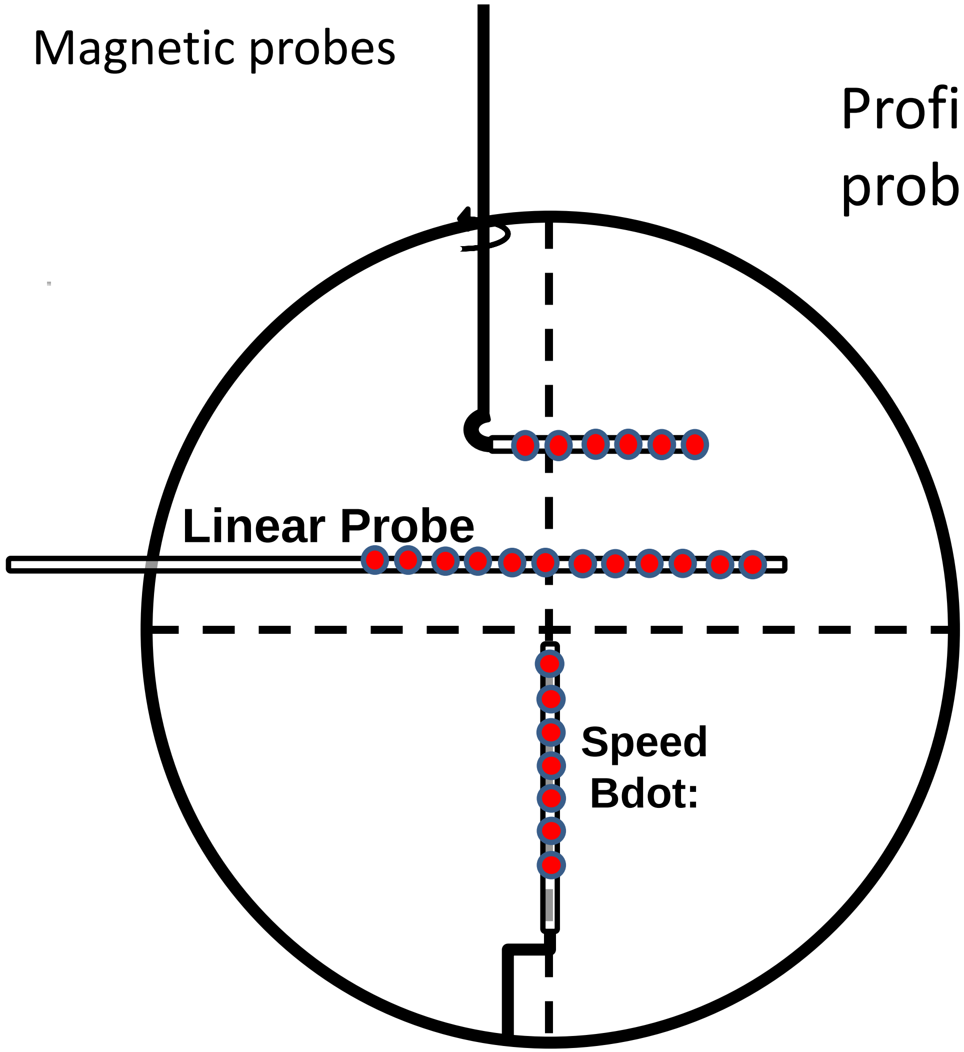

Profiles can be built from movable probe, using multiple shots

Magnetic field measurements

Magnetic probes

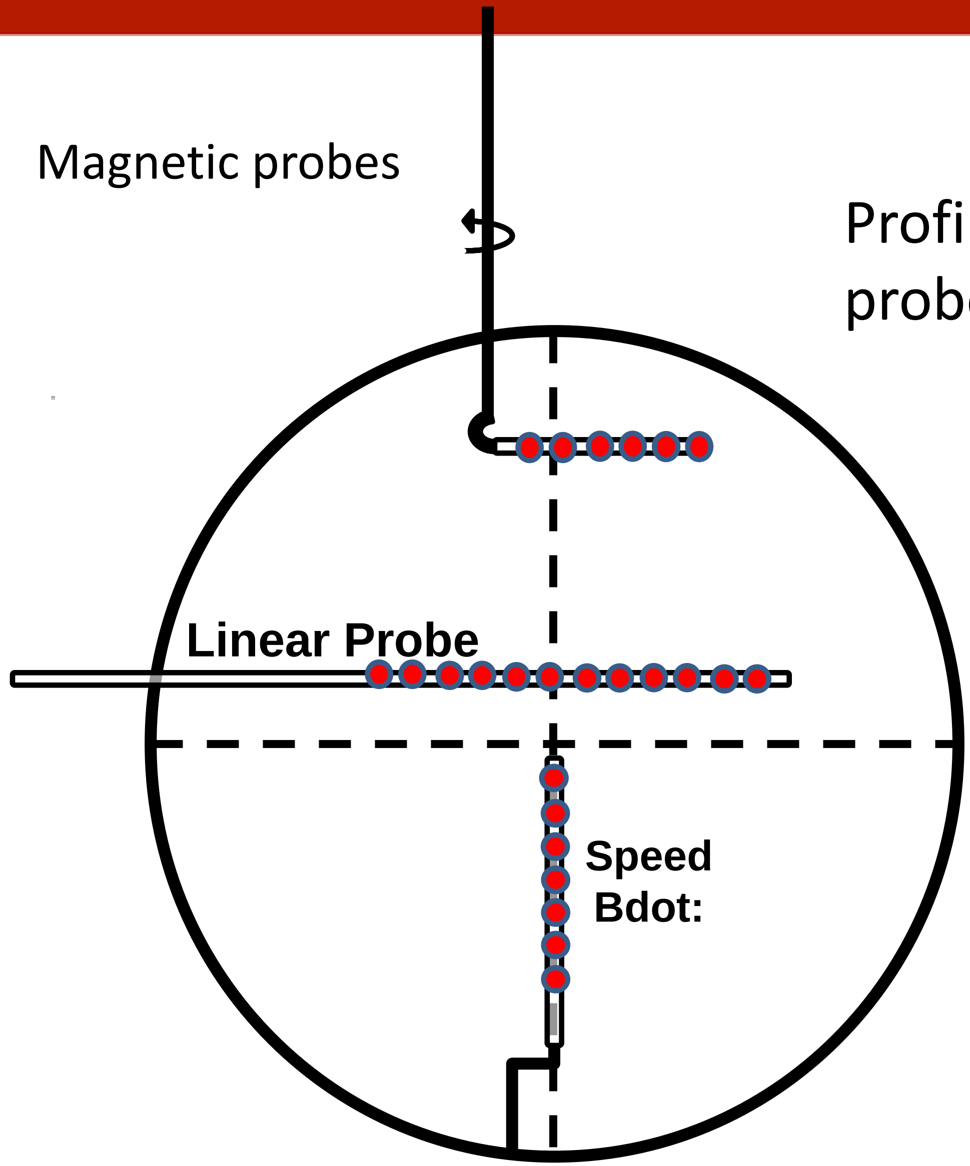

Profiles can be built from movable probe, using multiple shots

Magnetic field measurements

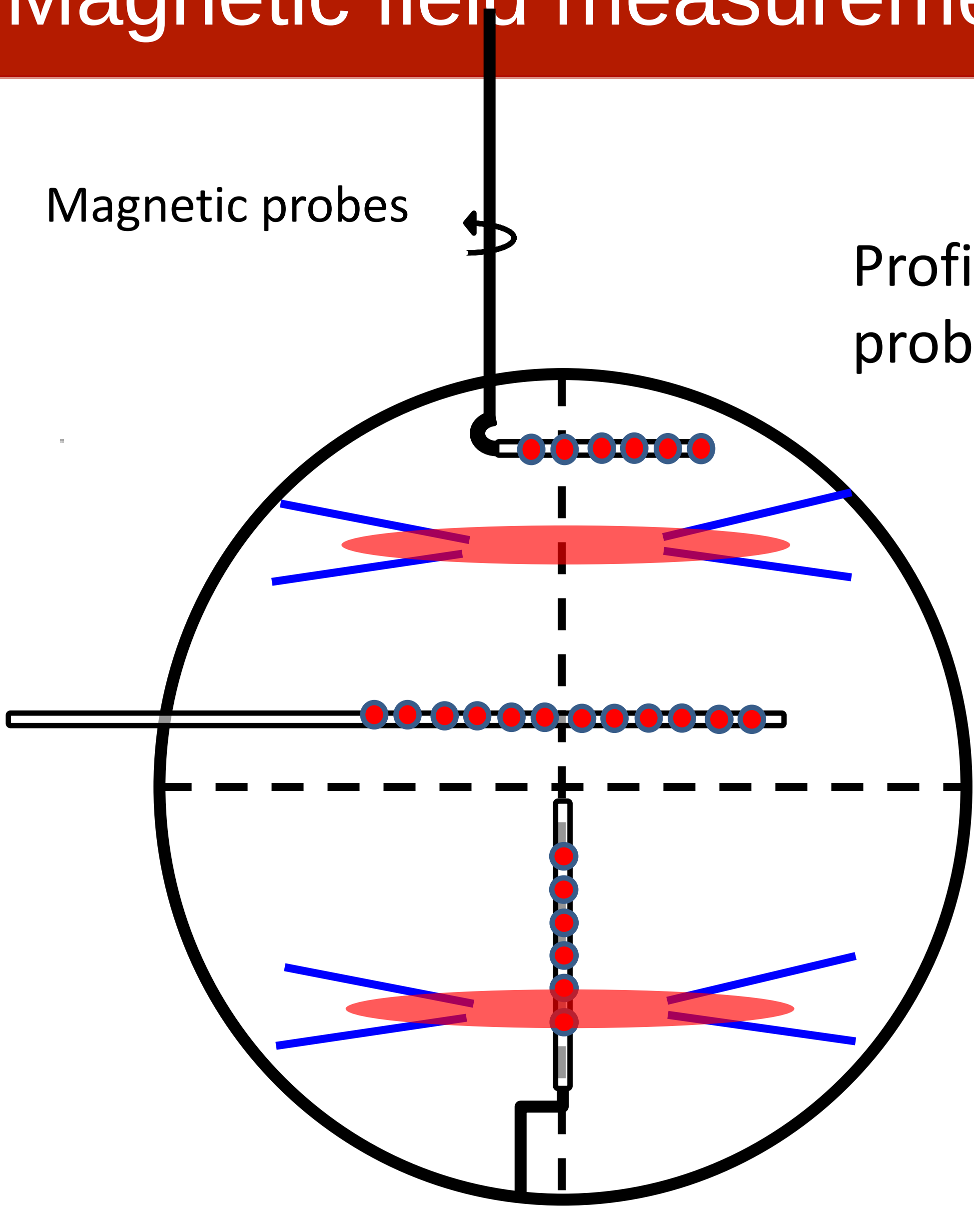

Profiles can be built from movable probe, using multiple shots

Magnetic field measurements

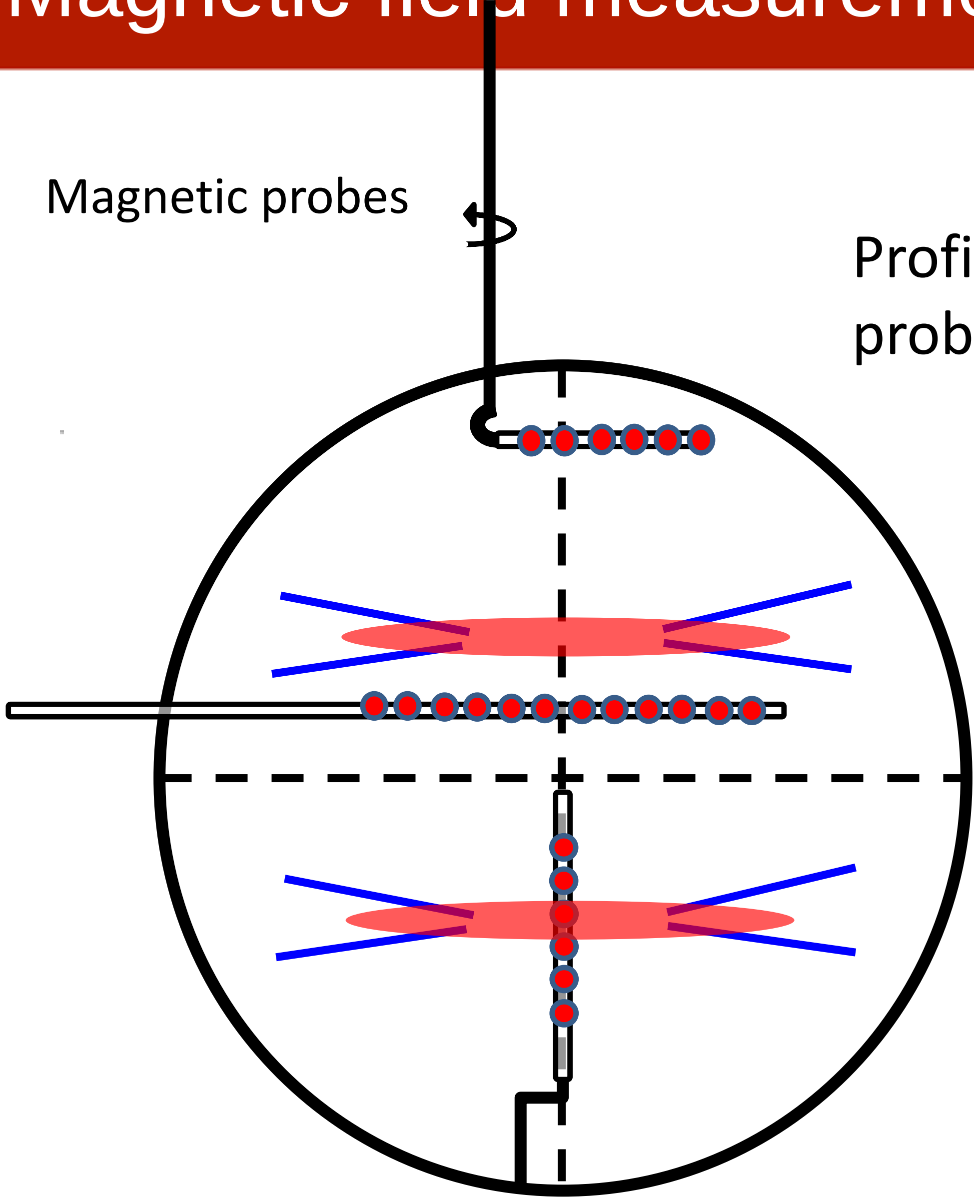

Profiles can be built from movable probe, using multiple shots

Magnetic field measurements

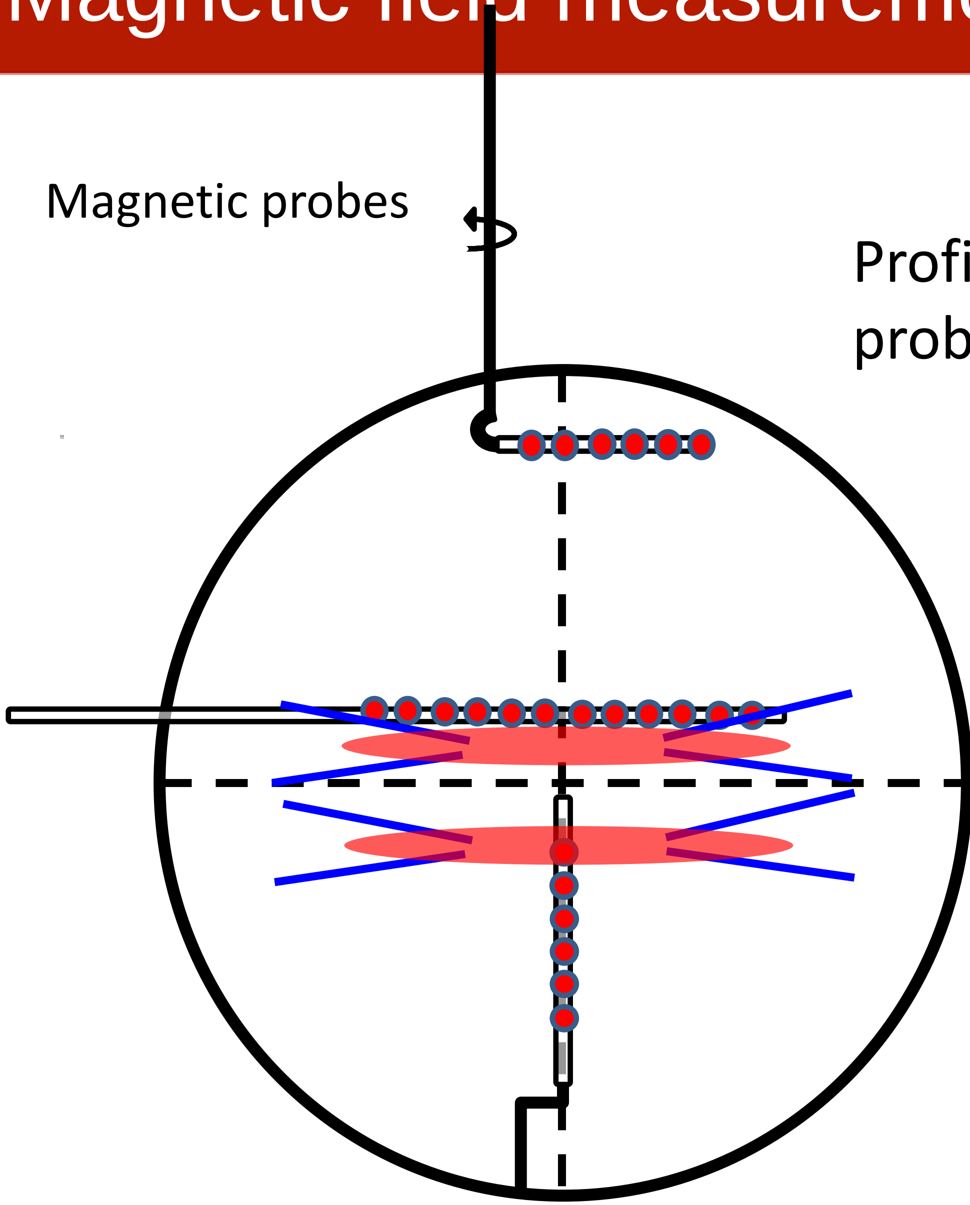

Profiles can be built from movable probe, using multiple shots

Magnetic field measurements

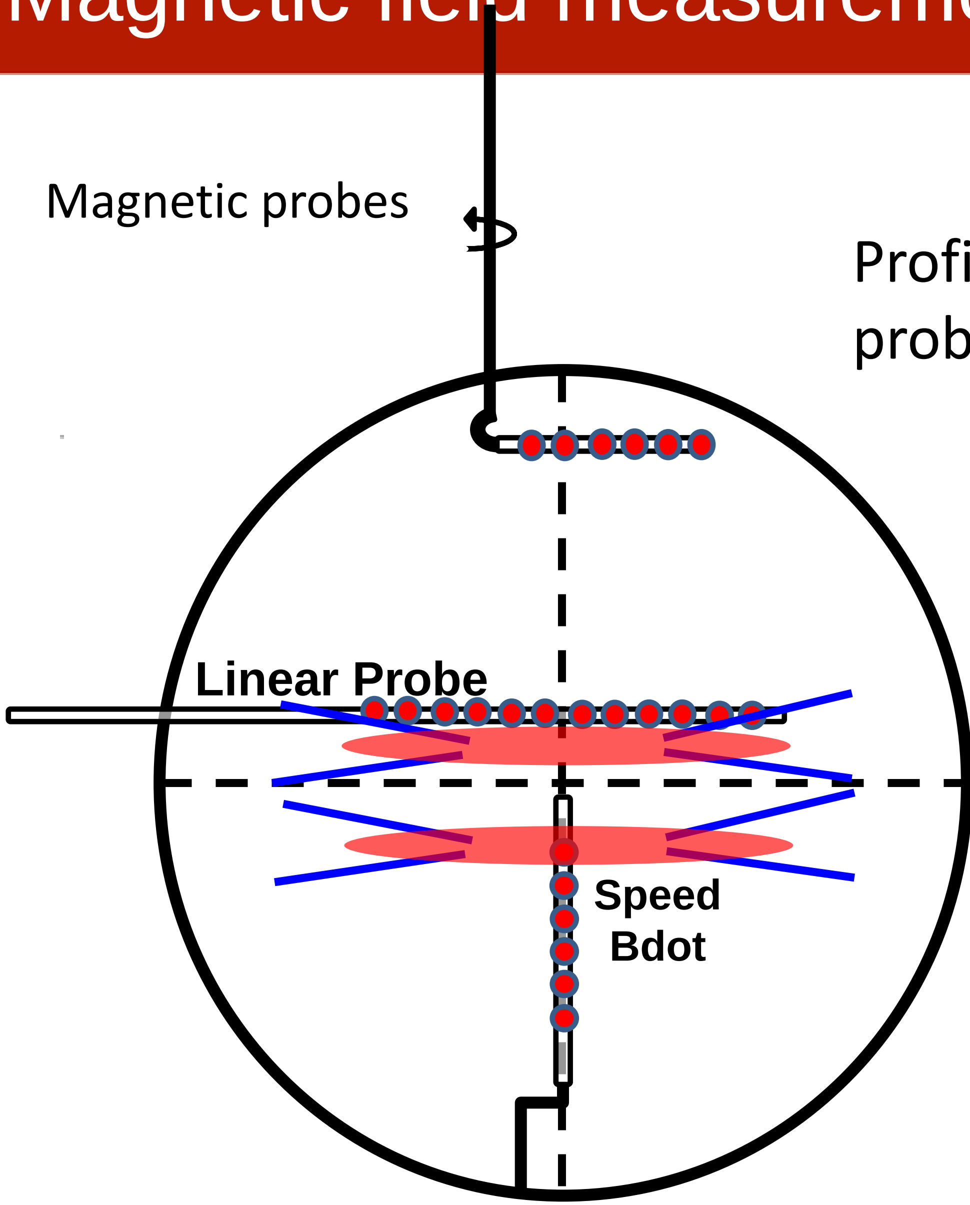

Profiles can be built from movable probe, using multiple shots

But jogging is great!

Speed probe yields the reconnection rate.

Linear probe yields reconnection geometry in a single shot.

High spatial resolution through Jogging-method

Elongated geometry: $\mu_0 J_\phi \approx dB_z/dR$

Jogging : $dR = V_{layer}\, dt$

$\rightarrow J_\phi \approx (dB_z/dt) / \mu_0 V_{layer}$

$J_z \approx (dB_\phi/dt) / \mu_0 V_{layer}$

Magnetic probes are optimized for high frequency response (10MHz)

V_{layer} ~ 40km/s $\rightarrow$ 4mm spatial resolutions!

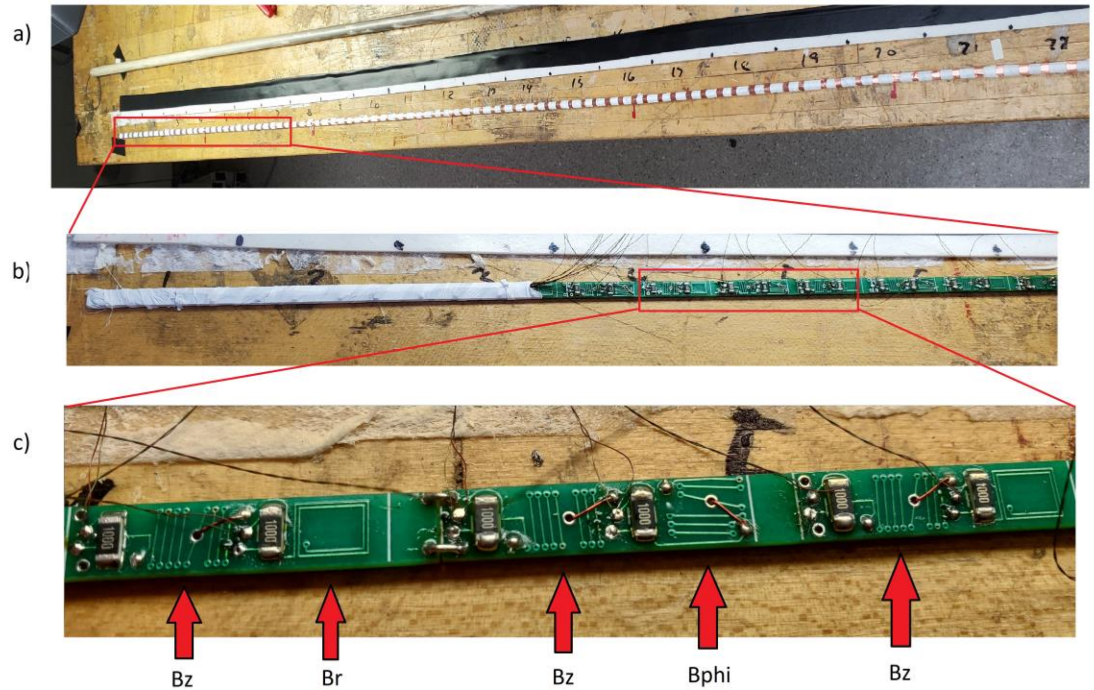

High spatial resolution through Jogging-method

Elongated geometry: $\mu_0 J_\phi \approx dB_z/dR$

Jogging : $dR = V_{layer}\, dt$

$\rightarrow$ $J_\phi \approx (dB_z/dt) / \mu_0 V_{layer}$

$J_z \approx (dB_\phi/dt) / \mu_0 V_{layer}$

Magnetic probes are optimized for high frequency response (10MHz)

V_{layer} ~ 40km/s $\rightarrow$ 4mm spatial resolutions!

High spatial resolution through Jogging-method

Elongated geometry: $\mu_0 J_\phi \approx dB_z/dR$

Jogging : $dR = V_{layer}\, dt$

$\rightarrow J_\phi \approx (dB_z/dt) / \mu_0 V_{layer}$

$J_z \approx (dB_\phi/dt) / \mu_0 V_{layer}$

Magnetic probes are optimized for high frequency response (10MHz)

V_{layer} ~ 40km/s $\rightarrow$ 4mm spatial resolutions!

Single shot data:

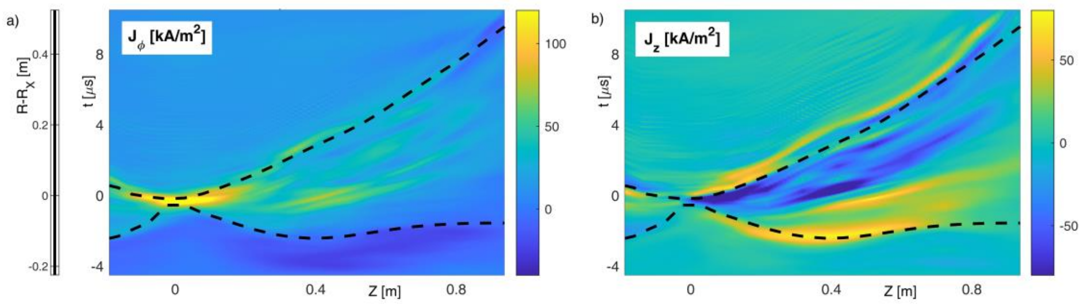

Multiple shots + Jogging-method

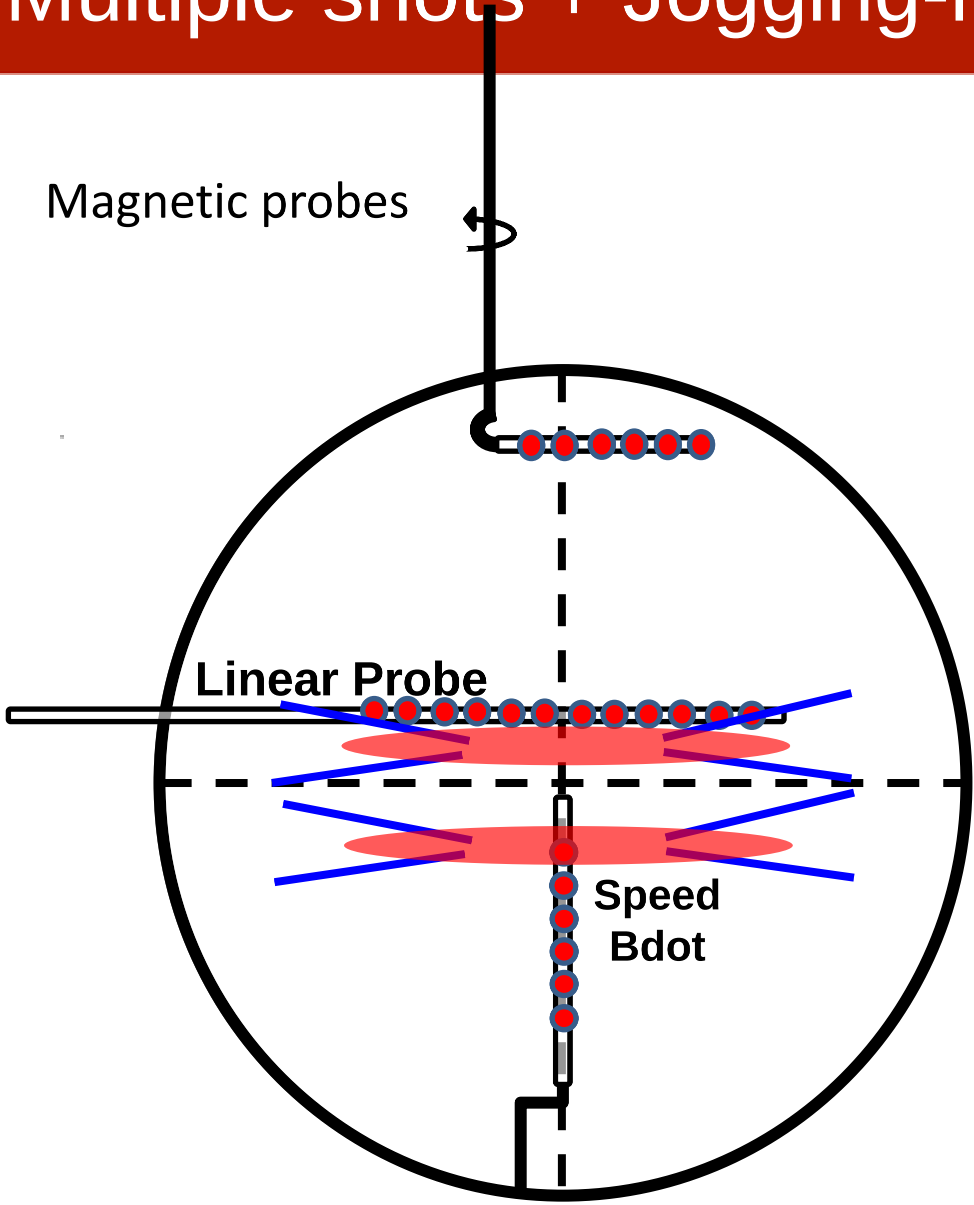

Multiple shots + Jogging-method

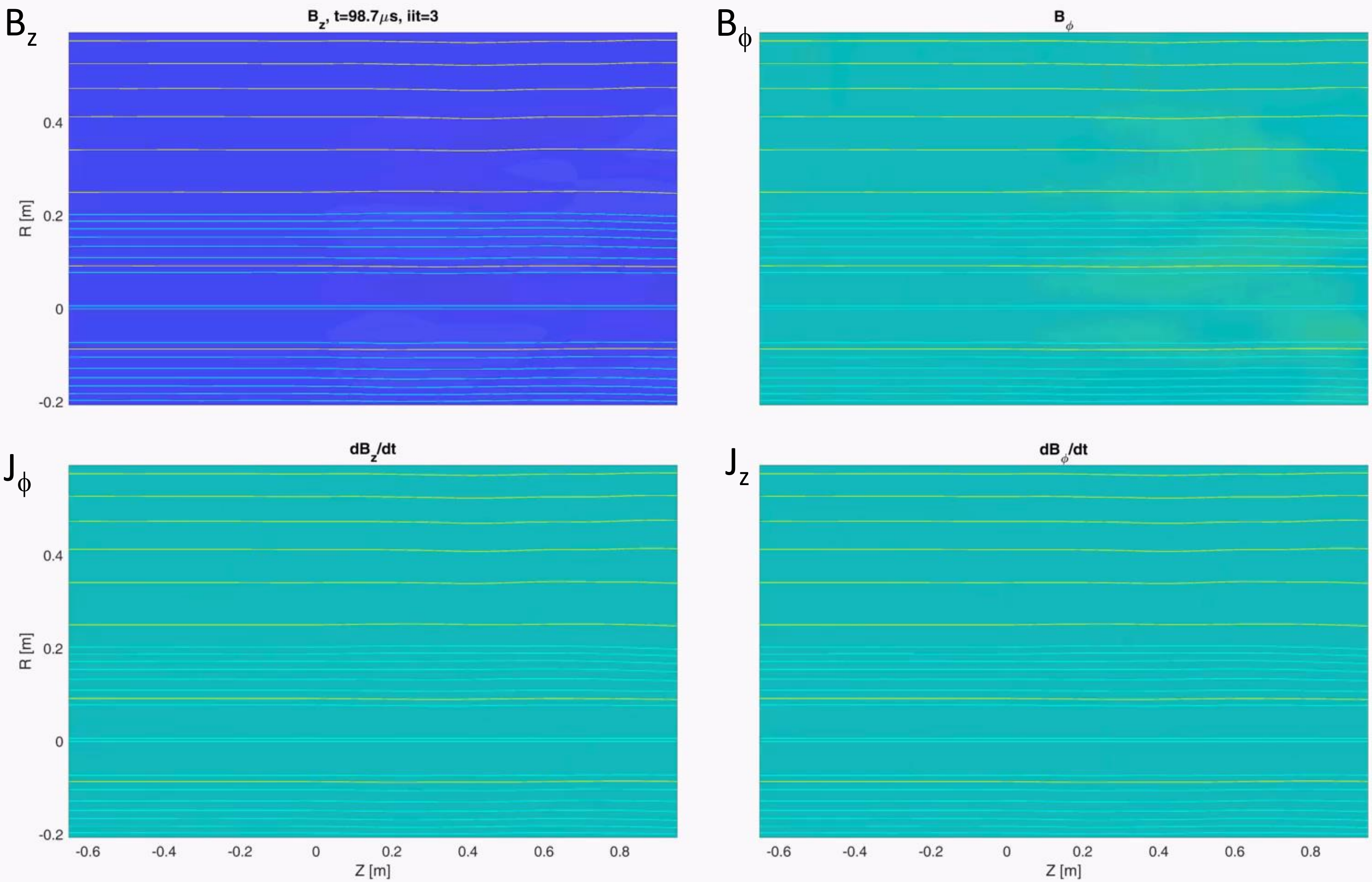

[Greess+, JGR, 2021]

Multiple shots + Jogging-method

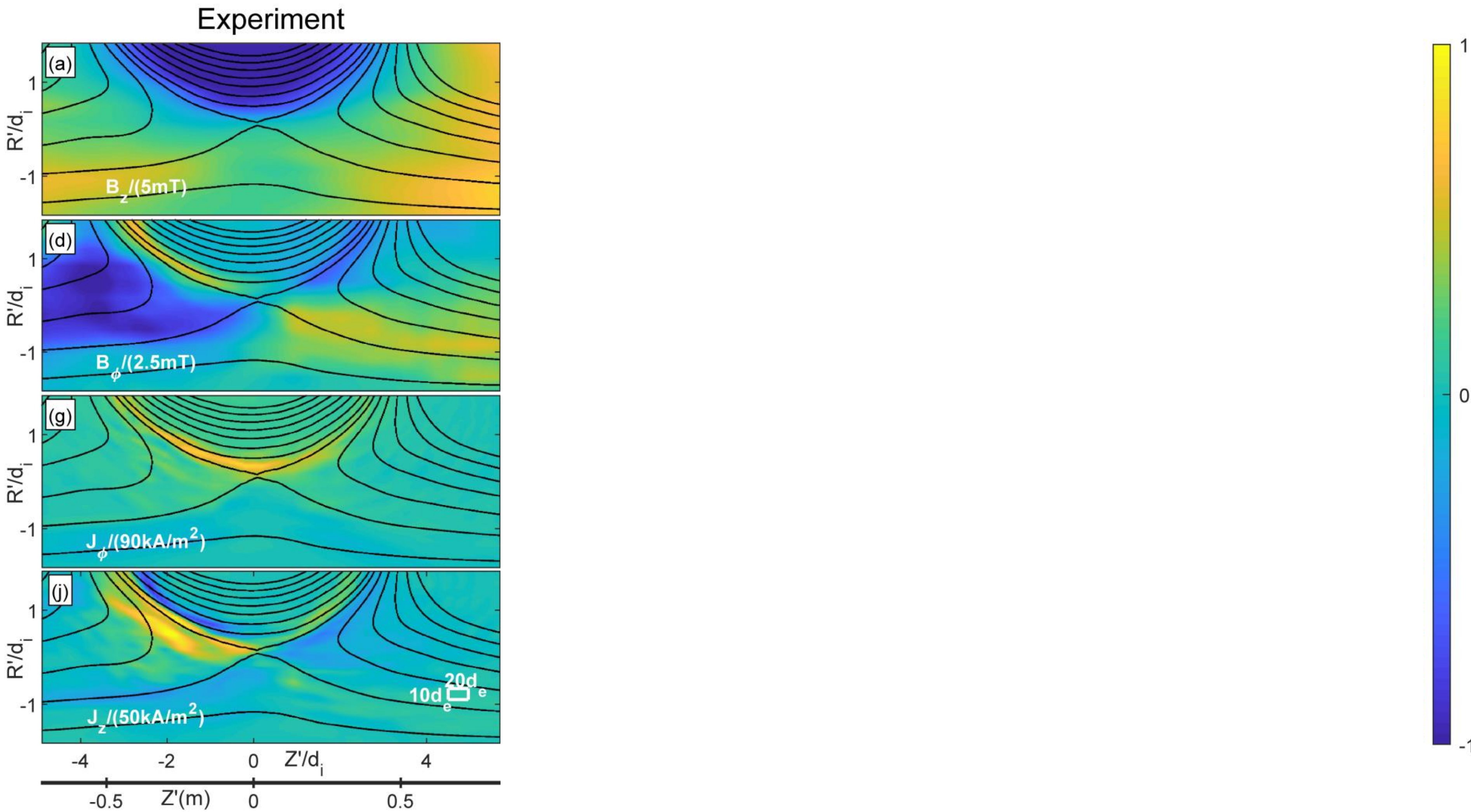

What breaks the Frozen-In-Law?

Reconnection requires:

Generalized Ohm's law

$$\mathbf{E} + \mathbf{v} \times \mathbf{B} \neq \eta_A \mathbf{J} + (\mathbf{J} \times \mathbf{B} - \nabla\cdot\mathbf{p}_e)/ne + \ldots$$

In 2D kinetic simulations, $\nabla\cdot\mathbf{p}_e$ is large when $\delta_j \sim d_e = c/\omega_{pe}$.

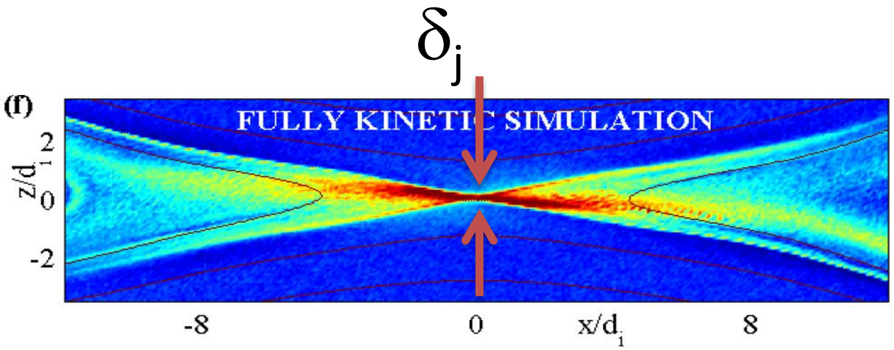

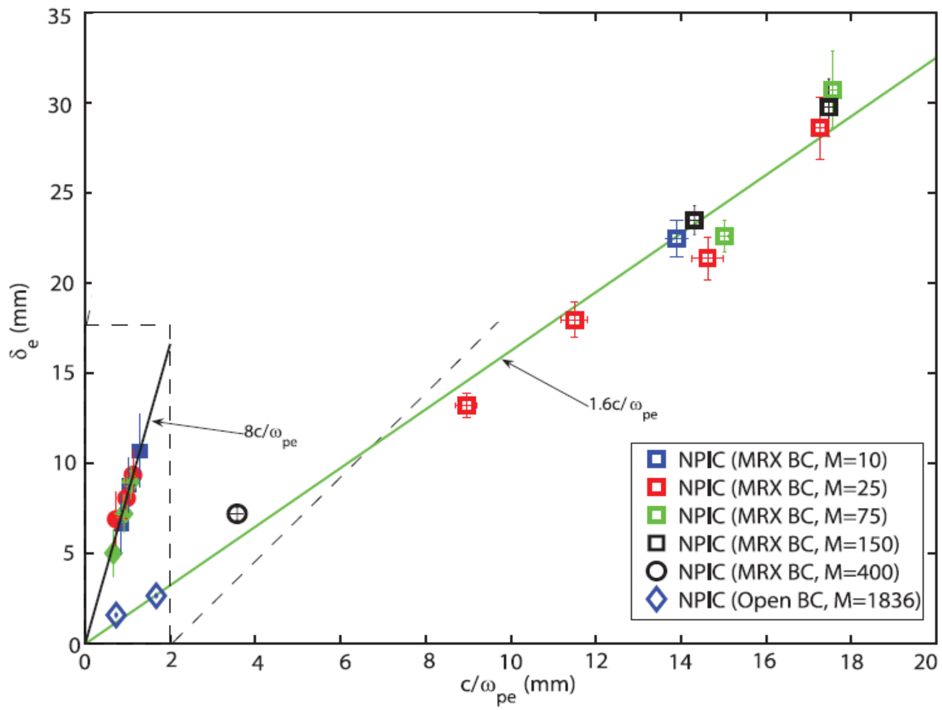

Experimental results at MRX:

Wide current layers,

➔ Anomalous Resistivity?

[Ji et al., GRL, 2008].

What breaks the Frozen-In-Law?

In TREX, the current layer widths coincide with kinetic simulation results ➔ $\nabla\cdot\mathbf{p}_e$ is likely large

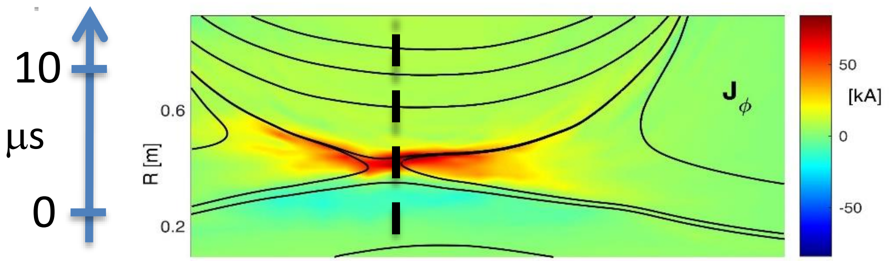

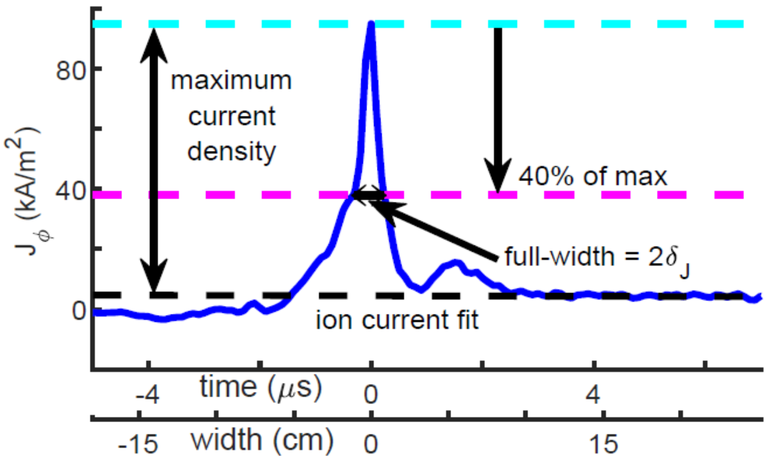

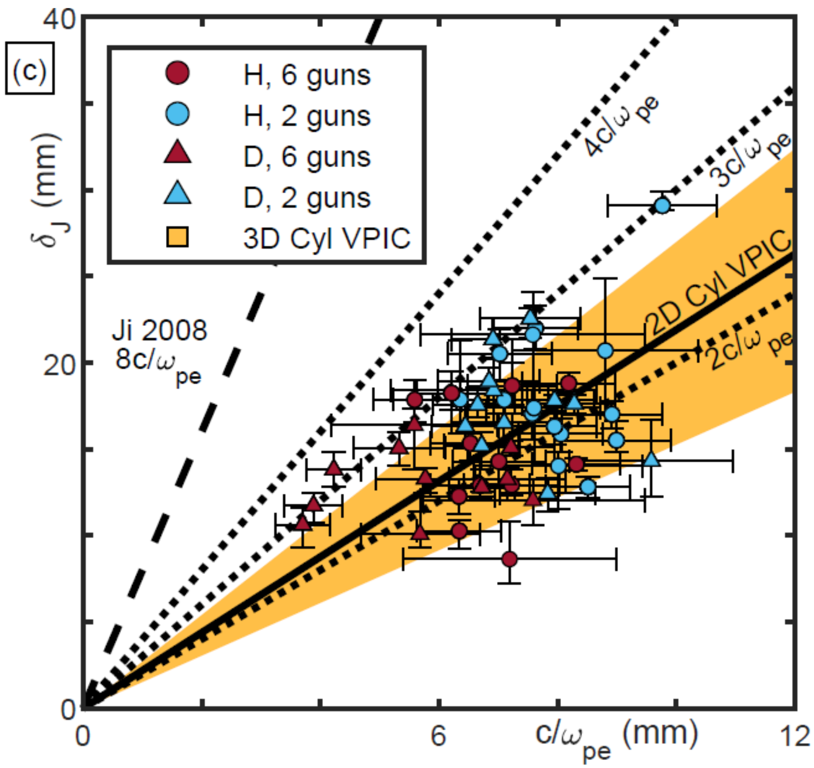

Fast reconnection observed in TREX

The absolute reconnection rate, E_{rec}, is mainly set by the Drive Voltage applied.

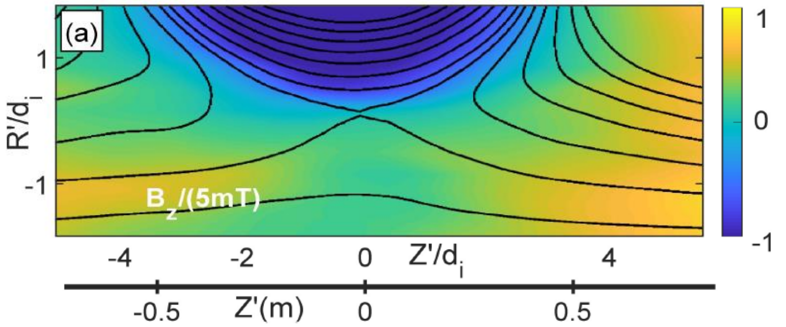

The absolute reconnection rate, E_{rec}, is mainly set by the Drive Voltage applied.

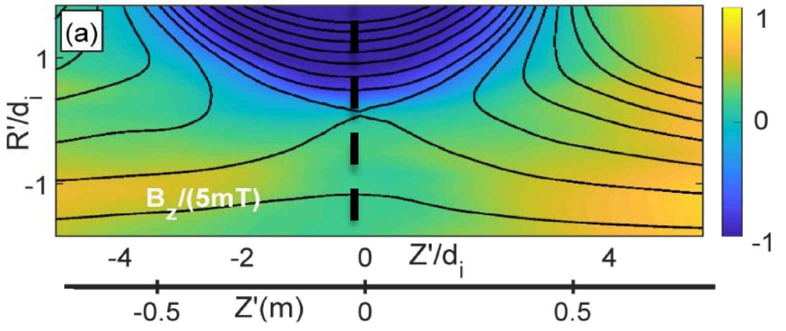

But reconnection physics regulates n_i and B_{rec}

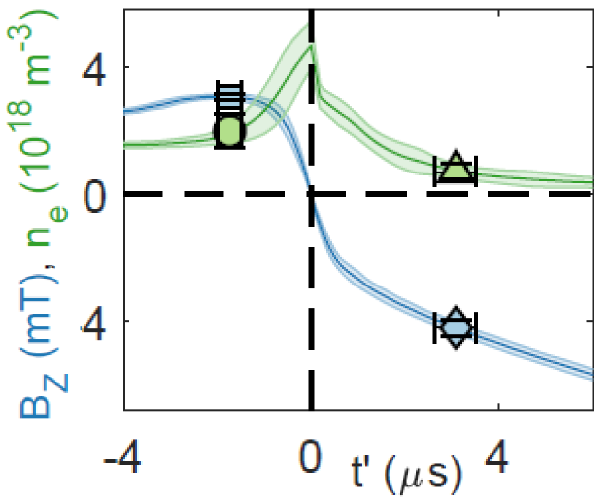

Fast reconnection observed in TREX

The absolute reconnection rate, E_{rec}, is mainly set by the Drive Voltage applied.

But reconnection physics regulates n_i and B_{rec}

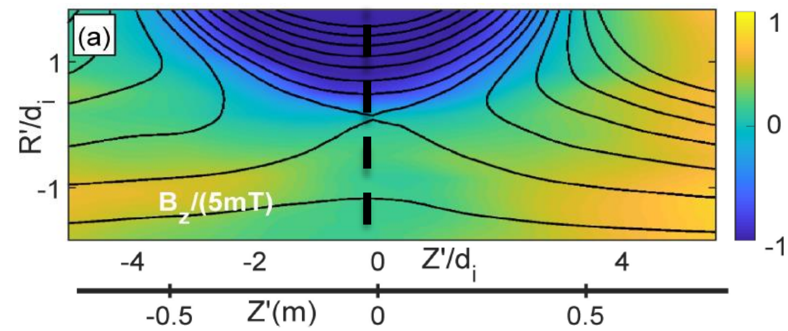

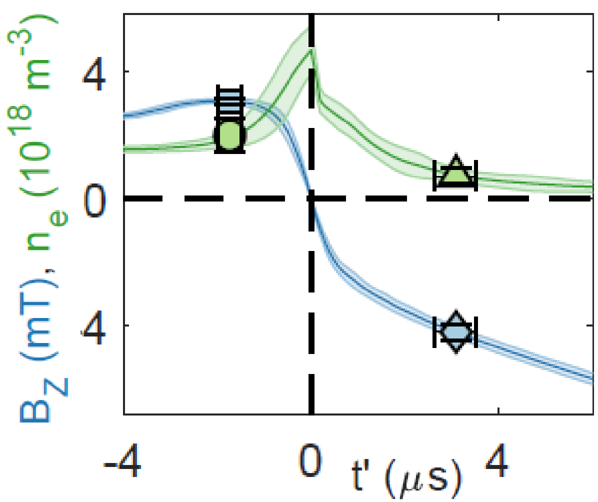

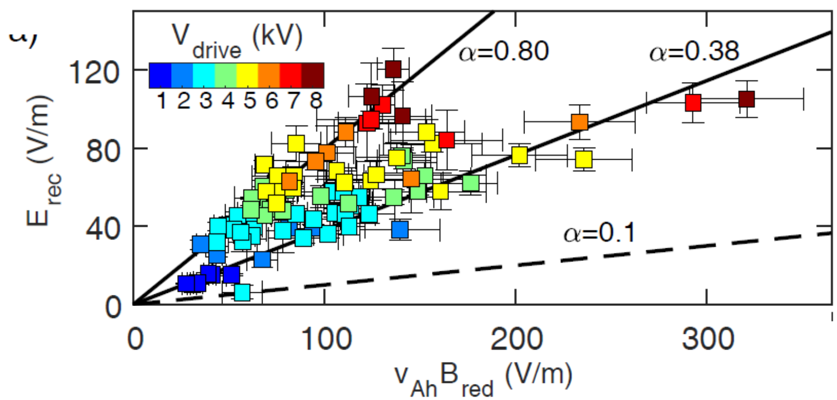

Fast reconnection observed in TREX

The absolute reconnection rate, E_{rec}, is mainly set by the Drive Voltage applied.

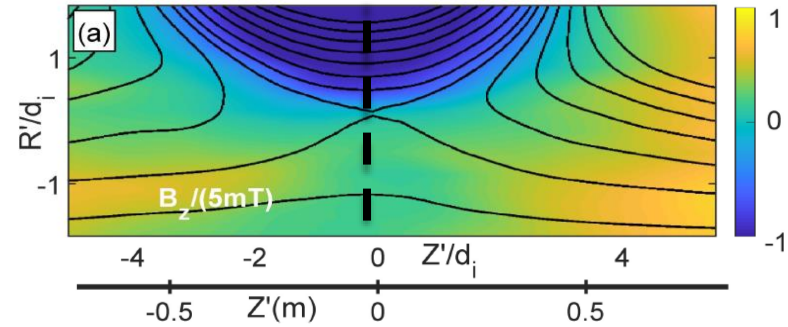

But reconnection physics regulates n_i and B_{rec}

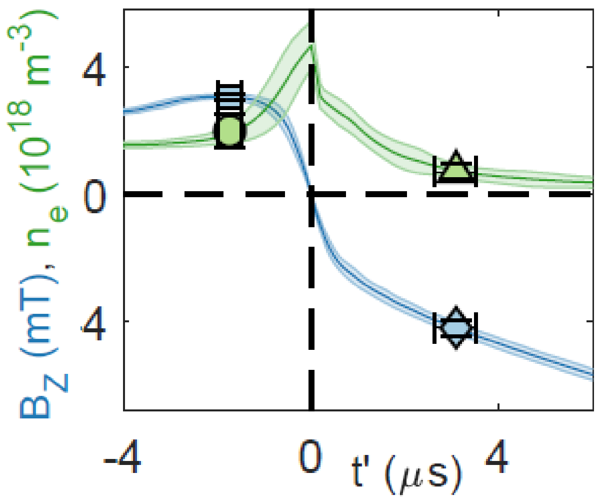

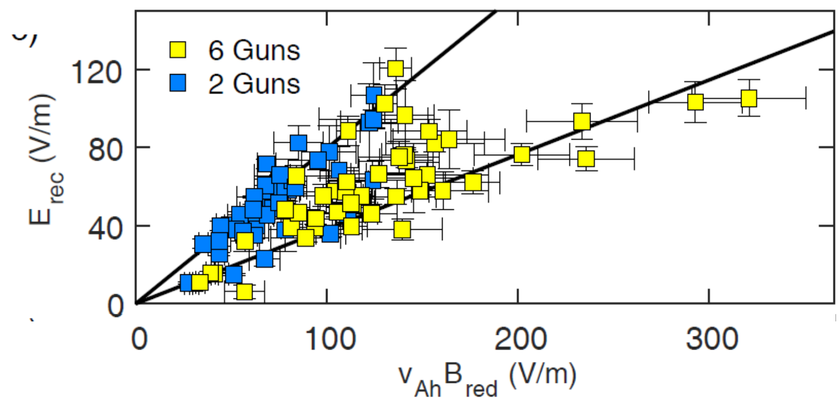

Fast reconnection observed in TREX

The absolute reconnection rate, E_{rec}, is mainly set by the Drive Voltage applied.

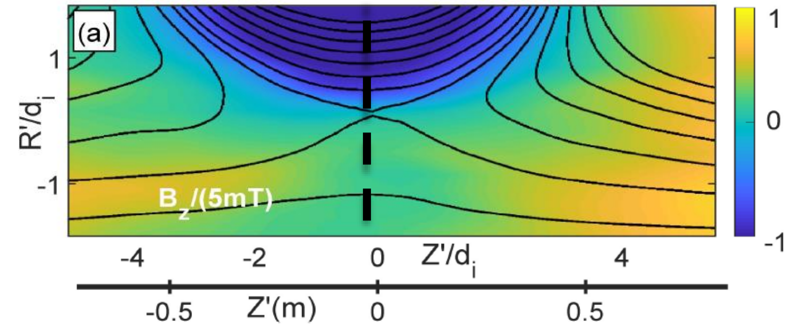

But reconnection physics regulates n_i and B_{rec}

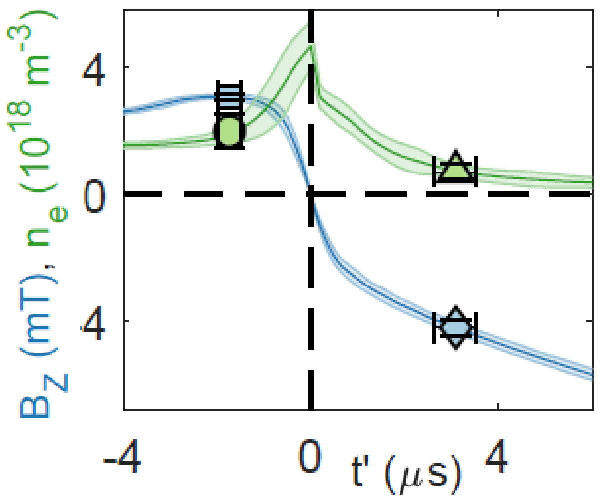

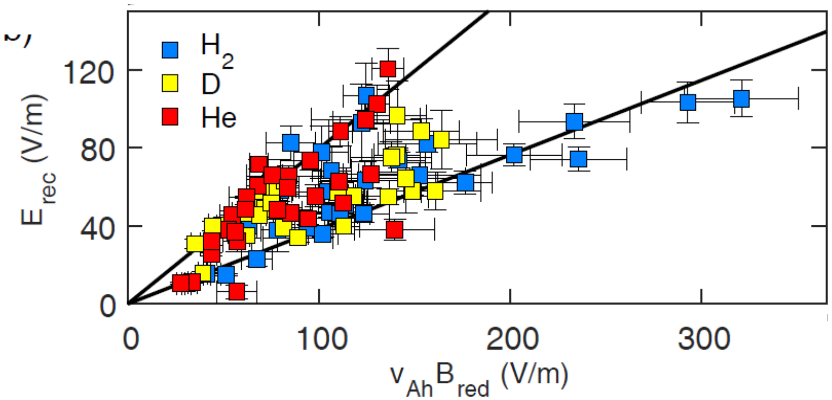

Fast reconnection observed in TREX

The absolute reconnection rate, E_{rec}, is mainly set by the Drive Voltage applied.

But reconnection physics regulates n_i and B_{rec}

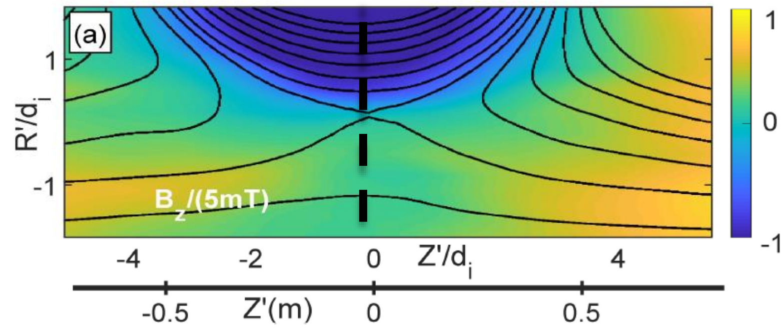

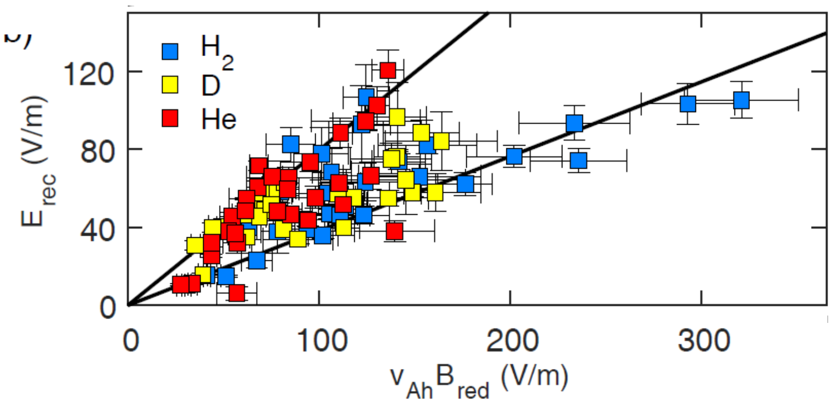

Fast reconnection observed in TREX

The absolute reconnection rate, E_{rec}, is mainly set by the Drive Voltage applied.

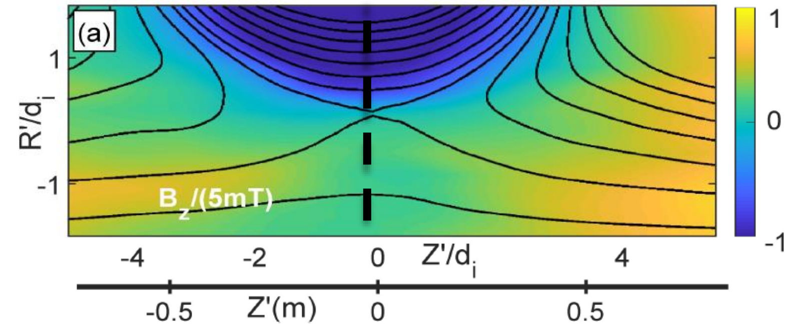

But reconnection physics regulates n_i and B_{rec}

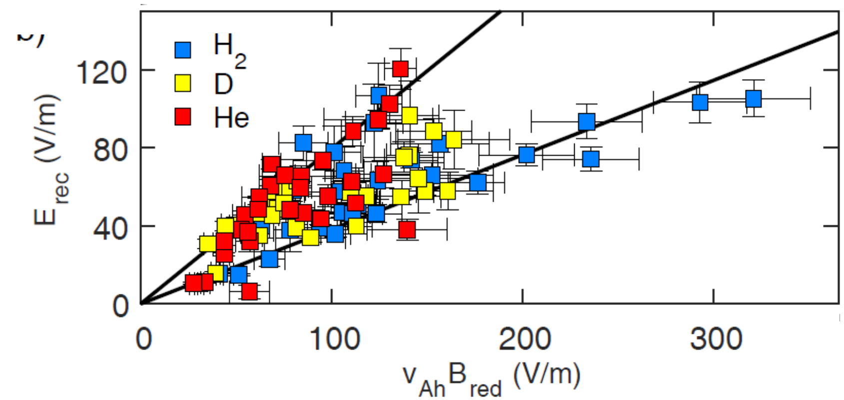

The normalized reconnection rate, $E_{rec} / (V_A B_{rec})$, depends on system size:

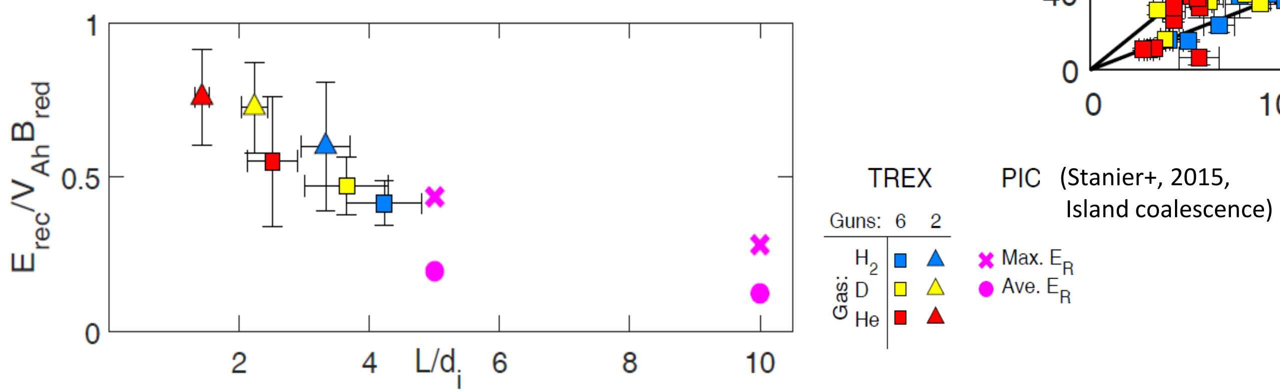

Fast reconnection observed in TREX

[Pyakurel+, PoP, 2019]

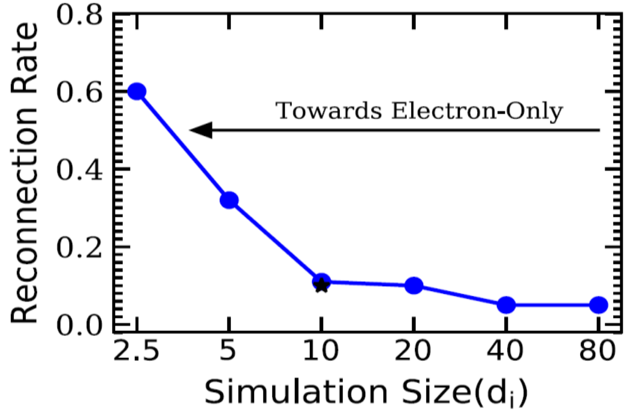

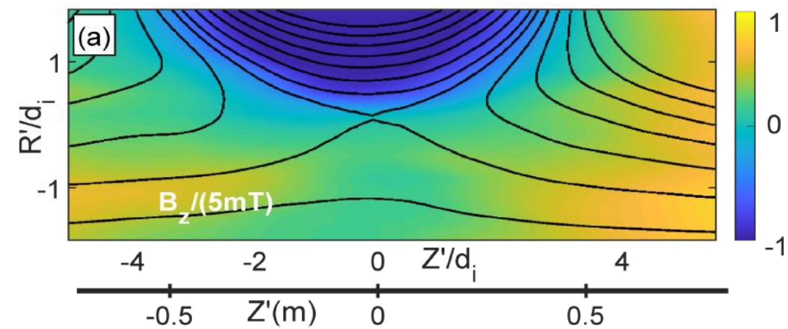

The normalized reconnection rate,

E_{rec} / (V_A B_{rec}), depends on system size:

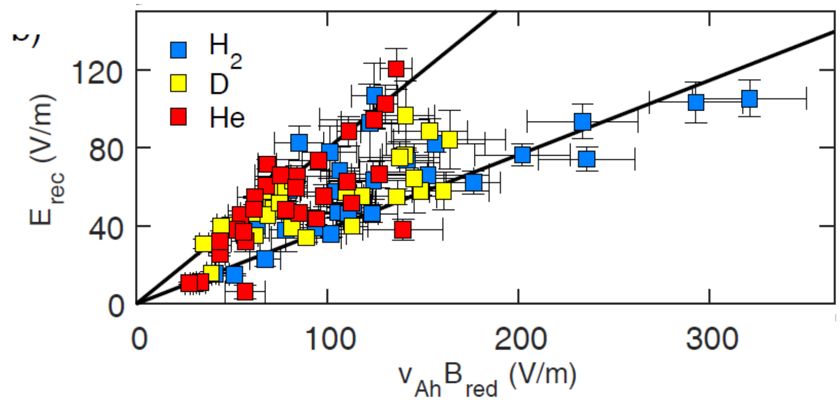

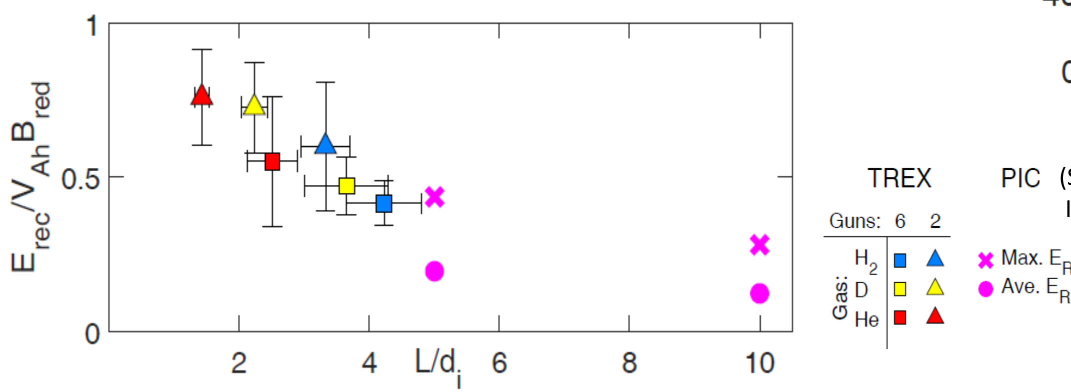

(Stanier+, 2015, Island coalescence)

Fast reconnection observed in TREX

[Pyakurel+, PoP, 2019]

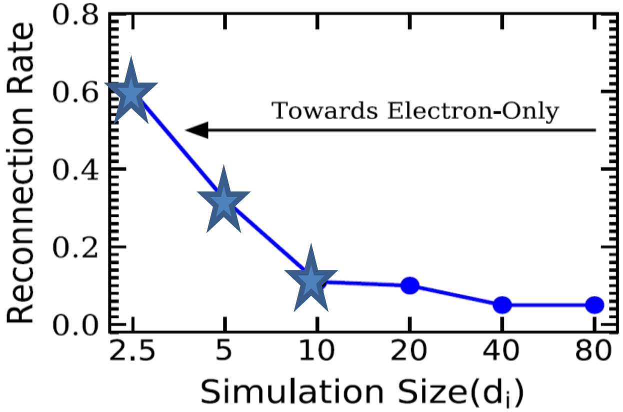

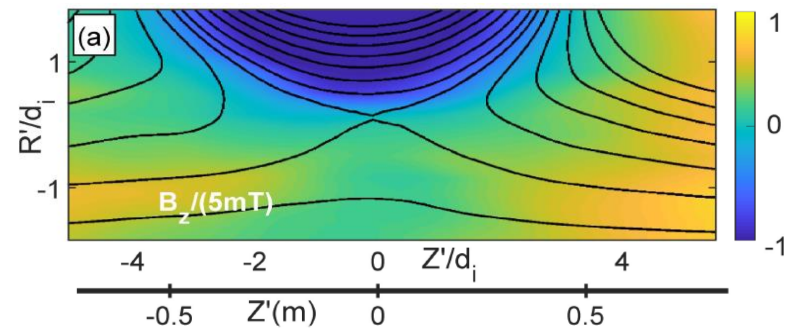

The normalized reconnection rate,

E_{rec} / (V_A B_{rec}), depends on system size:

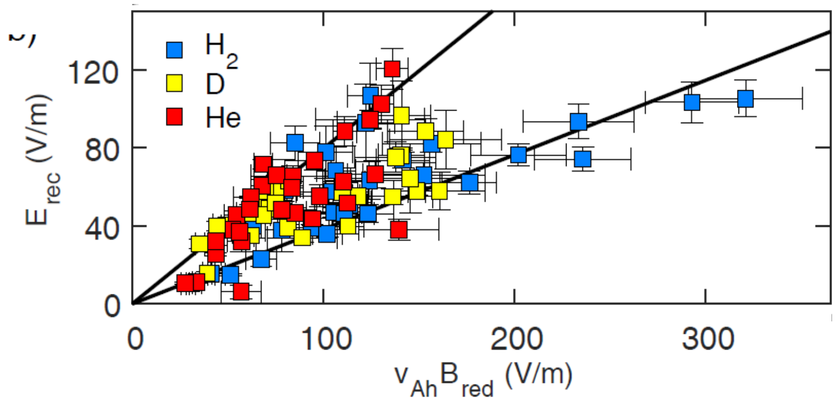

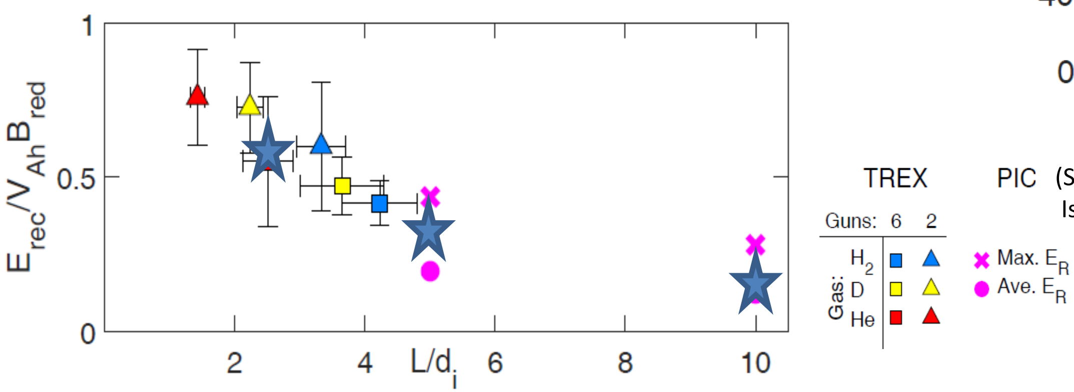

(Stanier+, 2015, Island coalescence)

TREX implemented at the WiPPL user facility

TREX Configuration

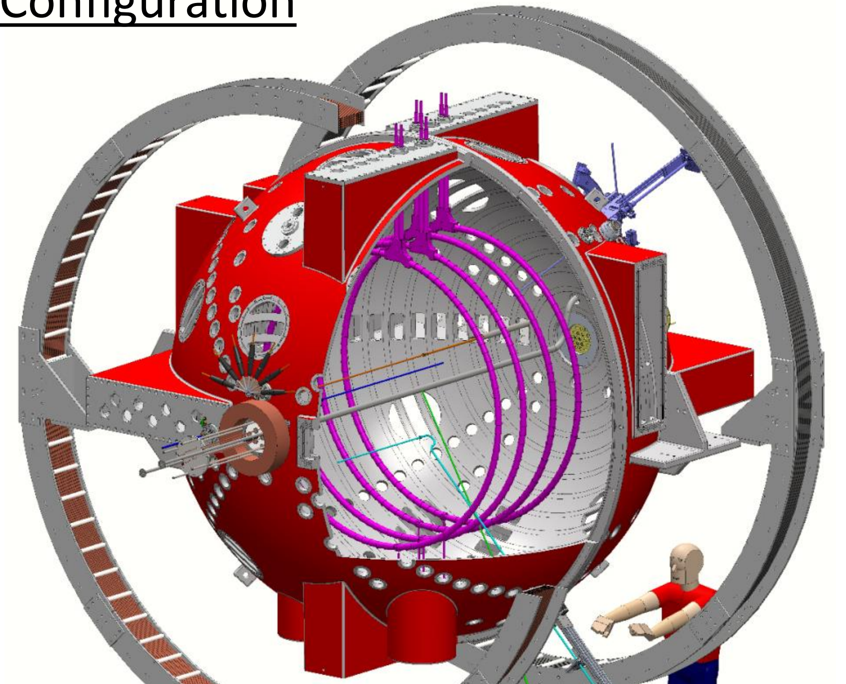

Phase diagram of magnetic reconnection. [Daughton,Roytershteyn & Ji , Daughton 2021]

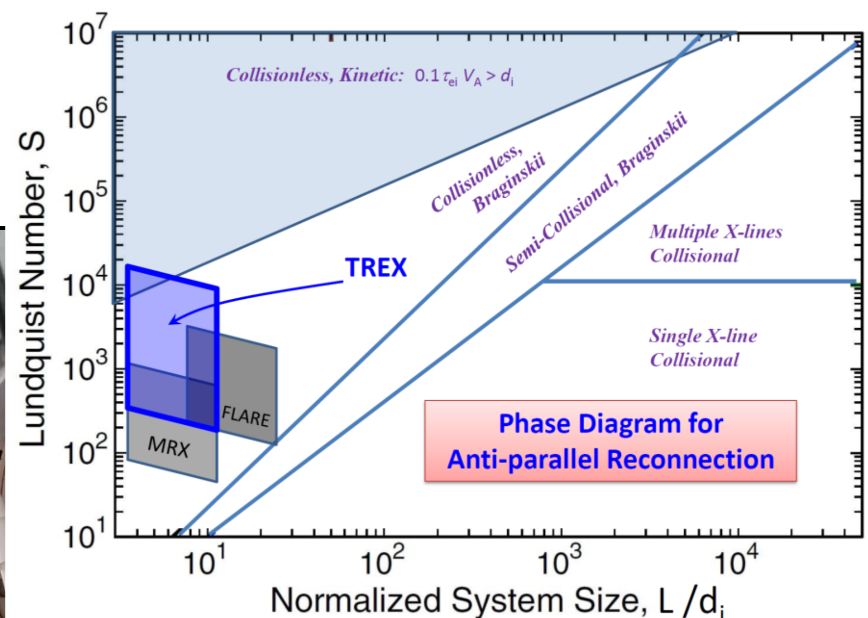

View during the TREX installation:

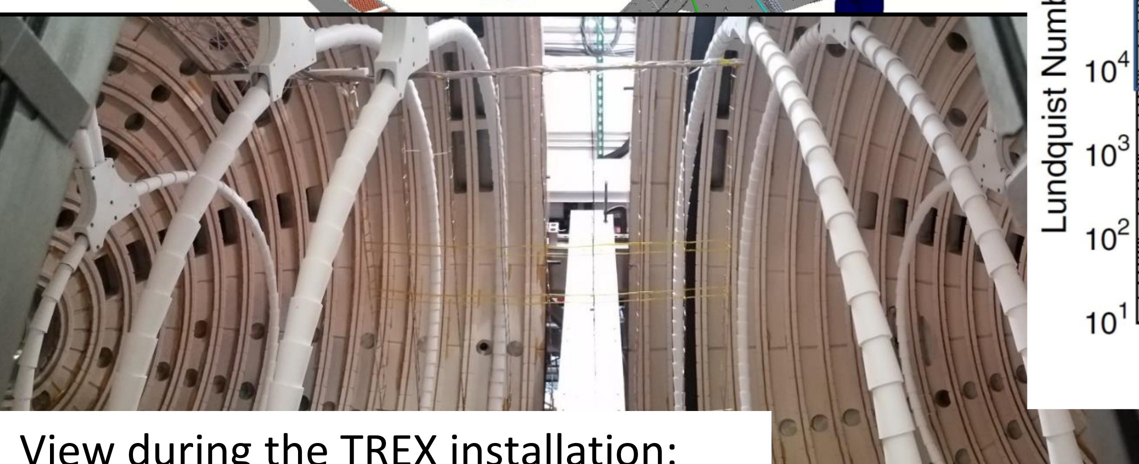

TREX implemented at the WiPPL user facility

TREX Configuration

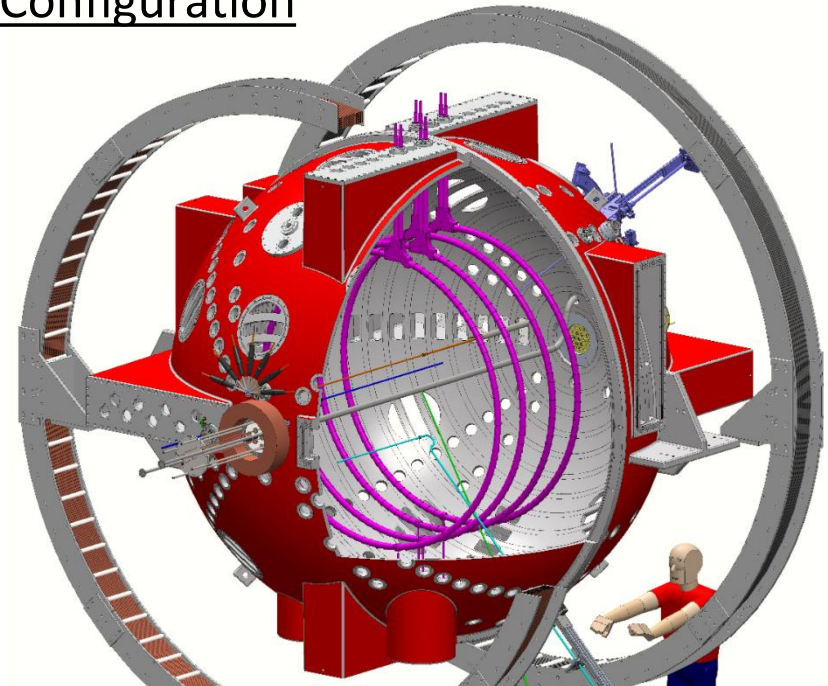

Phase diagram of magnetic reconnection.

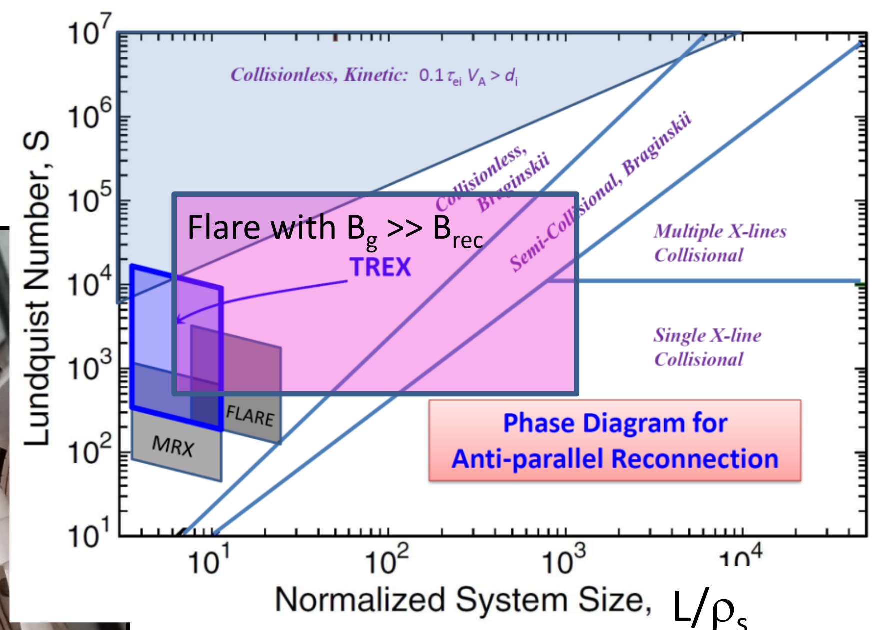

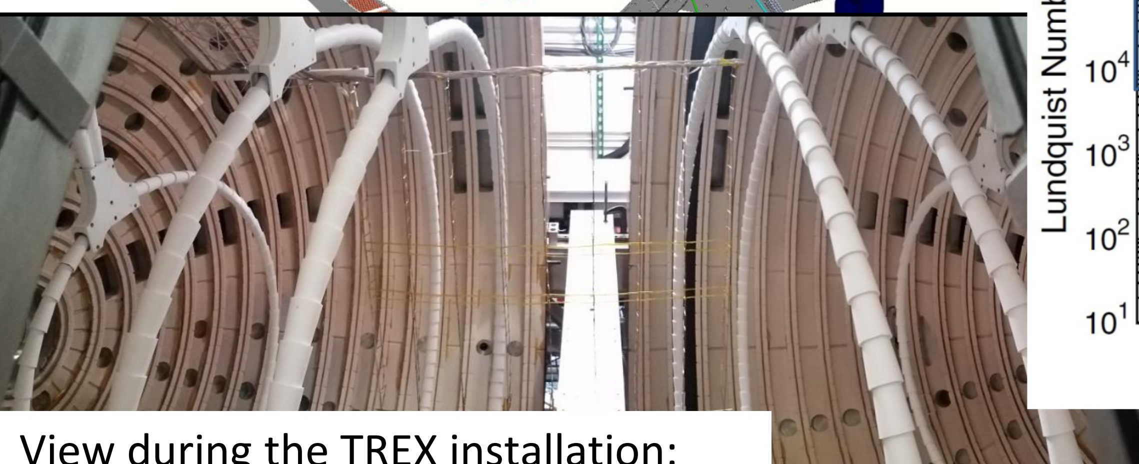

View during the TREX installation:

TREX implemented at the WiPPL user facility

TREX Configuration

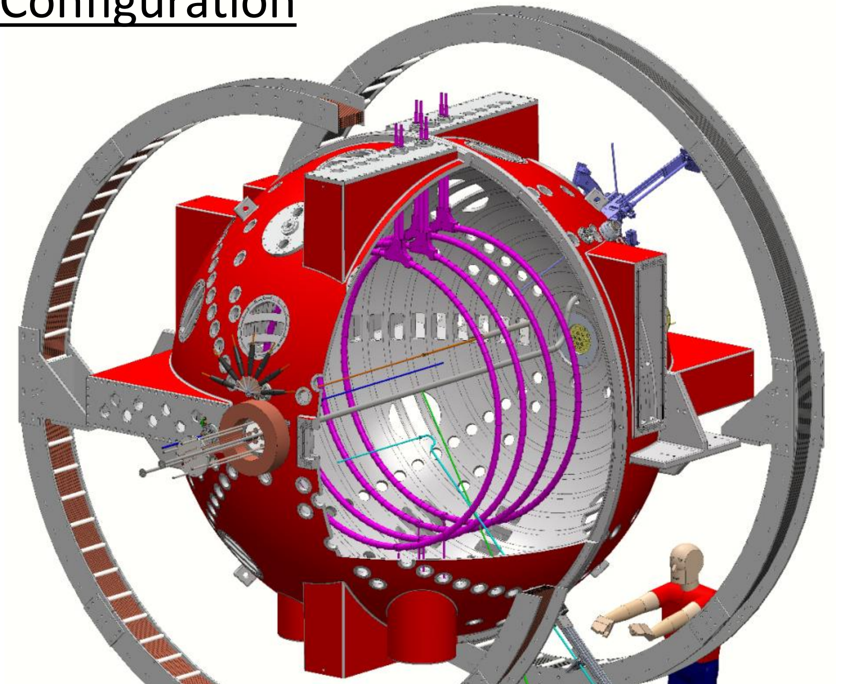

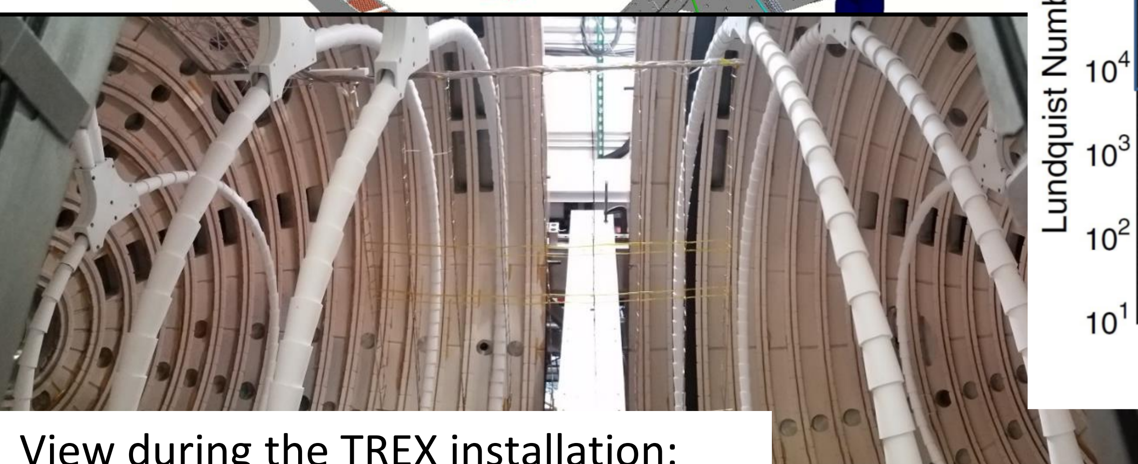

View during the TREX installation:

Phase diagram of magnetic reconnection.

8kV loop voltage ➔ collisionless regime with electron pressure anisotropy, $\tau_{ei} > d_i/(0.1V_A)$

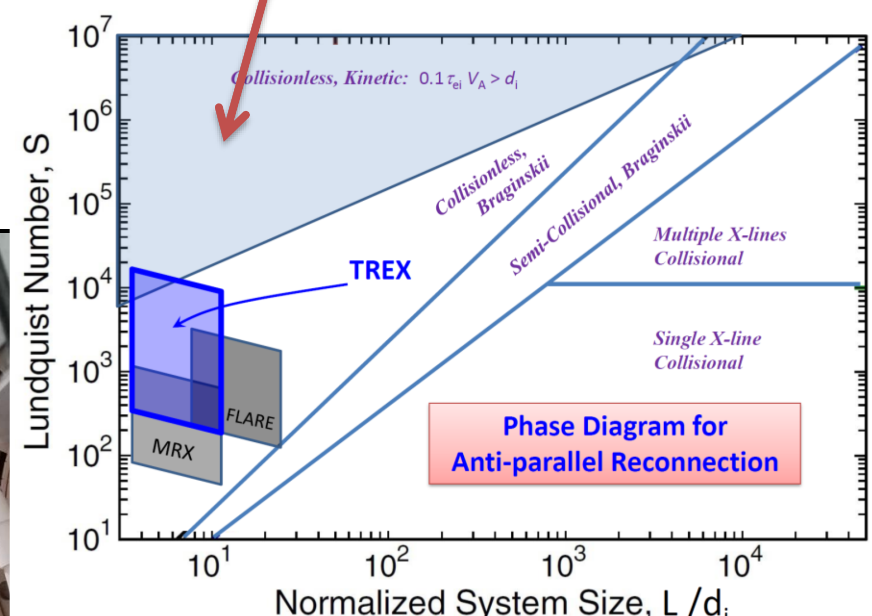

TREX implemented at the WiPPL user facility

<u>TREX Configuration</u>

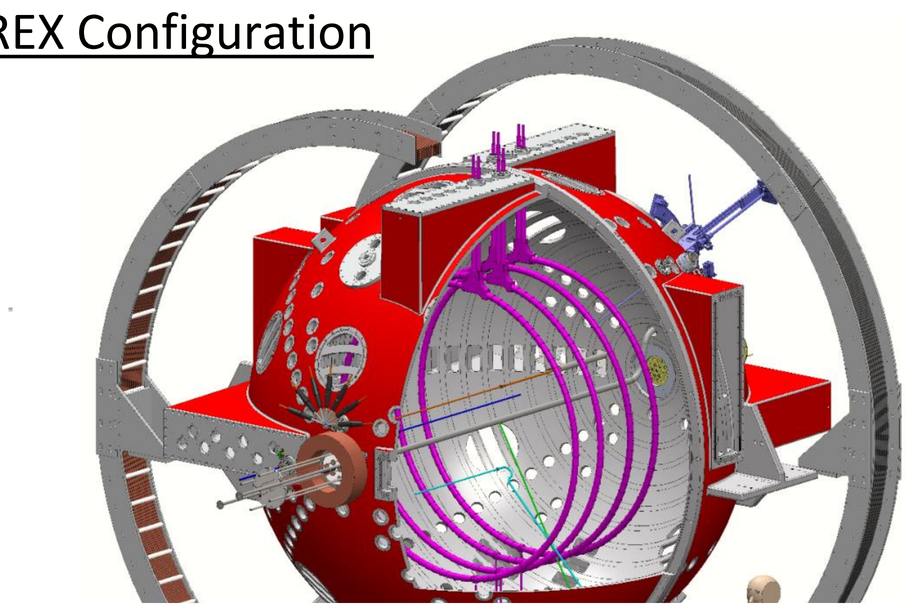

Phase diagram of magnetic reconnection.

8kV loop voltage ➔ collisionless regime with electron pressure anisotropy, $\tau_{ei} > d_i/(0.1V_A)$

Scan in S using kinetic simulations, for $B_g \sim 0.3\ B_r$

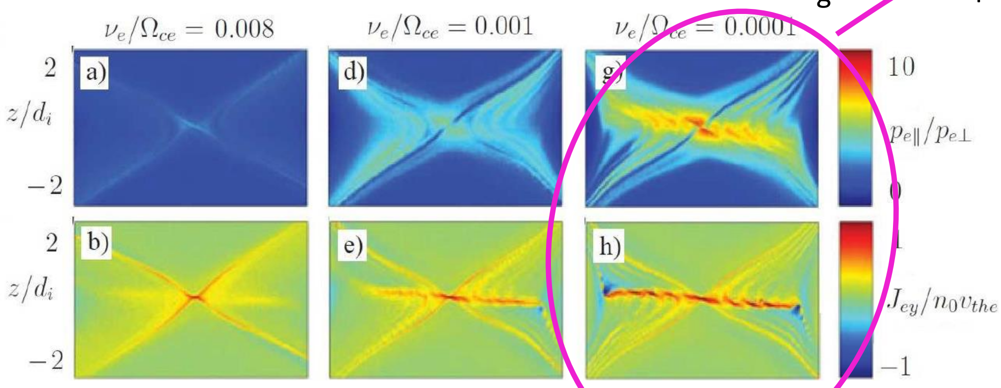

Le et al., JPP, 2015

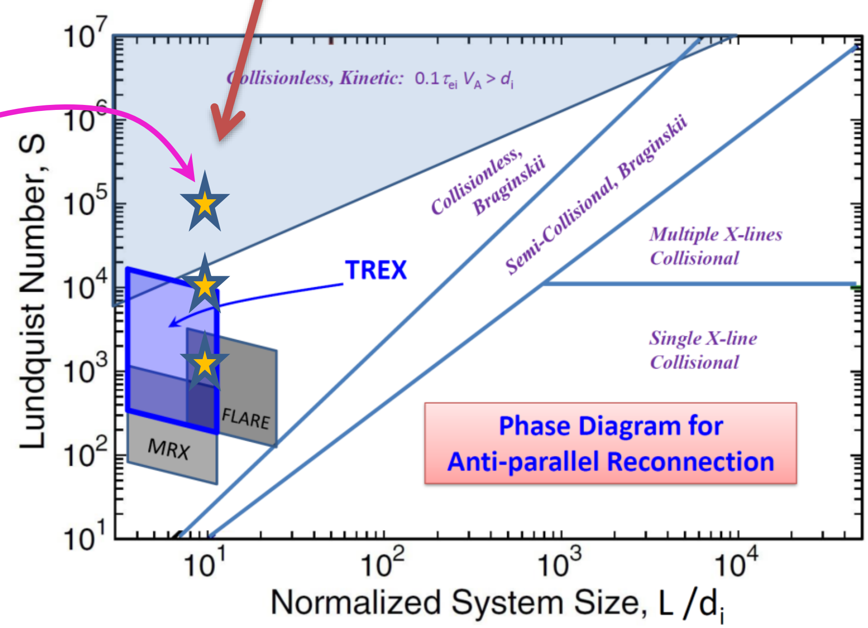

TREX implemented at the WiPPL user facility

TREX Configuration

Phase diagram of magnetic reconnection.

8kV loop voltage ➔ collisionless regime with electron pressure anisotropy, $\tau_{ei} > d_i/(0.1V_A)$

Scan in *S* using kinetic simulations, for $B_g \sim 0.3\ B_r$

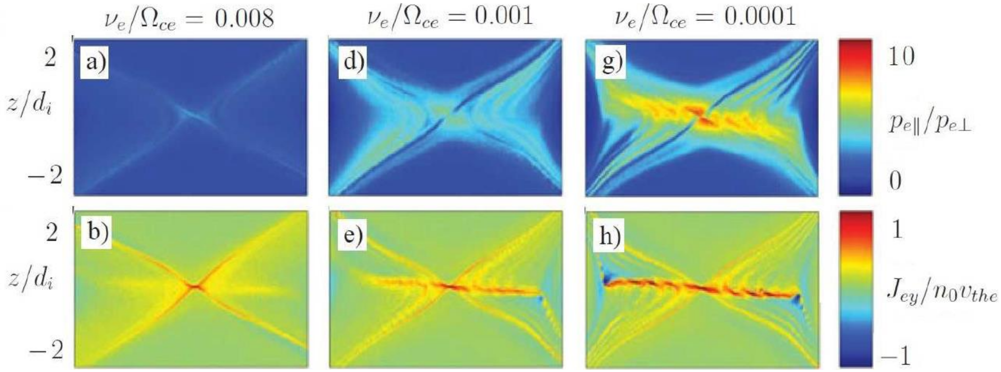

Le et al., JPP, 2015

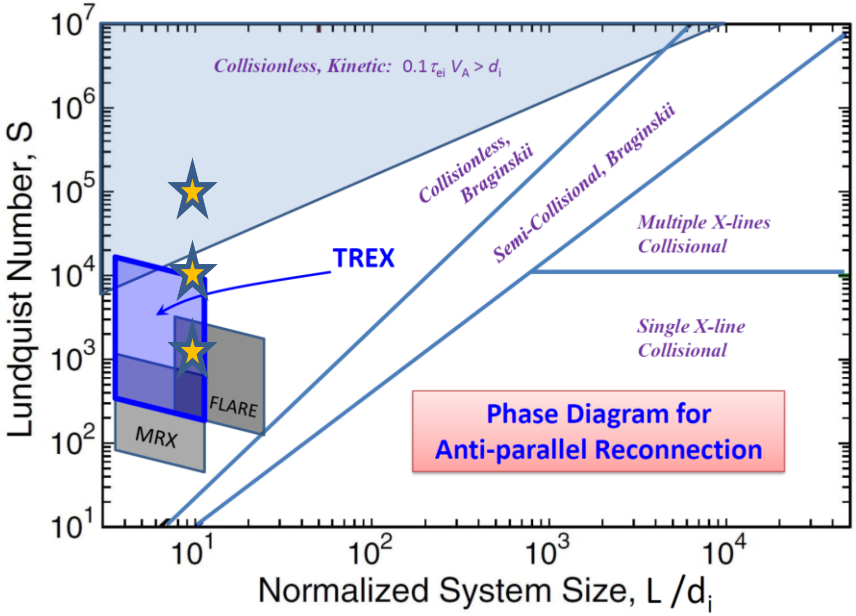

TREX implemented at the WiPPL user facility

WiPPL

New Regime of Reconnection (look at Ohm's law)

$$\mathbf{E} + \mathbf{v} \times \mathbf{B} = \eta\, \mathbf{J} + (\mathbf{J} \times \mathbf{B} - \nabla\cdot\mathbf{p}_e)/ne + \ldots$$

$ne\,\mathbf{E}_y \ll \mathbf{J} \times \mathbf{B} \sim \nabla\cdot\mathbf{p}_e$ (Kinetic reconnection)

$ne\,\mathbf{E}_y \sim \mathbf{J} \times \mathbf{B}$ (Hall or Whistler reconnection)

Phase diagram of magnetic reconnection.

8kV loop voltage ➔ collisionless regime with electron pressure anisotropy, $\tau_{ei} > d_i/(0.1V_A)$

Scan in S using kinetic simulations, for $B_g \sim 0.3\, B_r$

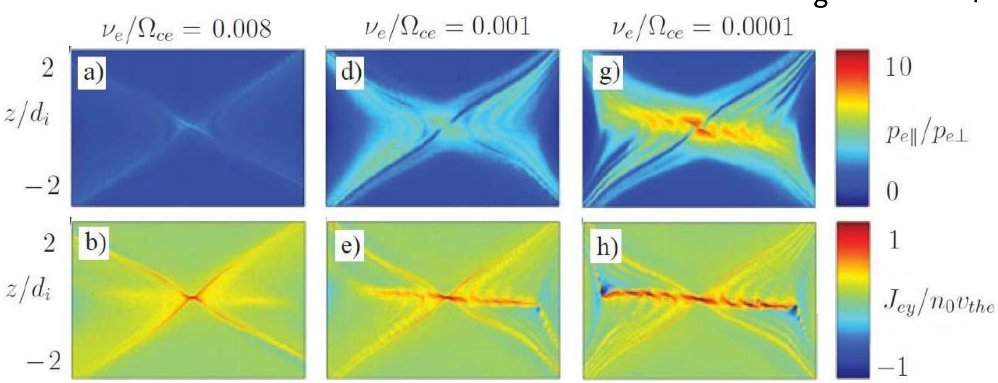

Le et al., JPP, 2015

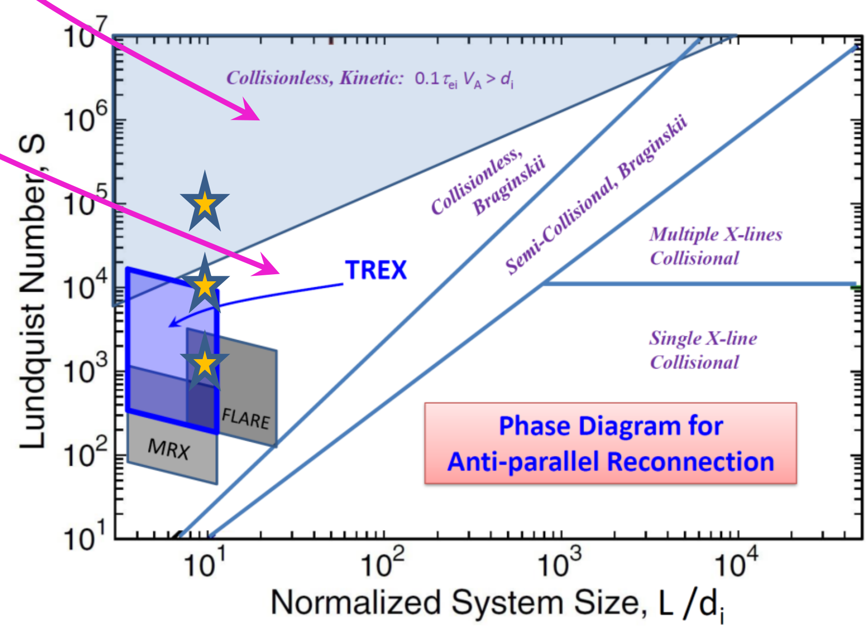

Future: Reach Fully Collisionless Regime

TREX Configuration

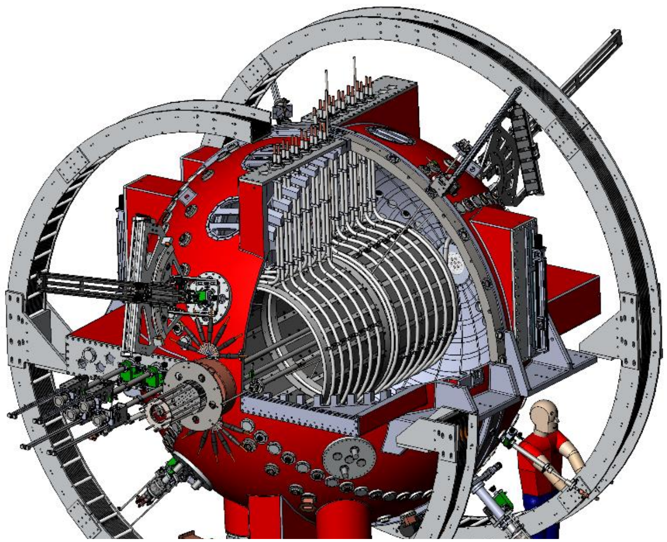

Phase diagram of magnetic reconnection.

8kV loop voltage ➔ collisionless regime with electron pressure anisotropy, $\tau_{ei} > d_i/(0.1V_A)$

Scan in *S* using kinetic simulations, for $B_g \sim 0.3\, B_r$

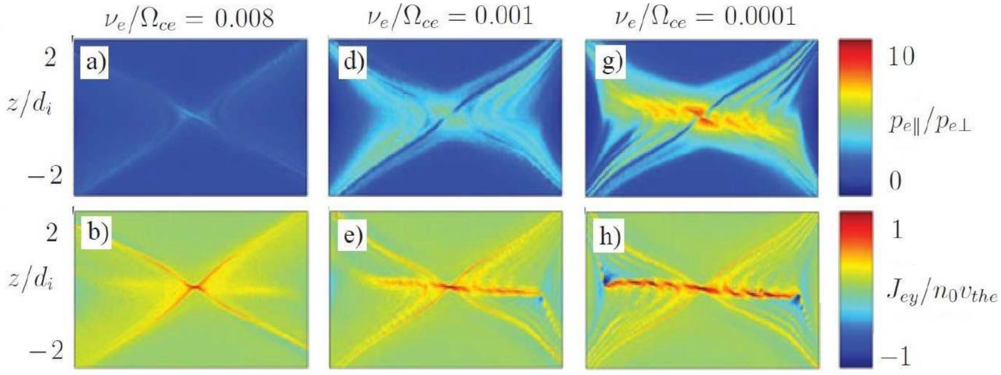

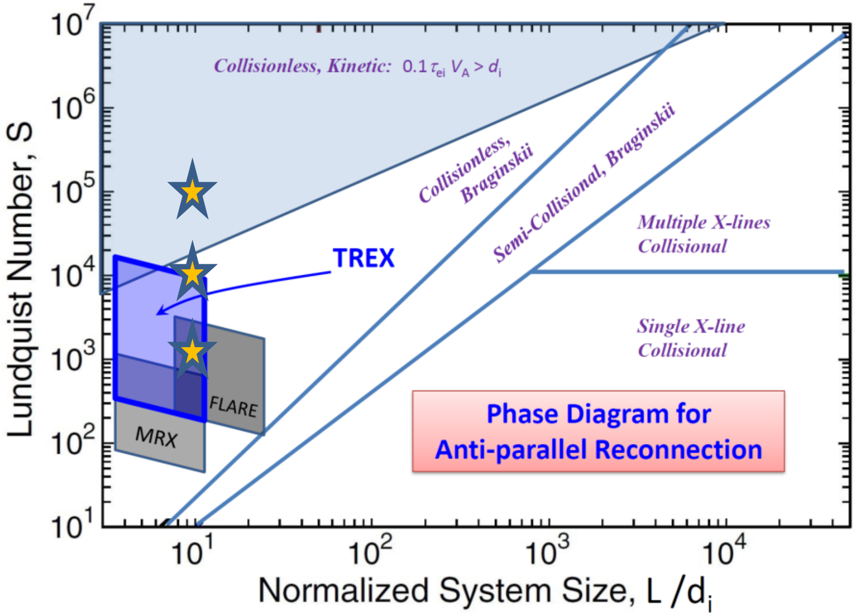

Le et al., JPP, 2015

Future: Reach Fully Collisionless Regime

<u>TREX Configuration</u>

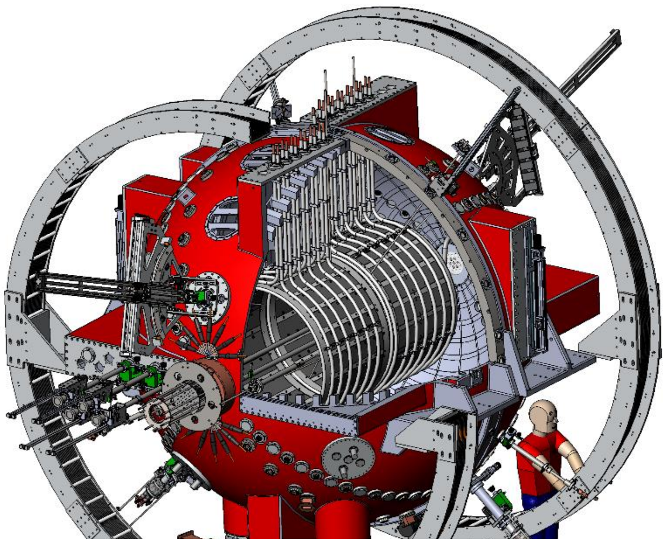

Phase diagram of magnetic reconnection.

8kV loop voltage ➔ collisionless regime with electron pressure anisotropy, $\tau_{ei} > d_i/(0.1V_A)$

Scan in S using kinetic simulations, for $B_g \sim 0.3\ B_r$

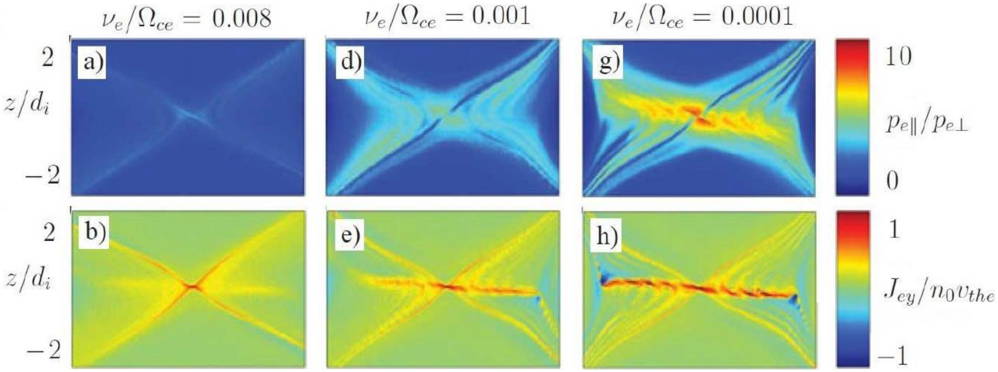

Le et al., JPP, 2015

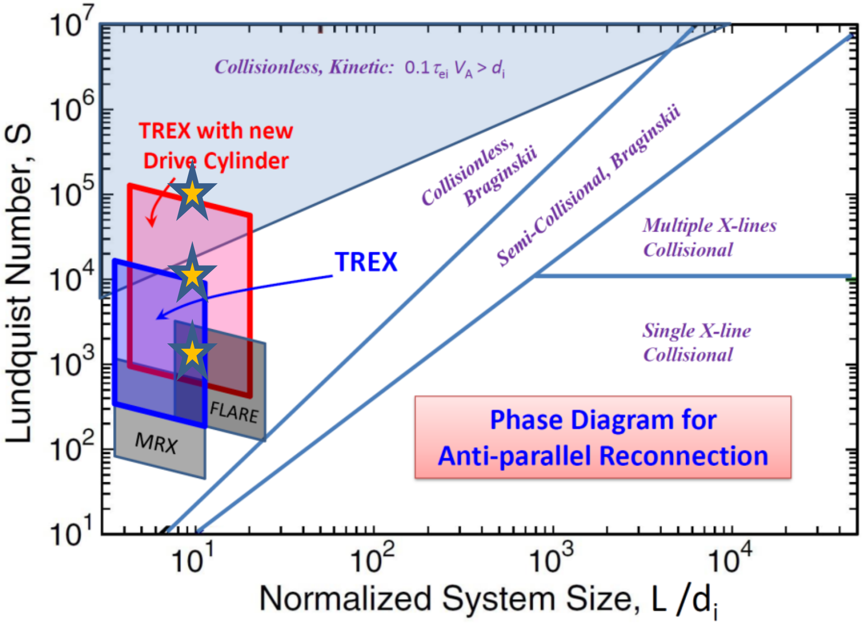

Future: Reach Fully Collisionless Regime

TREX Configuration

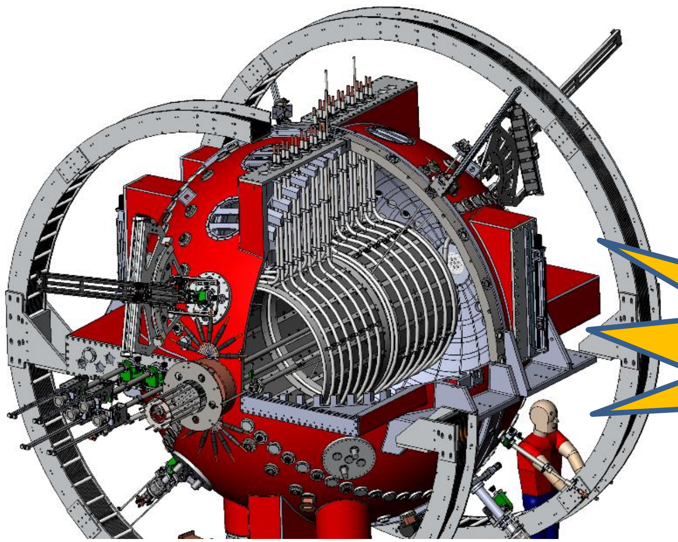

Phase diagram of magnetic reconnection.

8kV loop voltage ➔ collisionless regime with electron pressure anisotropy, $\tau_{ei} > d_i/(0.1V_A)$

New Data, from present config!

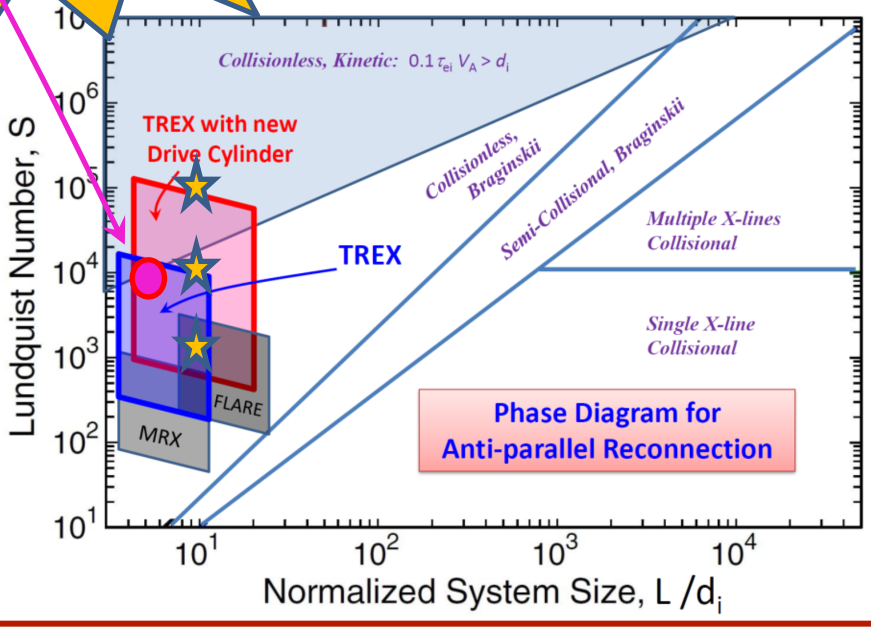

Scan in S using kinetic simulations, for $B_g \sim 0.3\ B_r$

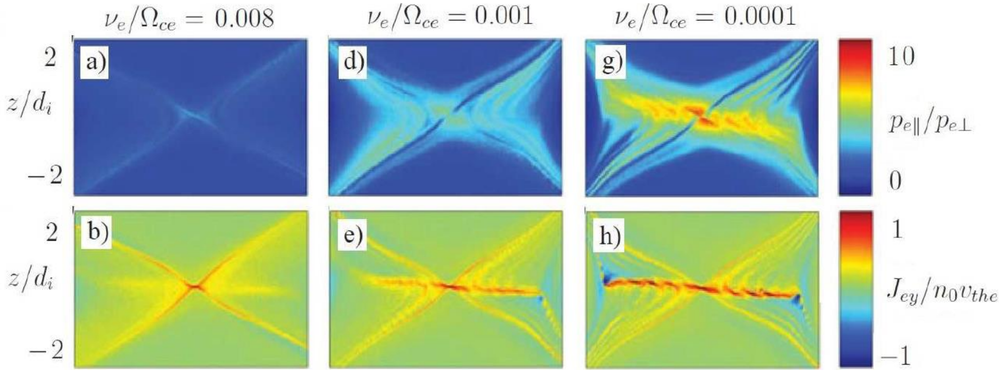

Le et al., JPP, 2015

Fully Collisionless Regime Reached

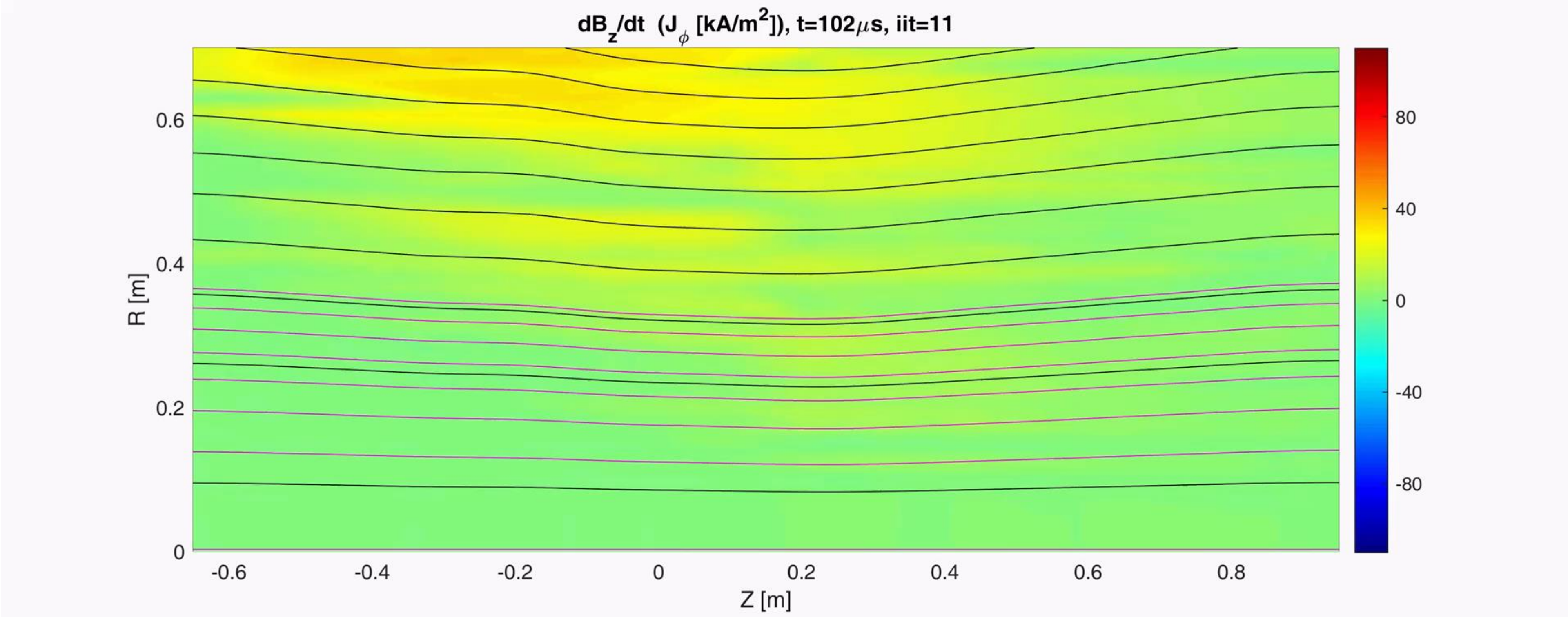

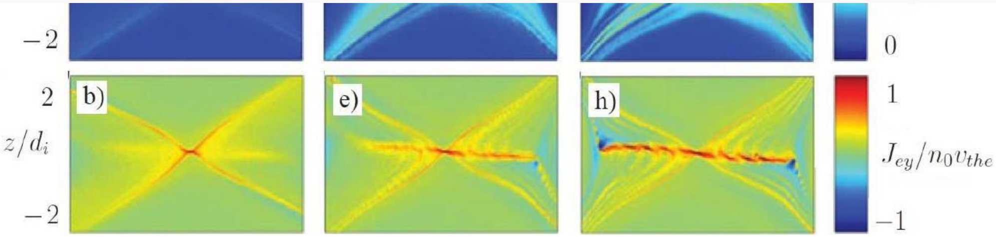

Le et al., JPP, 2015

Fully Collisionless Regime Reached

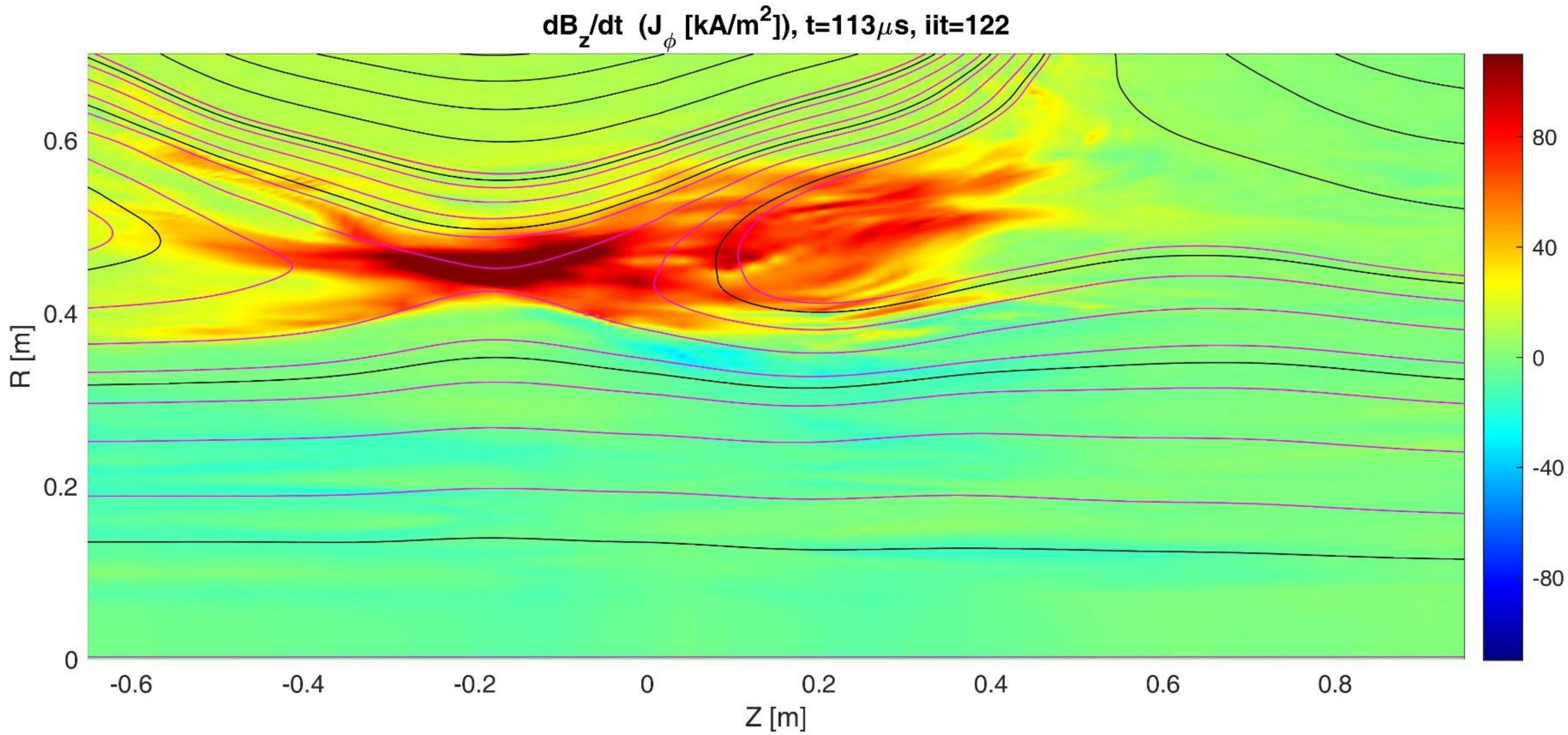

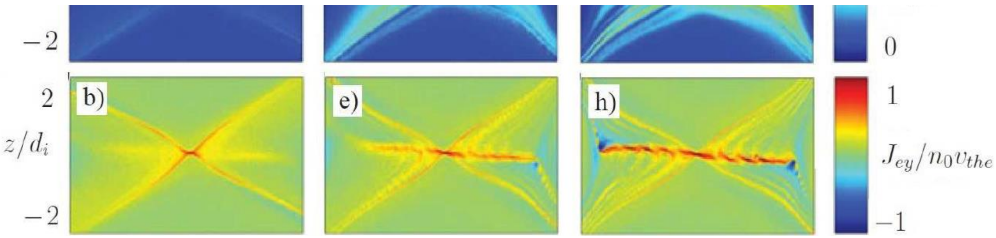

Le et al., JPP, 2015

Fully Collisionless Regime Reached

Data from 36 shots

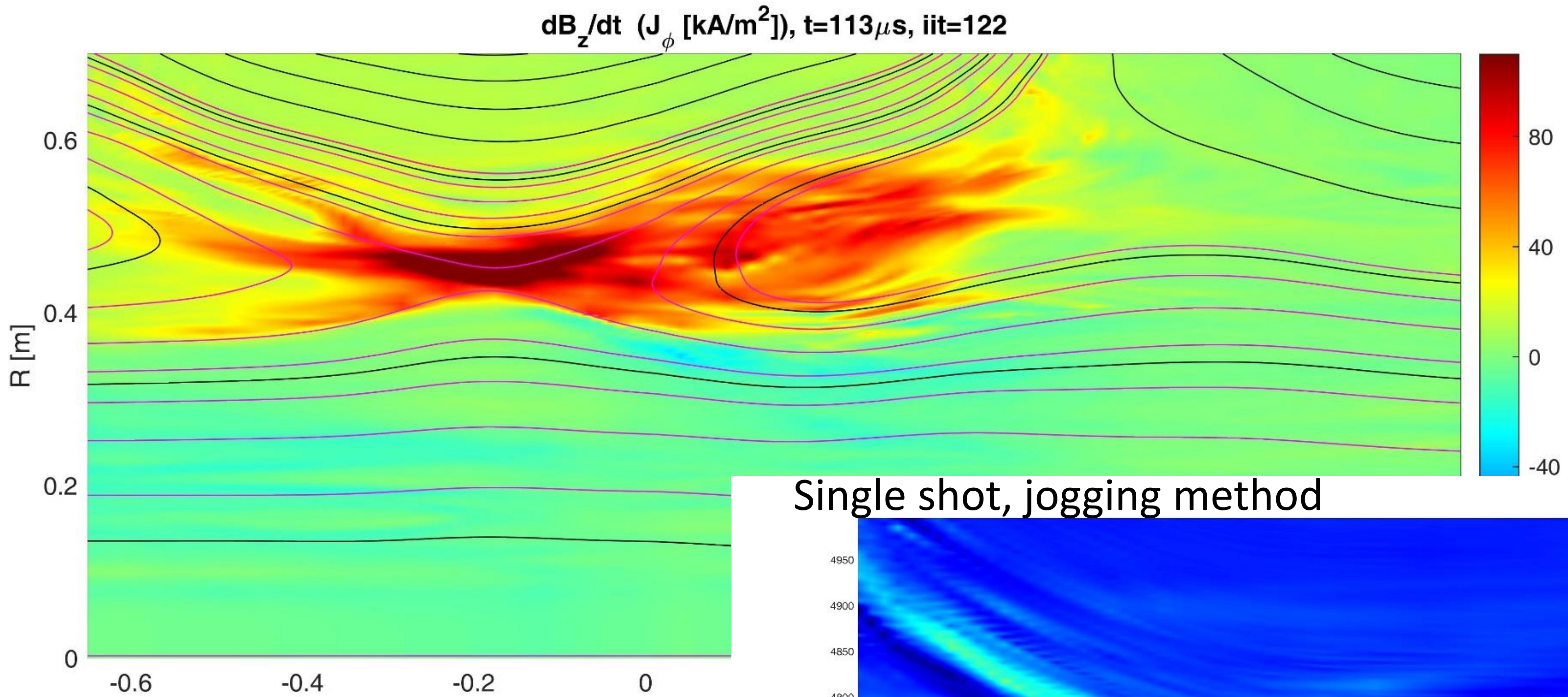

Single shot, jogging method

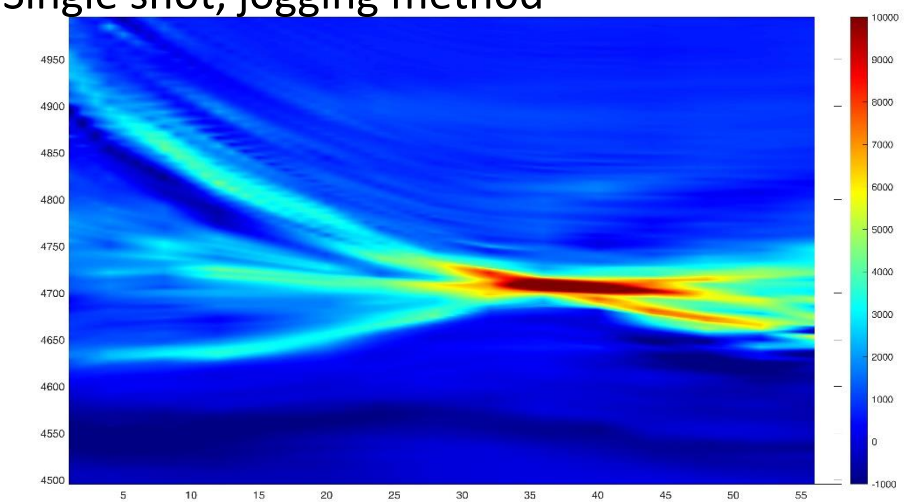

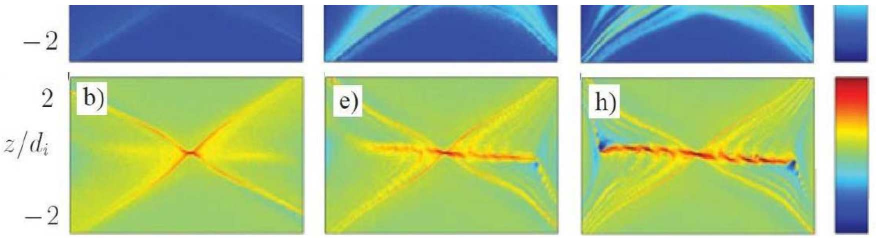

Le et al., JPP, 2015

Fully Collisionless Regime Reached

Cylindrical VPIC simulation

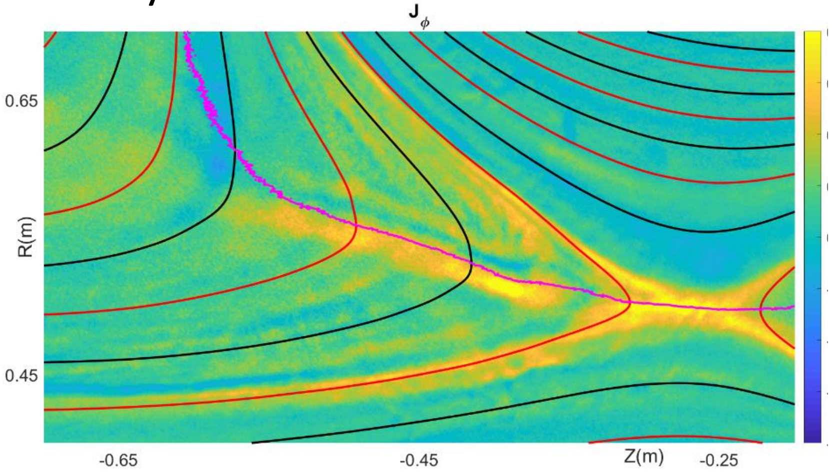

Marginal Firehose along the jet.

$\mathbf{J} \times \mathbf{B} \sim \nabla \cdot \mathbf{p}_e$

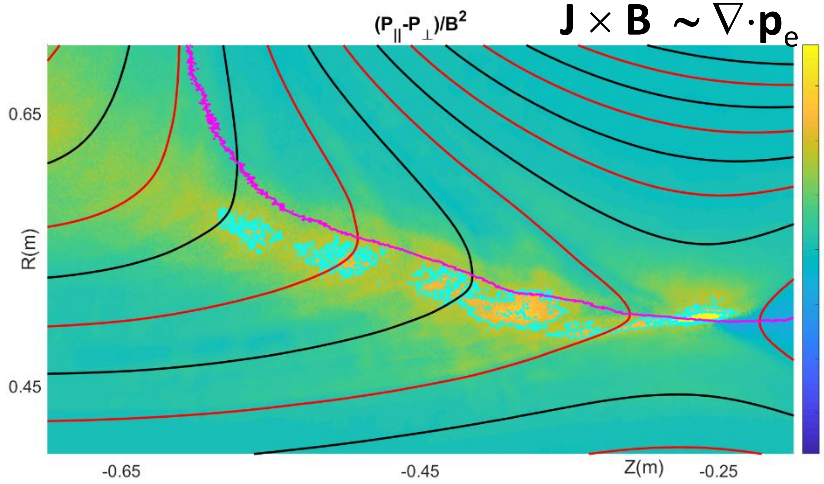

Scan in S using kinetic simulations, for B_g ~

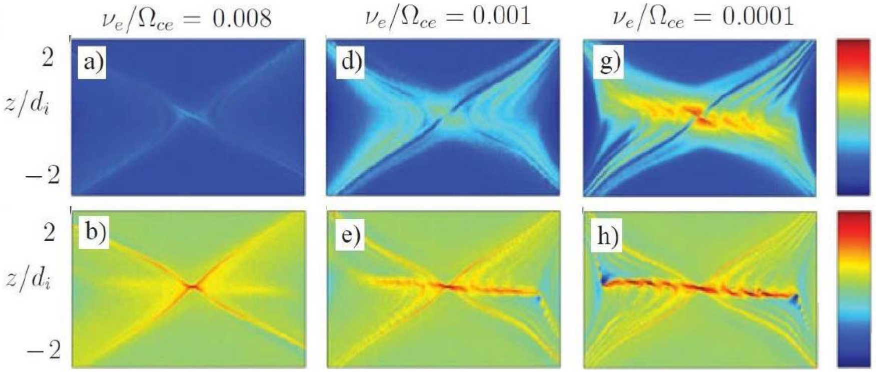

Le et al., JPP, 2015

Single shot, jogging method

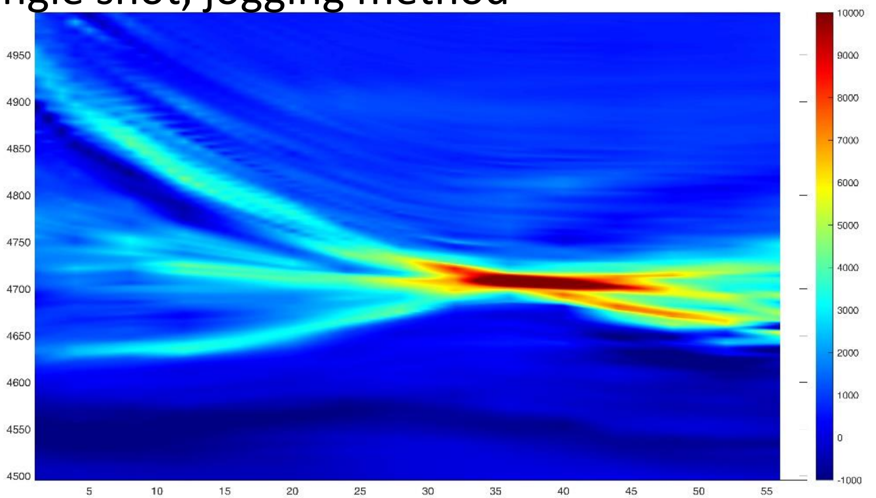

Conclusion

- Reconnection layers, ~1m, are characterized at mm resolution
- Strong drive yields high Lundquist number regime with electron pressure anisotropy
- Embedded current layers are observed.
- Reconnection is fast
- The current layer width is narrow ➔ $\nabla\cdot P_e$ likely breaks the Frozen-In-Law.
- TREX has now entered the regime of <u>kinetic reconnection</u>!
- The WiPPL user facility is open for business; see Cary Forest or visit: wippl.wisc.edu

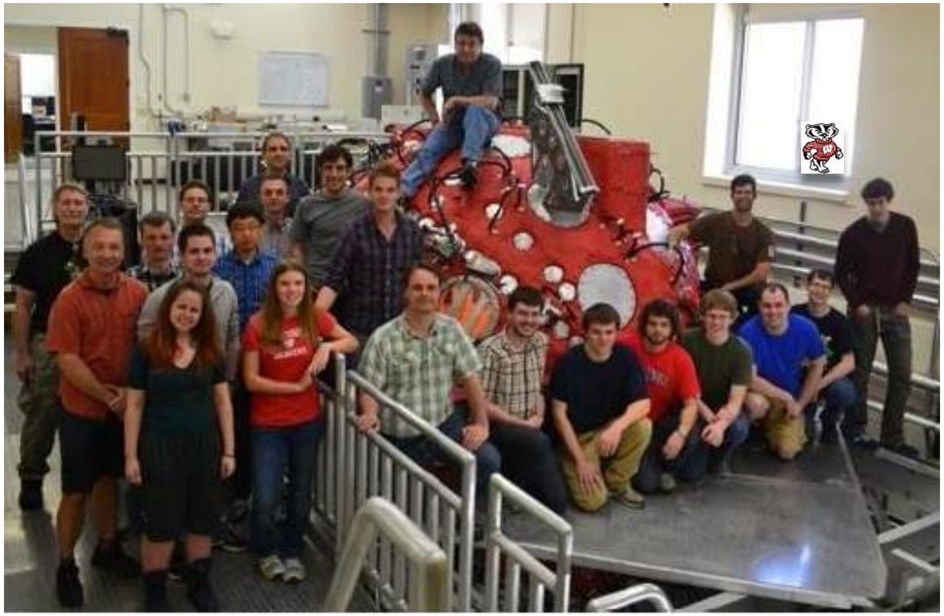

Thank you for your attention